Title
Skeletal effects induced by Maxillary Skeletal Expander (MSE) and Hyrax appliance in the midface

Author
Cantarella, Daniele

Publication Date
2017

Peer reviewed|Thesis/dissertation

UNIVERSITY OF CALIFORNIA

Los Angeles

Skeletal effects induced by Maxillary Skeletal Expander (MSE) and Hyrax appliance in the midface

A thesis submitted in partial satisfaction

of the requirements for the degree of Master of Science

in Oral Biology

by

Daniele Cantarella

2017

ABSTRACT OF THE THESIS

Skeletal effects induced by Maxillary Skeletal Expander (MSE)

and Hyrax appliance in the midface

by

Daniele Cantarella

Master of Science in Oral Biology

University of California, Los Angeles, 2017

Professor Won Moon, Co-Chair

Professor Sanjay Mallya, Co-Chair

Introduction: The purpose of this study was to evaluate the skeletal changes induced by Maxillary Skeletal Expander (MSE) and Hyrax appliance in the midface with the use of Cone-Beam Computed Tomographic images. A novel methodology to study the skeletal changes was developed. Our hypothesis is that MSE and Hyrax result in a dissimilar expansion pattern and magnitude.

Materials and Methods: A novel methodology was developed that included three main reference planes (maxillary sagittal plane, axial palatal plane and V-coronal plane), three axial CBCT sections through the maxilla and the pterygoid plates (axial palatal section, lower nasal section, and upper nasal section), one coronal section through the zygomatic and maxillary bones (coronal zygomatic section), and one axial section

through the zygomatic arch and maxillary bone (axial zygomatic section). Fifteen and six patients were included in the MSE and Hyrax groups respectively. Parametric or non-parametric tests as appropriate were used to evaluate the treatment changes observed in the MSE group and Hyrax group.

Results: In MSE patients, the midpalatal suture split, and the maxilla moved laterally and forward. Skeletal changes were largest in the axial palatal section, smaller in the lower nasal section and smallest in the upper nasal section. Also, skeletal changes were larger in the anterior than the posterior regions of the skull. The pterygoid processes of the sphenoid bone bent laterally with a center of rotation located in proximity of the cranial base. The pterygopalatine suture underwent substantial loosening in all parts. In the lower part, the pyramidal process of the palatine bone was pulled out from the pterygoid plates of the sphenoid bone, leaving detectable openings in 53% of the sutures. In the middle part, the tuberosity of the maxilla slid laterally and anteriorly relatively to the pterygoid processes. In the upper part, the posterior portion of the perpendicular plate of the palatine bone bent medially. In the coronal plane, the zygomaticomaxillary complex rotated outwards with a center of rotation located in proximity of the frontozygomatic suture in both MSE and Hyrax patients. In the horizontal plane, the zygomaticomaxillary complex rotated outwards with a center of rotation located in the proximal part of the zygomatic process of the temporal bone for MSE group. However, the center of rotation for the maxilla was located in proximity of the pterygoid process for Hyrax group.

Several differences were found between the MSE and Hyrax groups. Skeletal changes were considerably larger in MSE than in Hyrax patients for almost all parameters. The

pattern of lateral movement of the maxilla was more parallel in both coronal and horizontal planes with MSE. Moreover, in the horizontal plane, the center of rotation of the zygomaticomaxillary complex in MSE group was located more posteriorly and laterally than that of the Hyrax group. Furthermore, MSE was able to split the pterygopalatine suture while Hyrax appliance could not.

Conclusions: MSE induced significantly more skeletal changes in the midpalatal suture, pterygopalatine suture, maxilla and circummaxillary bones in post-pubertal age patients, compared to Hyrax appliance. MSE and Hyrax resulted in dissimilar expansion pattern and varying magnitude.

Keywords: Maxillary Skeletal Expander (MSE), Hyrax appliance, maxillary expansion, skeletal changes, orthopedic effects, midpalatal suture, circummaxillary sutures, midface.

The thesis of Daniele Cantarella is approved.

Sotirios Tetradis

Won Moon, Committee Co-Chair

Sanjay Mallya, Committee Co-Chair

University of California, Los Angeles

2017

TABLE OF CONTENTS

LIST OF FIGURES

LIST OF TABLES

LIST OF ACRONYMS

- MSP: maxillary sagittal plane
- APP : axial palatal plane
- VCP: V-coronal plane
- APS: axial palatal section
- LNS: lower nasal section
- UNS: upper nasal section
- CZS: coronal zygomatic section
- AZS: axial zygomatic section
- Rt: right
- Lt: left
- ANS: anterior nasal spine
- PNS: posterior nasal spine
- FZS: frontozygomatic suture
- ZMS: zygomaticomaxillary suture
- ZTS: zygomaticotemporal suture
- Up Ant Mx: most anterior point of maxillary bone in the UNS
- Up Post Mx: most posterior point of maxillary bone in the UNS

Acknowledgements

I would like to give special thanks to all the persons who collaborated in this research, offering their expertise and contributing to my professional growth. Particularly I would like to thank Dr. Won Moon who gave me the opportunity to work at this exciting research project and who stimulated my research with new ideas and different perspectives. I would like to thank the committee members, Dr. Sanjay Mallya for sharing his knowledge and time and Dr. Sotirios Tetradis for agreeing to serve on my committee.

Several other persons gave their valuable contribution to the project:

- Dr. Joseph Miller, from UCLA Division of Integrative Anatomy, clarifying some important aspects of the pterygopalatine suture
- Dr. Daniela Markovich, from UCLA Department of Biomathematics, assisting with the statistical analysis
- Dr. Hsin Chuan (Dan) Pan, helping with several illustrations
- Stephen Tran, from UCLA Dept. of Bioinformatics, helping with the data analysis
- My sister Enza, with the arrangement of Excel spreadsheet and tables
- Dr. Ramon Mompell, helping with the organization of the material
- Dr. Islam El-Kenawy, giving his support in all IT issues
- Dr. Christoph Moschik, Dr. Mohammed Alkahtani and Dr. Eliza Jaria

Finally a big thank to the residents and Professors of UCLA Section of Orthodontics, who made my stay at UCLA a pleasant experience.

INTRODUCTION

Rapid Palatal Expansion (RPE) is routinely used to treat transverse maxillary constriction by opening the midpalatal suture, providing correct and stable maxillary width [1-4]. Angell [5] first described this method in 1860 but it was popularized by Haas [1-3,6] 100 years later. Since then many types of Rapid Maxillary Expansion (RME) appliances have been developed with different rates of expansion and protocols [7-9] although the basic principles are essentially the same [10]. The most common design of RME is a tooth-borne anchored expander with or without an acrylic plate [11,12]. With tooth-supported expansion devices it is not possible to obtain pure skeletal movements [11,13,14]. Undesirable results in conventional RPE are limited skeletal movement, dentoalveolar tipping, root resorption, detrimental periodontal effects such as dehiscence and lack of long-term stability [11,12,15,16]. To moderate these side effects, clinicians in recent years have utilized micro-implant assisted rapid palatal expansion (MARPE) that can apply the expansion force directly to the maxillary bones while minimally loading the dentition [10,17-19]. Other authors reported that the mentioned side effects encountered with tooth-born expanders can be minimized using an hybrid Hyrax device, a tooth bone-borne palatal expander that is attached to the first molars and connected by two orthodontic micro-implants to the anterior palate [20].

The main purpose of RPE devices, regardless their design, is primarily to split the midpalatal suture [21]. For this reason one of the most important factors affecting the success of RPE is the age of the patient and therefore the stage of fusion of midpalatal suture. Even though the timing of palatal suture interdigitation varies among individuals, the most appropriate age for RPE is the pubertal or pre-pubertal period [22,23]. Due to

higher interdigitation of the midpalatal suture after puberty, some authors affirm that expansion of the maxillary arch in post-pubertal patients is not feasible [22,24] and surgically assisted rapid palatal expansion (SARPE) is a recognized approach for the correction of skeletal transverse maxillary deficiencies at this age [25-31]. It is assumed by these clinicians that RPE without a surgical approach is unsuccessful after the puberty, because the midfacial buttresses prevent the maxillary bones from moving [2,25,32-34]. However, SARPE has the disadvantage of being invasive since a surgical intervention is required. Recently the expansion of the midpalatal suture [35] in young adults has become more common and recent evidences suggest that it can be possible to successfully expand the palate at this age. Handelman [36] using a tooth-borne expander on 47 patients reported that RPE is a clinically successful and safe method for correcting transverse maxillary arch deficiency in adults without the need of SARPE. Nevertheless, bone-borne expanders have been more predictable in adults in opening the midpalatal suture as demonstrated more recently by some authors in clinical [18] and in Finite Element Method (FEM) studies [19].

It is believed that the main resistance to the opening of the midpalatal suture is probably not in the suture itself; rather, it is in the surrounding structures with which the maxilla articulates, particularly the sphenoid and the zygomatic bones [37,38]. Therefore the expansion force might affect all the circummaxillary sutures: internasal, nasomaxillary, frontomaxillary, frontonasal, frontozygomatic, zygomaticomaxillary, zygomaticotemporal, and pterygopalatine. This involvement has been hypothesized based on investigations that utilized histologic methods [39-41], radiologic imaging [18,42-44], photoelastic models [45,46], bone scintigraphy [47] and FEM [19,48-58].

Cranial sutures respond differently to the external orthopedic forces depending on their anatomic location and on the degree of interdigitation. To understand the biologic changes in the alveolar bone and at the circummaxillary sutures in response to RPE, it is necessary to analyze the forces received by these structures during palatal expansion. It has been reported that pressure is generated at various craniofacial areas during RPE. Some authors[29,59] cited various combinations of frontozygomatic suture, zygomaticomaxillary suture and zygomaticotemporal suture as the primary anatomic sites of resistance to RPE. Leonardi [42] found higher stress levels in the zygomatic process of the maxilla, external walls of the orbit, frontozygomatic suture, and in the frontal process of the maxilla. These same locations were observed also in different FEM studies [48,49,53-55,57]. Garib [60] and Babacan [61] report that the maximum stresses were experienced by the medial aspect of the frontomaxillary suture, the superior portion of the nasomaxillary suture and the lateral aspect of the frontonasal suture, supporting the results found by Gautam [50] in a FEM study. In relation to this aspect, a recent study [19] distinguishes between conventional RPE and micro-implant assisted rapid palatal expansion (MARPE). Stress distribution from conventional expansion is located along the three maxillary buttresses: the zygomaticomaxillary suture, the nasomaxillary suture and the pterygopalatine suture. In comparison, stress distribution from MARPE showed less propagation to the buttresses and adjacent locations in the maxillary complex.

Due to the resistance of all the circummaxillary sutures during the expansion process the separation of maxillary bones in the coronal plane occurs in a triangular fashion with the apex toward the nasal cavity and the base at the same level as the palatine processes [6,38,62-68]. On the horizontal plane the greatest opening of the

midpalatal suture has been found anteriorly, with progressively less separation toward its posterior part [1,2,6,69-71]. Other authors have reported more parallel expansion in both planes [18,19,49,72]. Recent systematic reviews [73,74] concluded that RPE is an effective procedure that is always able to produce transverse skeletal effects on the maxilla by opening the midpalatal suture in growing subjects regardless of the type of palatal expander. Bazargani [75] also in a systematic review determines that the opening of the midpalatal suture amounted to 20%–50% of the total screw expansion, but there was no consistent evidence on whether the opening of the midpalatal suture was parallel or triangular, regardless of the expander that was used.

Regarding the fulcrum of rotation of the maxillary bone in the coronal plane, it is still being debated where it is located. The majority of FEM studies affirm that it is located at the frontomaxillary suture [19,48,49,51]. Gardner [40] in his study with rhesus monkeys and Gautam [50] in his FEM study define this center of rotation close the superior orbital fissure. This last author also mentioned that the center of rotation of the maxilla in the horizontal plane was somewhere between the lateral and the medial pterygoid plates of the sphenoid bone.

When we analyze the effects induced by RPE on the sphenoid bone, we need to consider the pterygopalatine suture and the spheno-occipital synchondrosis [22,40,43,44,46-52,76-84]. Melsen [82] and Baccetti [83] affirm that in dry human skulls a spontaneous opening of the pterygopalatine suture is not expected during rapid palatal expansion because of the extensive interlocking of the corresponding bone surfaces. Disarticulation of the palatal bone from the pterygoid process is possible only on infantile and juvenile (early mixed dentition) skulls. Attempted disarticulation in the

late juvenile (late mixed dentition) and adolescent periods was always accompanied by fracture of the heavily interdigitated osseous surfaces. However, other authors consider that the splitting of the pterygopalatine suture can be the explanation of the sagittal and vertical movement of the maxilla during the expansion. Garib [60] and Jafari [48] believe that the reduction of the fusion at the circummaxillary sutures will explain this displacement of the maxilla. Lastly, other clinicians in different investigations in humans [43,79], monkeys [40], mice [80,81] and in FEM studies [49,52] have reported indirect effects of RPE on the spheno-occipital synchondrosis producing antero-posterior movements of the maxilla. Also, Stepanko [76] and Kudlick [84] hypothesized that the sphenoid bone may be affected by RPE and they found that there were no significant changes regardless of sex or treatment type (tooth-borne or bone-borne expander). Their study focused on the sphenoid bone alone and not on the articulation of the sphenoid with surrounding bones.

In relation with the zygomatic bone, sutures frequently studied are the frontozygomatic, zygomaticomaxillary and zygomaticotemporal. Although high stress levels in the zygomatic bone have been reported [19,46,50-59, 85], no study has described the motion path performed by the zygomatic bone during RPE. In the same context, the internasal suture, the nasomaxillary suture and the frontonasal suture were also analyzed in the literature. It has been reported that high levels of stress are generated at these areas [19,21,39,40,42.44,46,50,61,86-88]. Changes at these sutures are related to an increase of the dimensions of the nasal cavity and therefore to a reduction in the nasal airflow resistance [2,6,18,44,61,72,89-93]. A systematic review [75] concludes that the effect of

RPE on the dimensions of the nasal cavity seems to be apparent and indicates an enlargement between 17% and 33% of the total screw expansion.

Modifications of the midpalatal suture, dental position and inclination, and changes at circummaxillary sutures during RPE have been previously analyzed using study models [63,79], two-dimensional imaging [1-3,6,94-97], and more recently three-dimensional imaging based on computed tomographic data [18,42-44,60,72,76,77,89-91]. The limitations of clinical examinations and two-dimensional radiography are the impossibility to analyze what is occurring at the suture level in orthodontic patients. The introduction of cone beam computed tomography (CBCT) in the orthodontic field and the development of new computer software allow to obtain multiplanar, 3-dimensional (3D) reconstructions contributing to extend the possibilities in diagnosis of the craniofacial complex in living subjects [98-101]. Comparisons between tooth-borne and bone-borne expanders have been published using this technology. However, these studies either compare both distractors in young patients [17,60] or evaluate them in adult patients when these expanders accompany SARPE [102-105]. No study has compared conventional RPE in pre-pubertal patients versus MARPE without surgical assistance in post-pubertal patients, accounting for various bones of the craniofacial complex. Thus, the aim of this thesis is to evaluate the effects on the maxillary and circummaxillary structures induced by two distraction modes, a bone-borne expander (Maxillary Skeletal Expander) and a conventional tooth-borne expander (Hyrax), using high-resolution CBCT. Maxillary Skeletal Expander (MSE) is a specific type of MARPE used in UCLA Orthodontic Clinic.

Particularly the following inquiries must be addressed: exploring the possibility of splitting the midpalatal and pterygopalatine sutures in post-pubertal age, and identifying the centers of rotation for the maxillary and zygomatic bones in the coronal and axial planes. Finally, a novel methodology should be developed in order to accurately evaluate various skeletal displacements in 3D during the midfacial expansion.

Our hypothesis is that MSE and Hyrax result in dissimilar expansion pattern and varying magnitude.

MATERIALS AND METHODS

The study received approval from the Institutional Review Board at UCLA. Two groups of patients were selected: Maxillary Skeletal Expander (MSE) and Hyrax groups. All patients were treated in the Orthodontic Clinic at UCLA School of Dentistry. It was a retrospective study and inclusion criteria were the following: 1) transverse maxillary deficiency based on Andrew's transverse analysis of elements, 2) treatment with MSE or Hyrax as part of the overall treatment, 3) CBCT was taken before and right after expansion, 4) absence of craniofacial syndromes, and 5) no previous orthodontic treatment.

The group of patients treated with MSE was composed of 15 subjects (9 males and 6 females) with the mean age of 17.2 $\pm$ 4.2 years. The group of patients treated with Hyrax had 6 subjects (4 males and 2 females) with the mean age 12.2 $\pm$ 2.8 years.

The MSE appliance made by Biomaterials Korea Inc. was made up of four components: a central body containing expansion jackscrew, four tubes (1.5 mm internal diameter and 2 mm length) in the anterior and posterior corners of the central body serving as jigs for placing 4 micro-implants (1.5 mm in diameter and 11 mm in length), four soft supporting arms connecting the central body to maxillary molars providing a stable MSE position during expansion, and two molar bands around maxillary first molars (Fig 1).

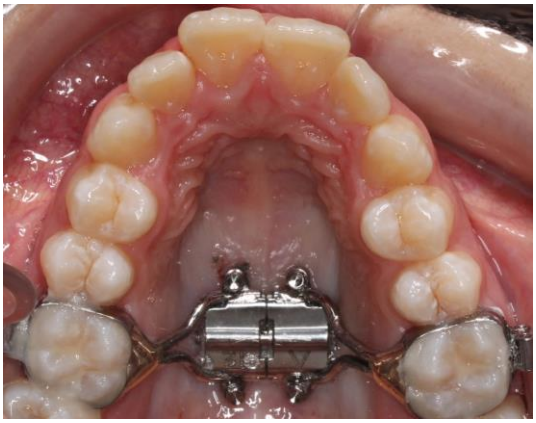
Fig 1. MSE appliance in situ

This 1.5 mm diameter micro-implant inside 1.5 mm tubes created a tight fit of the micro-implants and minimized unwanted tipping of micro-implants and subsequent lateral forces on the molars during maxillary expansion. The 11 mm micro-implant length ensured a bi-cortical engagement of the micro-implants at the palatal bone and nasal floor, which in turn, prevented unwanted tipping of the micro-implants during the expansion and also promote skeletal expansion (Fig 2).

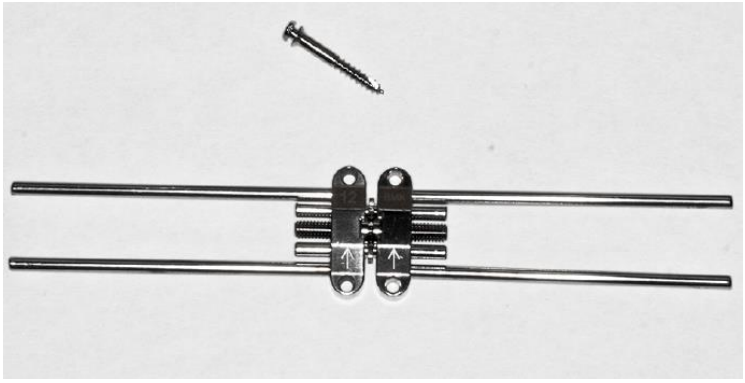
Fig 2. Prefabricated MSE appliance made by Biomaterials Korea Inc. Company

Each appliance was fabricated by sizing the molar bands, taking a pick-up impression and pouring it in stone, placing the central body 1-2 mm anterior to the junction of the

hard and soft palate, fitting the supporting arms to the lateral walls of the palate with 2-3 mm clearance, and soldering the arms to the molar bands. The central jackscrew expander was flush against to the palatal vault and the supporting arms had 2-3 mm clearance off the lateral walls of the palate. This completed appliance was then cemented intra-orally, and four micro-implants were placed under local anesthesia. Patients were instructed to complete two activations of the expansion screw each day until the desired expansion was achieved, each turn producing 0.25 mm of expansion.

The Hyrax appliance used consisted of a central expansion screw attached to two molar bands with rigid supporting arms on maxillary first molars and lingual bar extensions (Fig 3). These appliances were fabricated in a similar manner as the MSE appliances and were cemented intra-orally. Patients were instructed to complete one activation of the expansion screw each day until the desired expansion was achieved, with each turn producing .25mm of expansion.

Fig 3. Hyrax appliance

CBCT scans were taken both before and immediately after the completion of expansion on all patients. All CBCT scans were taken by a NewTom 5G in an 18x16 Field of view with 14-bit gray scale. Scan times were 18 seconds (3.6 seconds emission time), with 110 kV, utilizing an automatic exposure control that adjusted the milliampere based upon the patient's anatomic density. The NewTom 5G Safebeam control reduced the radiation the patient was exposed to, based on the patient's size. Data from the CBCT was reconstructed to produce .3mm slices.

A novel methodology utilizing customized reference planes to evaluate skeletal changes in the midface: maxillary sagittal plane (MSP), axial palatal plane (APP), V-coronal plane (VCP)

Several methods have been proposed to evaluate the skeletal morphology of the midface and the skeletal changes induced by orthopedic appliances. In the coronal plane, a line perpendicular to the line connecting the right and left frontozygomatic suture and passing through Crista Galli of the ethmoid bone is commonly used in 2D cephalometric analysis (Fig 4). One problem with this reference line is that often it is not located in the center of palate and nasal cavity, and subsequently the critical landmarks such as anterior nasal spine (ANS) and posterior nasal spine (PNS) will fall significantly off to the right or left sides of the vertical reference line.

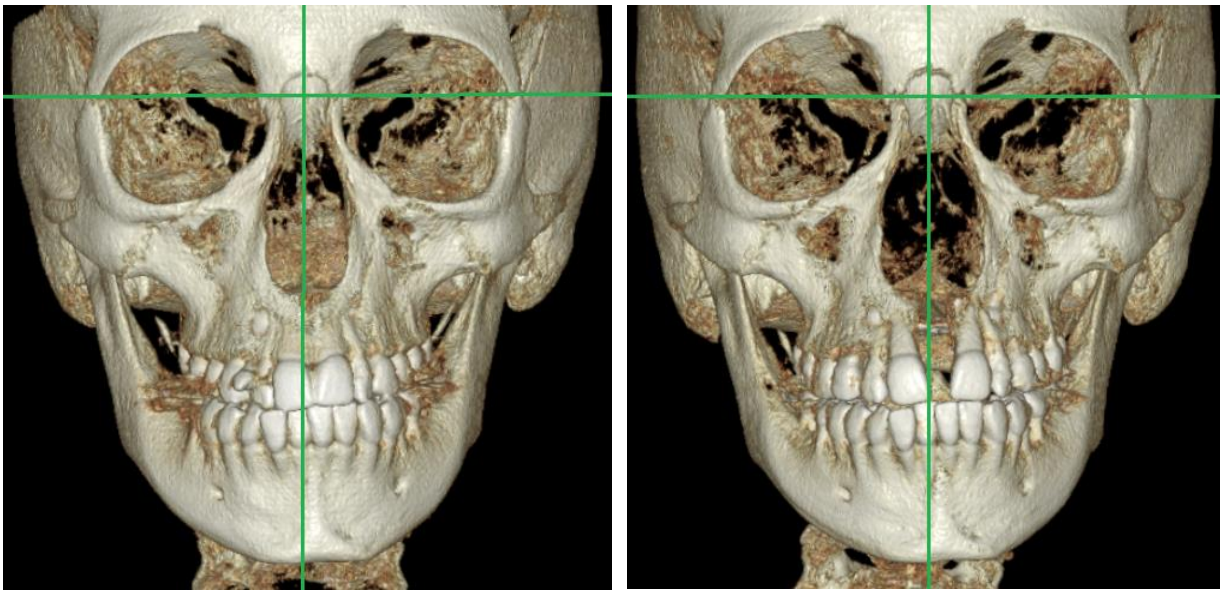

Fig 4. Reference lines used in conventional 2D postero-anterior cephalometrics for a MSE patient. A: pre-expansion and B: post-expansion. Anterior nasal spine is clearly located on the left side of the vertical reference line in the pre-expansion CBCT.

This makes it difficult to analyze the lateral displacement of landmarks located in the maxillary and circummaxillary bones induced by expanders, especially in patients presenting a skeletal asymmetry.

Other 3D cephalometric studies[106] also used reference planes based on the cranial base that do not necessarily cross the midpalatal suture, posing the similar problems.

In order to overcome the above problems, novel reference planes have been developed in this study. Using the OnDemand3D software from Cybermed Inc., the pre- and post-expansion CBCTs of the patients were superimposed using the grey level intensity of the voxels in the entire cranial base in adults and the anterior cranial fossae in growing children. This automated superimposition method will be explained further in the discussion section. After this superimposition, a plane passing through the anterior nasal spine (ANS), posterior nasal spine (PNS) and Nasion (N) on the pre-expansion CBCT was identified. The plane was named the “Maxillary Sagittal Plane” (Fig 5).

Fig 5. Maxillary Sagittal Plane (MSP), a novel reference plane, for evaluating skeletal movements of the midface induced by MSE. A: pre-expansion. B: post-expansion.

The distance from the maxillary sagittal plane (MSP) to various landmarks on maxillary and circummaxillary bones are the parameters used for evaluating lateral skeletal displacements induced by MSE and Hyrax appliance.

The maxillary sagittal plane (MSP) crosses the “center of the face” and maxilla, and the lateral movements of maxillary and circummaxillary bones can be accurately described by tracking the landmarks moving away from this reference plane during the expansion. This reference plane was established from the pre-expansion CBCT and applied to the post-expansion CBCT. The positions of the bony landmarks between pre- and post-expansion CBCT were analyzed relative to this reference plane.

Importantly, the lateral movement of the two halves of maxilla can be quantified independently by measuring the relative displacement of ANS and PNS against MSP during the expansion for each half. The extent of asymmetry during expansion can be quantified by tracking the relative displacements of ANS and PNS of the two halves, and its association with the circummaxillary structures can be explored.

The **maxillary sagittal plane (MSP)** passes through the anterior nasal spine (ANS), posterior nasal spine (PNS), and through Nasion (N) in the pre-expansion CBCT as shown in figures 6 and 7.

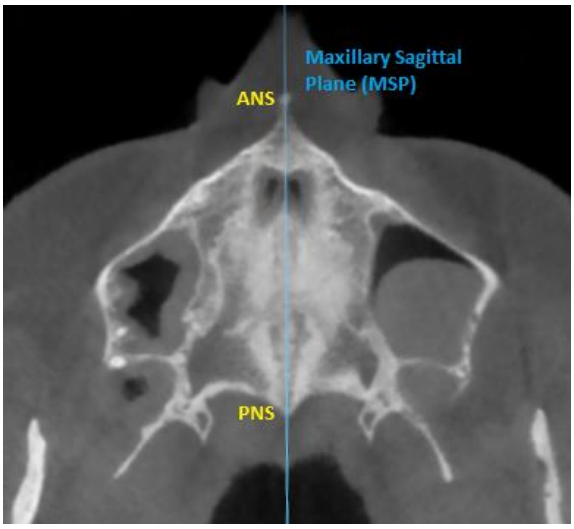

Fig 6. Axial section showing the maxillary sagittal plane (MSP) passing through ANS and PNS.

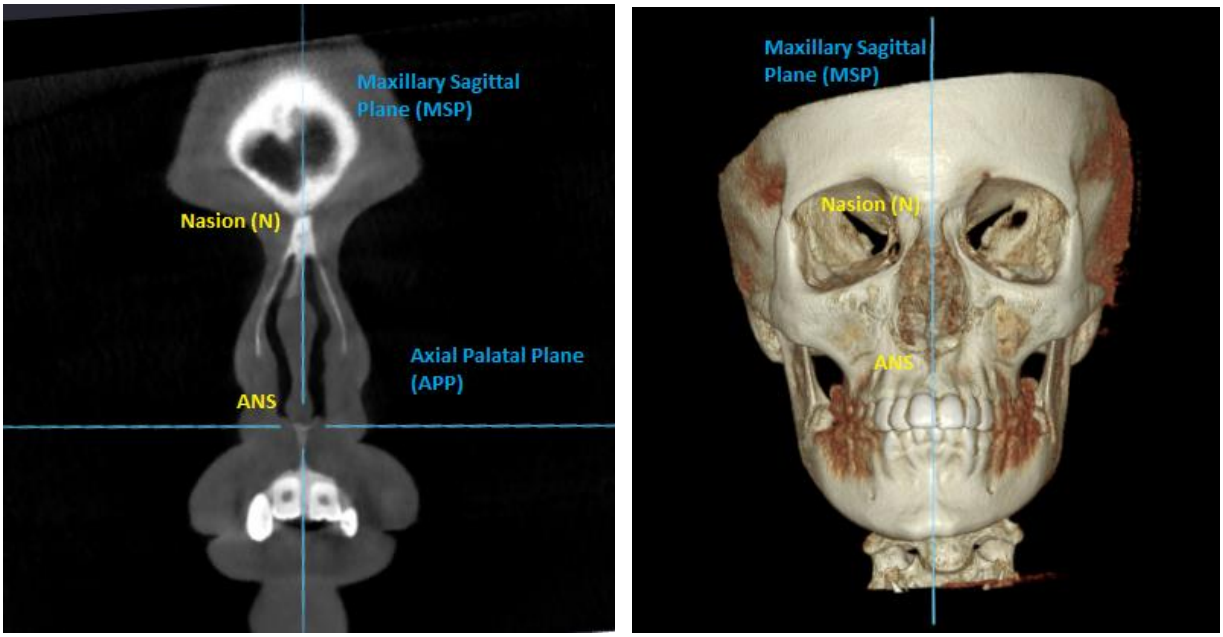

Fig 7. Coronal section (A) and 3D rendering (B) showing the maxillary sagittal plane (MSP) passing through ANS and Nasion (N).

The **axial palatal plane (APP)** is perpendicular to the maxillary sagittal plane (MSP) and passes through the anterior nasal spine (ANS) and the posterior nasal spine (PNS) as shown in Fig 8- 9.

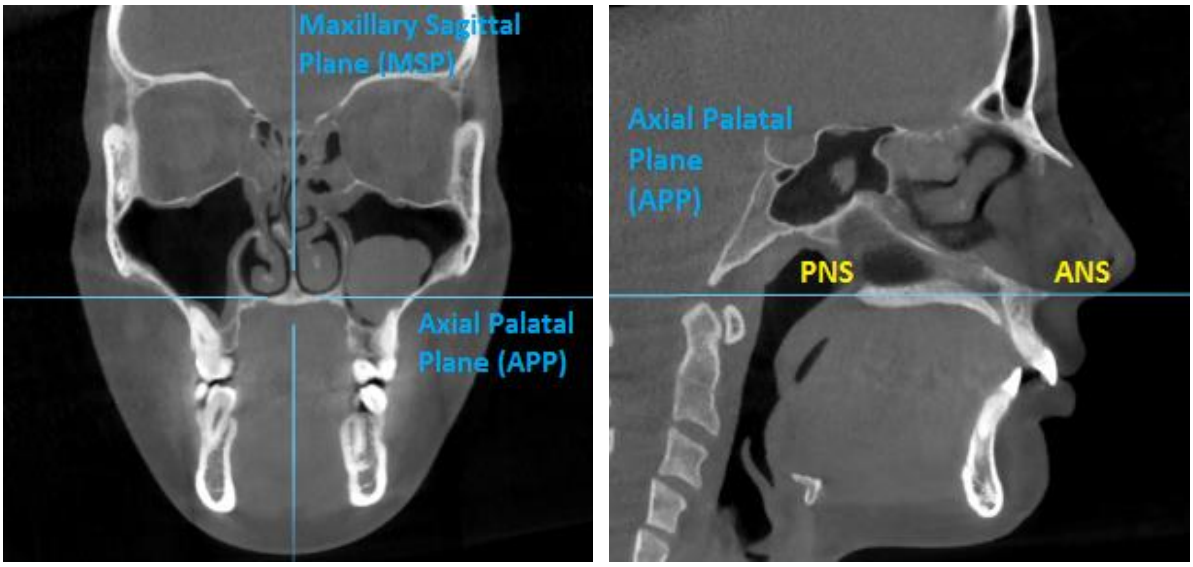

Fig 8. Coronal section (A) and sagittal section (B) showing the axial palatal plane (APP), perpendicular to the maxillary sagittal plane (MSP) and passing through ANS and PNS.

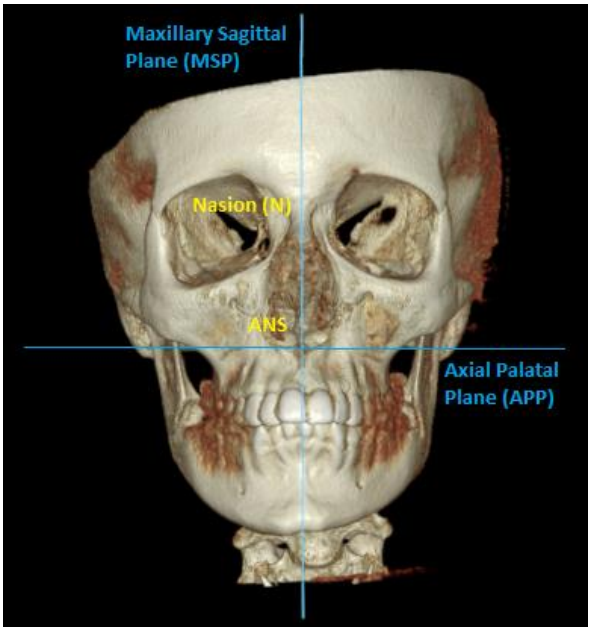

Fig 9. 3D rendering showing the axial palatal plane (APP) perpendicular to maxillary sagittal plane (MSP).

The **V-coronal plane (VCP)** is perpendicular to the maxillary sagittal plane (MSP) and to the axial palatal plane (APP) and passes through the most posterior point of the vomer (V point) as shown in Fig 10.

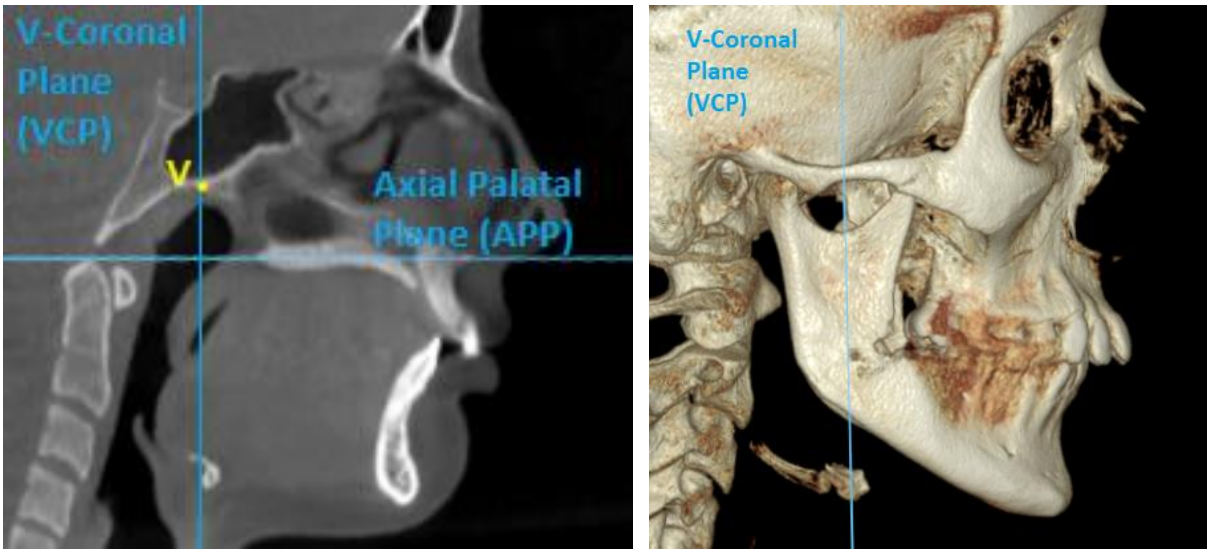

Fig 10. Sagittal section (A) and 3D rendering (B) showing the V-coronal plane (VCP).

These three main reference planes utilized to evaluate the skeletal movement of maxilla and circummaxillary structures in the transverse and sagittal directions are schematically summarized in Fig 11.

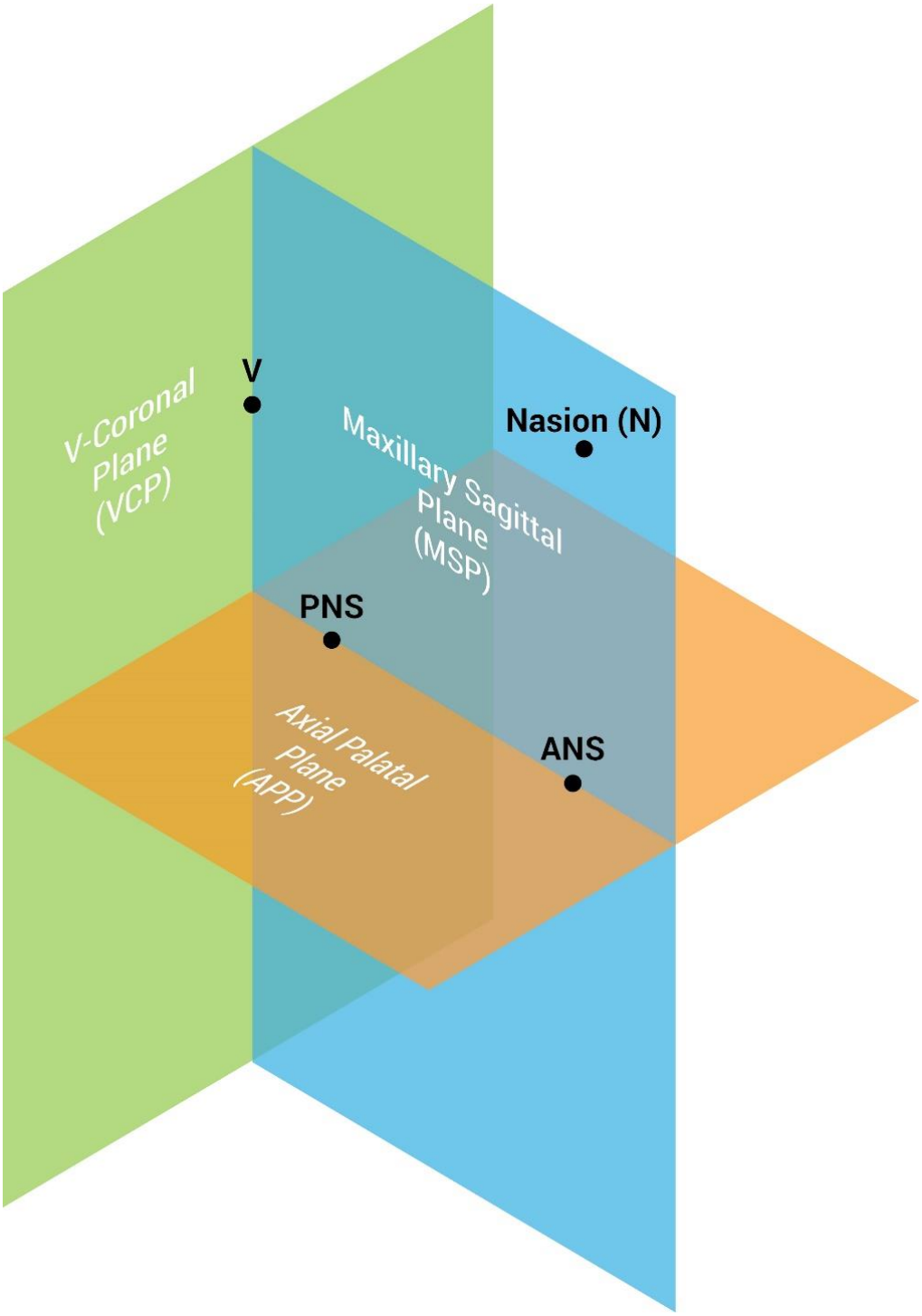

Fig 11. Schematic representation of the three main reference planes utilized in the study to evaluate the displacement of maxilla and circummaxillary structures: maxillary sagittal plane (MSP), axial palatal plane (APP), V-coronal plane (VCP).

The three main axial sections utilized to evaluate the maxillary and sphenoid bones: axial palatal section (APS), lower nasal section (LNS), upper nasal section (UNS)

In order to analyze the skeletal changes induced by the expanders in the maxillary bones and the pterygoid processes of the sphenoid bone, three sections were selected on the pre- and post-expansion CBCT of the patients. They were the axial palatal section (APS), the lower nasal section (LNS) and the upper nasal section (UNS).

The **axial palatal section (APS)** is a slice passing through the axial palatal plane as defined above in this section (Fig 8-9).

The **lower nasal section (LNS)** is a slice parallel to APS and found in the following manner. The distance from the V point to the axial palatal plane (APP) is measured as shown in Fig 12, and then the distance is divided by 3 segments.

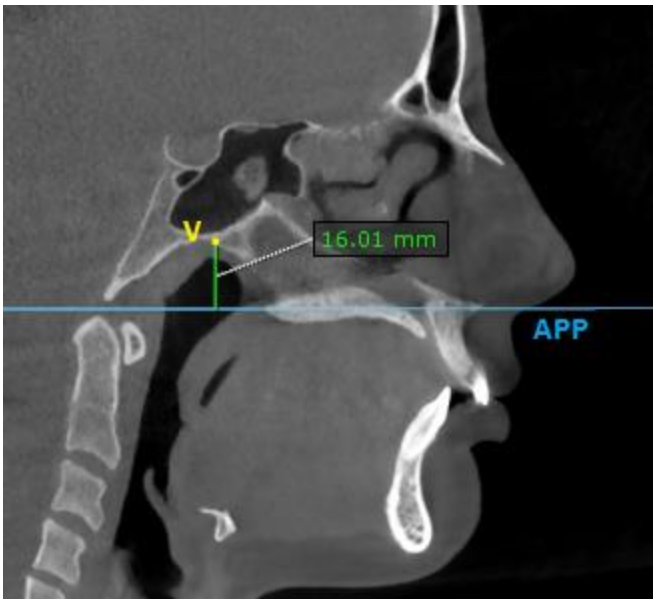

Fig 12. The distance between the most posterior point of vomer (V point) and the axial palatal plane (APP).

The lower nasal section (LNS) is parallel to the axial palatal plane (APP) and passes below the V point at 2/3 of the total distance between V and the axial palatal plane (APP) as shown in Fig 13.

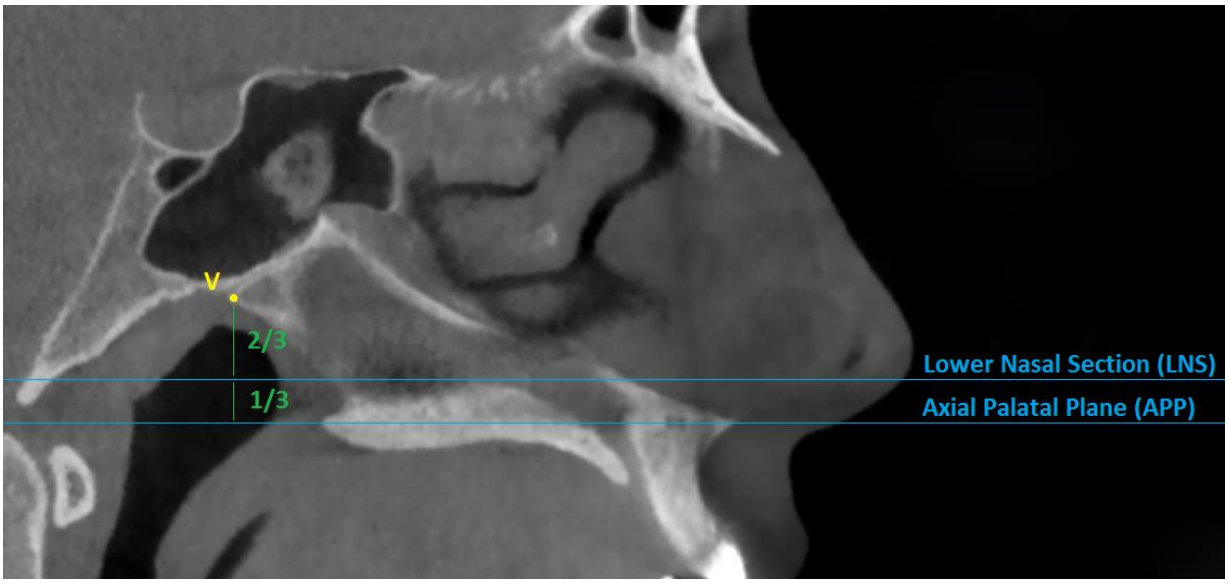

Fig 13. Lower Nasal Section (LNS)

The **upper nasal section (UNS)** is parallel to the axial palatal plane (APP) and passes through the V point (Fig 14).

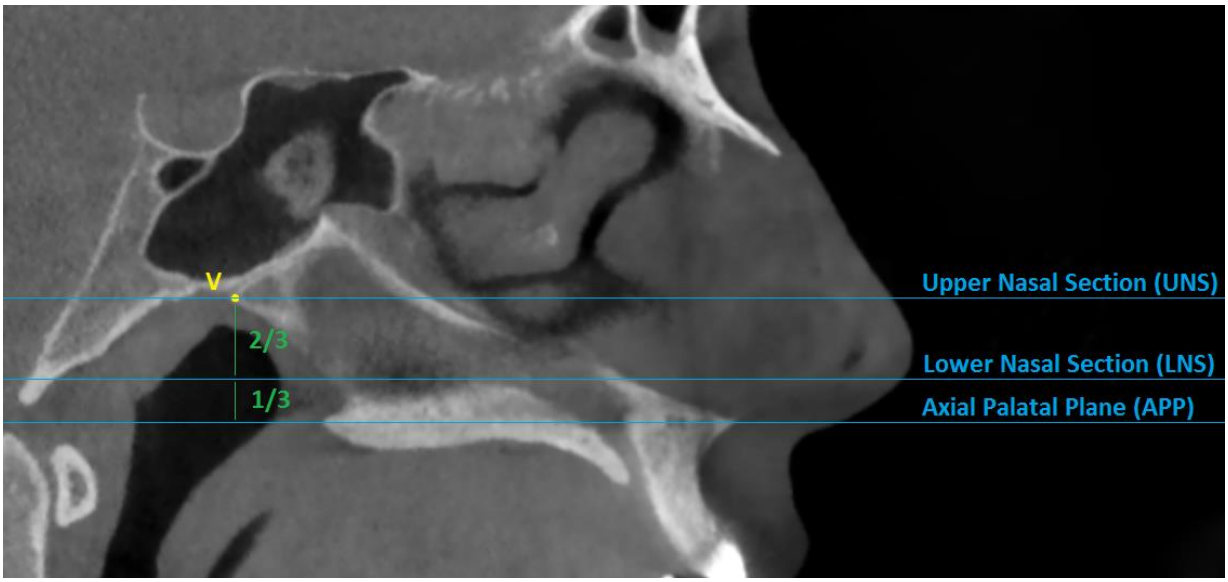

Fig 14. Upper Nasal Section (UNS) passing through the V point.

Fig 15 shows the three axial sections utilized to evaluate the skeletal changes in the maxilla and in the pterygoid processes of the sphenoid bone: axial palatal section (APS), lower nasal section (LNS) and upper nasal section (UNS).

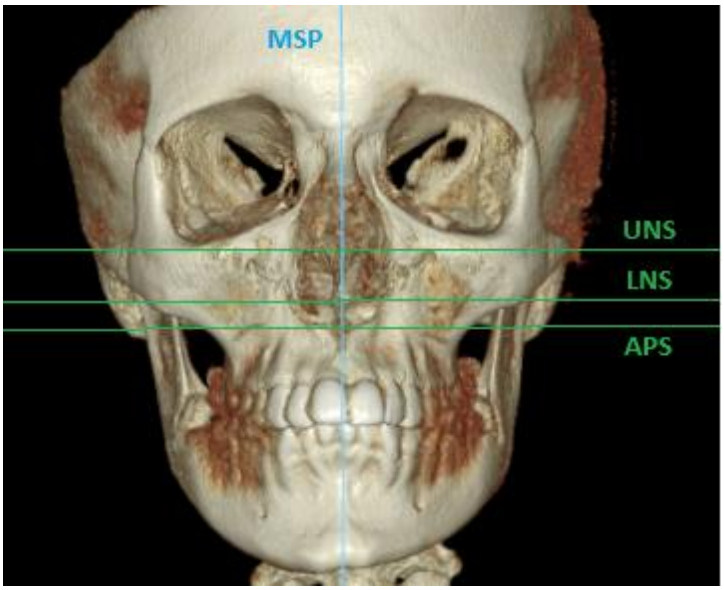

Fig 15. 3D rendering with the three axial sections (APS, LNS, UNS).

The three axial sections APS, LNS, UNS have been chosen because they cut through the pterygopalatine suture in three distinct areas as shown in Fig 16 and 17.

The axial palatal section (APS) cuts the pterygopalatine suture in an area where the “pyramidal process” of the palatine bone articulates with the “pterygoid notch” located between the lateral plate and the medial plate of the pterygoid process. The changes in this area due to the maxillary expansion will be described as “openings” between the lateral and medial pterygoid plates. The frequency of openings (i.e. the percentage of patients and the percentage of sutures with openings between these

plates) and the width of the openings will be described as indicators for loosening of the suture in MSE and Hyrax patients.

The lower nasal section (LNS) cuts through the pterygopalatine suture in an area where the posterior border of the perpendicular plate of the palatine bone articulates with the anterior surface of the pterygoid process of the sphenoid. In this area the pterygomaxillary fissure becomes extremely narrow and the tuberosity of the maxilla comes in close proximity with the pterygoid process, however the tuberosity of maxilla does not form a suture with the pterygoid process. The “lateral slide” of the most posterior point of the maxilla along the most anterior point of the pterygoid fossa will be described as an indicator for loosening of the pterygopalatine suture in MSE and Hyrax patients.

The upper nasal section (UNS) cuts through the pterygopalatine suture in an area where the perpendicular plate of the palatine bone forms the medial wall of the pterygopalatine fossa. The perpendicular plate of the palatine bone in its upper portion presents the “sphenopalatine notch” where nerves (posterior superior lateral nasal nerve and nasopalatine nerve) and vessels (sphenopalatine artery and vein) pass from the pterygopalatine fossa to the superior meatus of the nose. The upper portion of the perpendicular plate of the palatine bone presents also the “sphenoidal process” that articulates with the medial surface of pterygoid process of the sphenoid and the “orbital process” that articulates with the maxilla. During maxillary expansion, the perpendicular plate of the palatine bone can be pulled laterally by the maxilla. However, the “sphenoidal process” of the palatine bone cannot move laterally because it articulates with the medial surface of the pterygoid process of the sphenoid, and consequently it

could be forced to bend in medial direction. The morphological changes of the perpendicular plate during maxillary expansion in MSE and Hyrax patients will be assessed with angular measurements which are described later in this section.

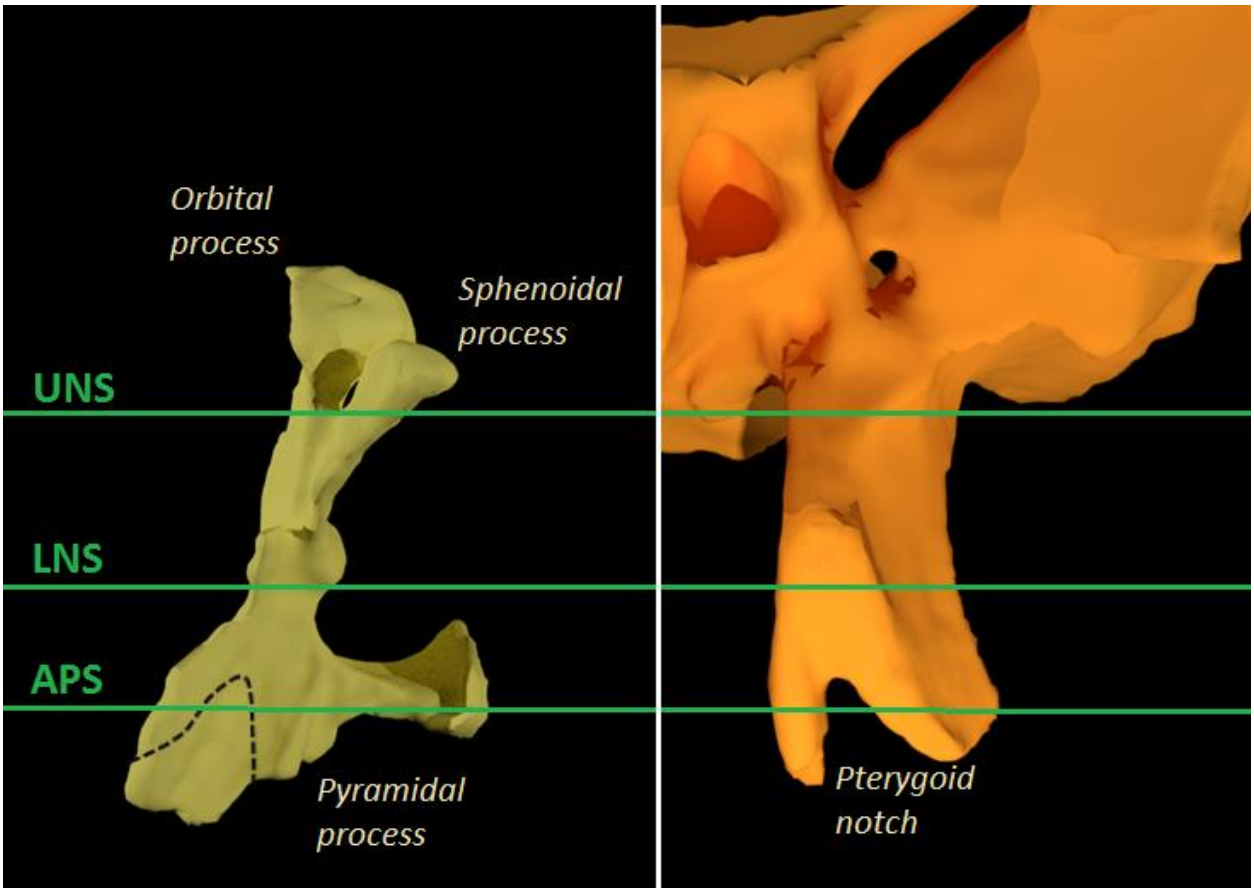

Fig 16. Axial palatal section (APS), lower nasal section (LNS) and upper nasal section (UNS) crossing the left palatine bone (posterior view in A) and the left pterygoid process of the sphenoid bone (anterior view in B).

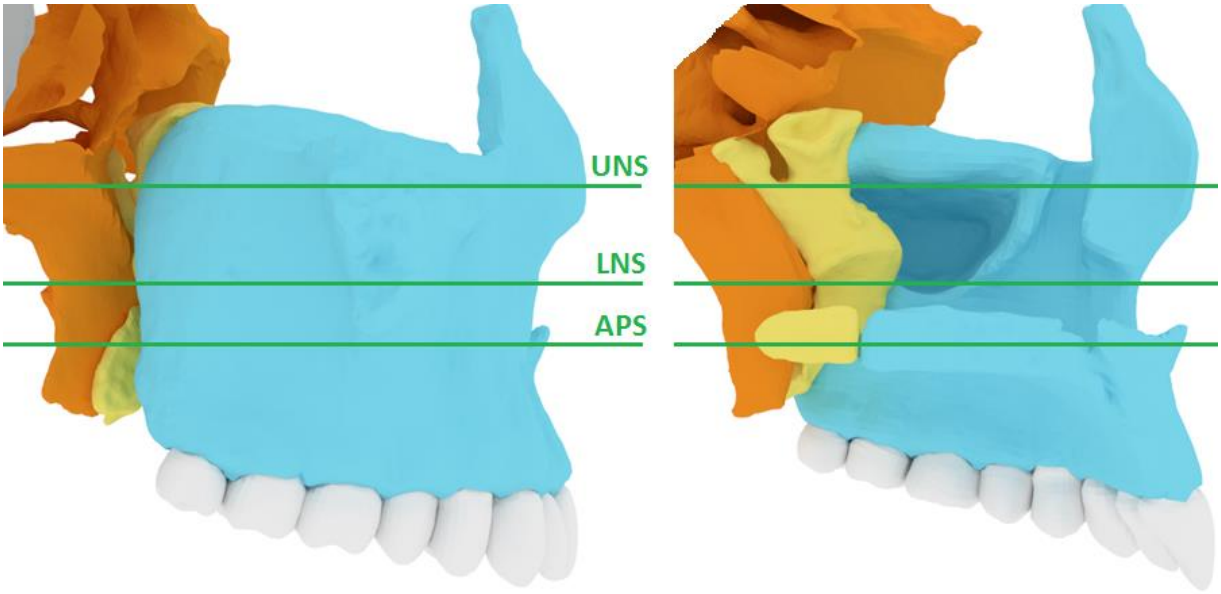

Fig 17. Illustration showing the axial palatal section (APS), lower nasal section (LNS) and upper nasal section (UNS) crossing the pterygomaxillary region. A: lateral view. B: medial view. Sphenoid bone in orange, palatine bone in yellow, maxillary bone in light blue.

The procedure to assess the displacement of maxillary bones and pterygoid processes is explained in Fig 18. The post-expansion CBCT is superimposed on the pre-expansion CBCT on the anterior cranial base (Fig 18 A). The maxillary sagittal plane (MSP), axial palatal plane (APP) and V-coronal plane (VCP) are identified in the pre-expansion CBCT. Then the axial palatal section (Fig 18 B), lower nasal section (Fig 18 C), and upper nasal section (Fig 18 D) are selected for the measurements. The slice through the anterior cranial base (Fig 18 E) was checked in every patient before taking the measurements in order to verify the accuracy of automated superimposition by the software.

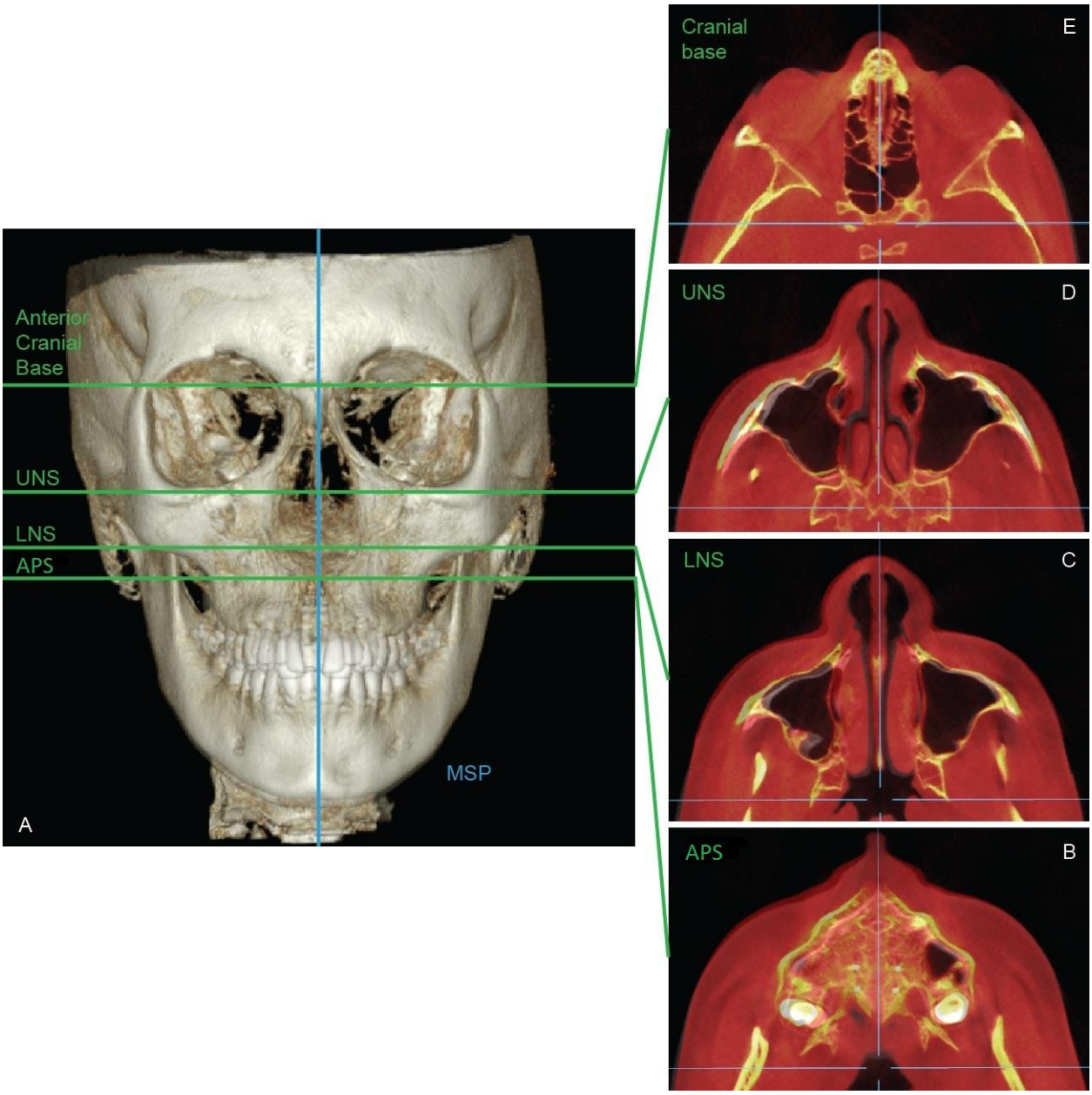

Fig 18. Illustration showing the procedure followed to assess the displacement of the maxilla and pterygoid processes of the sphenoid. A: 3D superimposition rendering of the skull. B: axial palatal section (APS). C: lower nasal section (LNS). D: upper nasal section (UNS). E: section through the anterior cranial base.

Measurements on the axial palatal section (APS)

The axial palatal section (APS) was used to measure the lateral movement of ANS and PNS, and the openings between the lateral and medial plates of the pterygoid process. The landmarks identified in APS are shown in Fig 19. These landmarks could be detected only in the post-expansion CBCT. In the pre-expansion CBCT, ANS and PNS for right and left halves are in contact, and no gaps between the lateral and medial plates of the pterygoid processes exist since the pterygoid notch is occupied by the pyramidal process of the palatine bone. A value equal to zero was assigned to these landmarks as distance measurement in the pre-expansion CBCT.

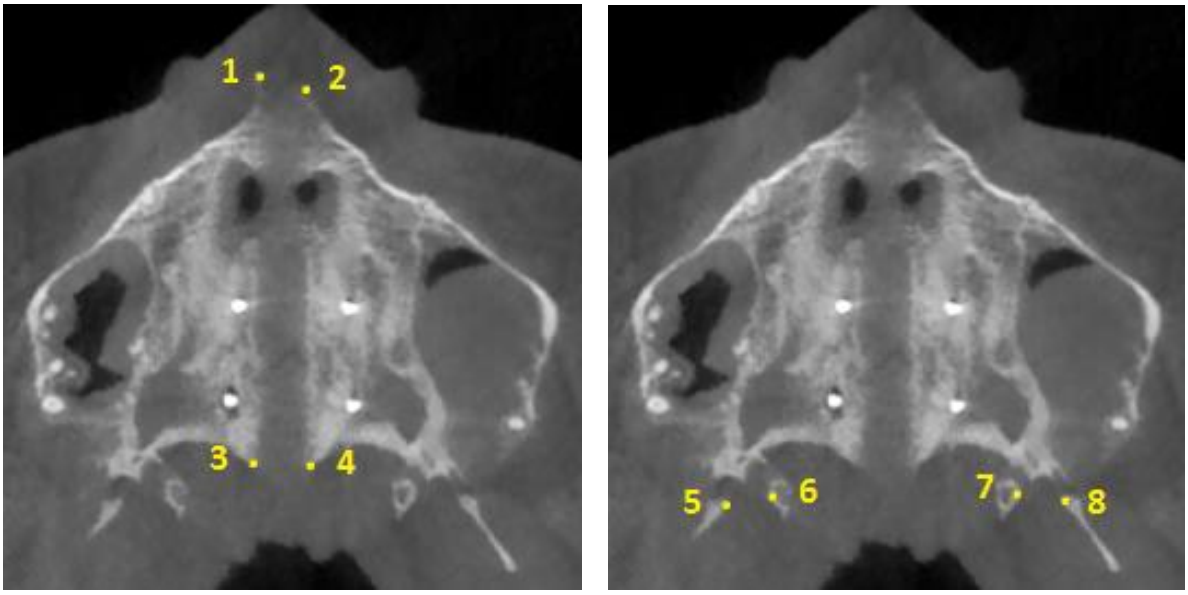

Fig 19. Landmarks identified in the axial palatal section (APS) for the post-expansion CBCT. A: Landmarks in the midpalatal suture. B: Landmarks in the pterygoid processes of the sphenoid bone. 1: Right anterior nasal spine (Rt ANS); 2: Left anterior nasal spine (Lt ANS); 3: Right posterior nasal spine (Rt PNS); 4: Left posterior nasal spine (Lt PNS); 5: Most medial point of the lateral plate of the right pterygoid process (Rt Lat Pter); 6: Most lateral point of the medial plate of the right pterygoid process (Rt Med Pter); 7: Most lateral point of the medial plate of the left pterygoid process (Lt Med Pter); 8: Most medial point of the lateral plate of the left pterygoid process (Lt Lat Pter).

The parameters evaluated in the axial palatal section (APS) are listed in Table I.

Table 1. Parameters evaluated in the axial palatal section (APS)

1	Distance of Rt ANS from maxillary sagittal plane
2	Distance of Lt ANS from maxillary sagittal plane
3	Distance of Rt PNS from maxillary sagittal plane
4	Distance of Lt PNS from maxillary sagittal plane
5	Lateral displacement of Rt ANS + Lt ANS
6	Lateral displacement of Rt PNS + Lt PNS
7	Width of opening in Rt pterygoid process
8	Width of opening in Lt pterygoid process

The post-expansion CBCT of the patient was superimposed on the pre-expansion CBCT on the stable structures of anterior cranial base; MSP, APP and VCP were identified in the pre-expansion CBCT; and then the axial palatal section (APS) was selected (Fig 20).

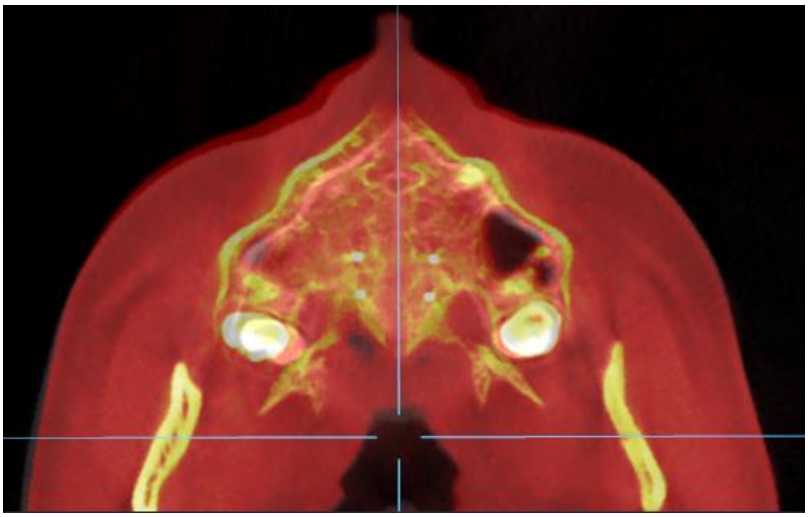

Fig 20. Axial palatal section (APS): example of the superimposed image of a MSE patient. The blue lines are MSP and VCP determined from the pre-expansion CBCT.

During maxillary expansion the midpalatal suture splits, and the anterior nasal spine (ANS) and the posterior nasal spine (PNS) are split in two halves producing Rt ANS,

Lt ANS, Rt PNS and Lt PNS which can be identified in the post-expansion CBCT (Fig 19). The distance from the maxillary sagittal plane (MSP) to Rt ANS, Lt ANS, Rt PNS and Lt PNS were measured as shown in Fig 21 and 22.

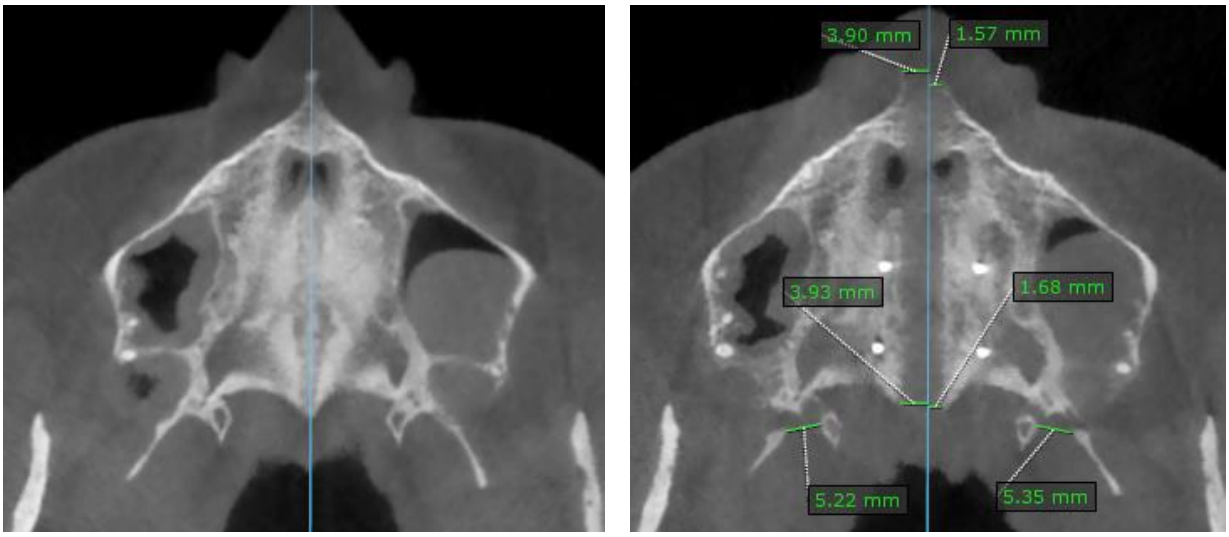

Fig 21. Transverse measurements on the axial palatal section (APS) in MSE patient. A: pre-expansion. B: post-expansion. Blue line: maxillary sagittal plane (MSP). MSP passes through ANS and PNS in the pre-expansion CBCT and becomes a reference line for measuring the lateral movements of skeletal landmarks in the post-expansion CBCT.

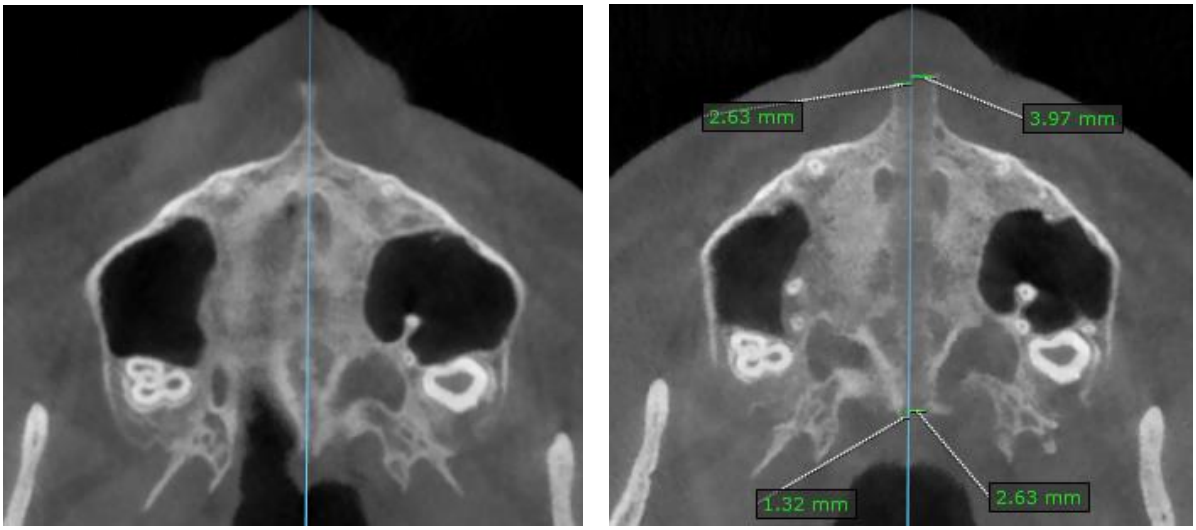

Fig 22. Transverse measurements on the axial palatal section (APS) section in Hyrax patient. A: pre-expansion. B: post-expansion. Blue line: maxillary sagittal plane (MSP).

The distance from the maxillary sagittal plane (MSP) to Rt ANS, Lt ANS, Rt PNS and Lt PNS in the pre-expansion CBCT was given a value of zero. In the post-expansion CBCT, the distance for each landmark from the maxillary sagittal plane was averaged, and then the Wilcoxon sign rank test was used to compare the pre-and post-expansion distances for statistical significance.

The symmetry of the split was also evaluated. If the ANS moved more than 0.5 mm (which means 0.6 mm or more) on one side than the other, the expansion was judged “asymmetrical”. The frequencies of symmetrical splits, asymmetrical splits with greater movement on the right side, and asymmetrical split with greater movement on the left side were calculated. ANS was chosen as a parameter for judging asymmetrical split of the suture because ANS reflects the changes in the anterior part of the midface and subsequently may have a significant impact on the soft tissues changes induced by the expanders. For each patient, the distance difference between greater and lesser sides was calculated; then these values were averaged in order to evaluate the overall asymmetrical expansion comparing the contralateral halves. The opening between the lateral and medial pterygoid plates is due to the fact that the pyramidal process of the palatine bone is pulled away from the pterygoid plates during maxillary expansion. The size of the opening is measured as the distance from the most medial point of the lateral pterygoid plate to the most lateral point of the medial pterygoid plate (Fig 21 B).

When the opening was not visible in the axial palatal section (APS), the other axial slices between the axial palatal section (APS) and the lower nasal section (LNS) where checked because the openings sometimes appeared in the slices slightly above APS

(Fig 23-24). If these openings were observed in several axial sections, the section with the largest opening was chosen for the measurement.

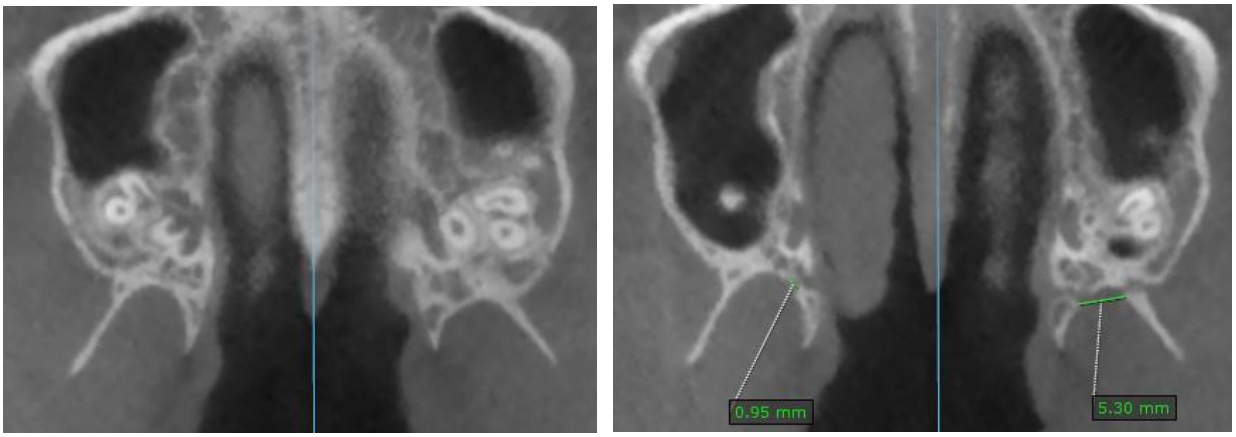

Fig 23. CBCT of a MSE patient. A: pre-expansion. B: post-expansion. Openings between the lateral and medial pterygoid plates detected on an axial slice situated between the axial palatal section (APS) and the lower nasal section (LNS) in the post-expansion CBCT.

Fig 24. CBCT of a Hyrax patient. A: pre-expansion. B: post-expansion. Openings between the lateral and medial pterygoid plates detected on an axial slice situated between the axial palatal section (APS) and the lower nasal section (LNS) in the post-expansion CBCT.

In the case of a partial disengagement of the pyramidal process from the pterygoid notch, the width of the opening was measured from the pyramidal process to the

pterygoid plate adjacent to the opening as shown in Fig 23 B and 24 B, right pterygopalatine suture.

The frequency of the openings (i.e. the percentage of patients and sutures with openings) and the average width of the opening were calculated, and they were used as parameters for loosening of the pterygopalatine suture. In the pre-expansion CBCT, the frequency and width of the openings were given a value of zero. The Fisher's exact test was used to evaluate the statistical significance of the changes for the frequency of openings within and between groups. The non-parametric Wilcoxon sign rank test was used to compare the average width of the openings before and after expansion for statistical significance.

Measurements in the lower nasal section (LNS)

The lower nasal section was used to evaluate the displacement of the maxilla and of the pterygoid processes of the sphenoid bone in the transverse and sagittal directions. The landmarks analyzed were the most anterior point of the right and left maxilla (Rt Lo Ant Mx and Lt Lo Ant Mx), the most posterior point of the right and left maxilla (Rt Lo Po Mx and Lt Lo Po Mx), the most anterior point of the right and left pterygoid fossa (Rt Lo Pter and Lt Lo Pter) as shown in Fig 25.

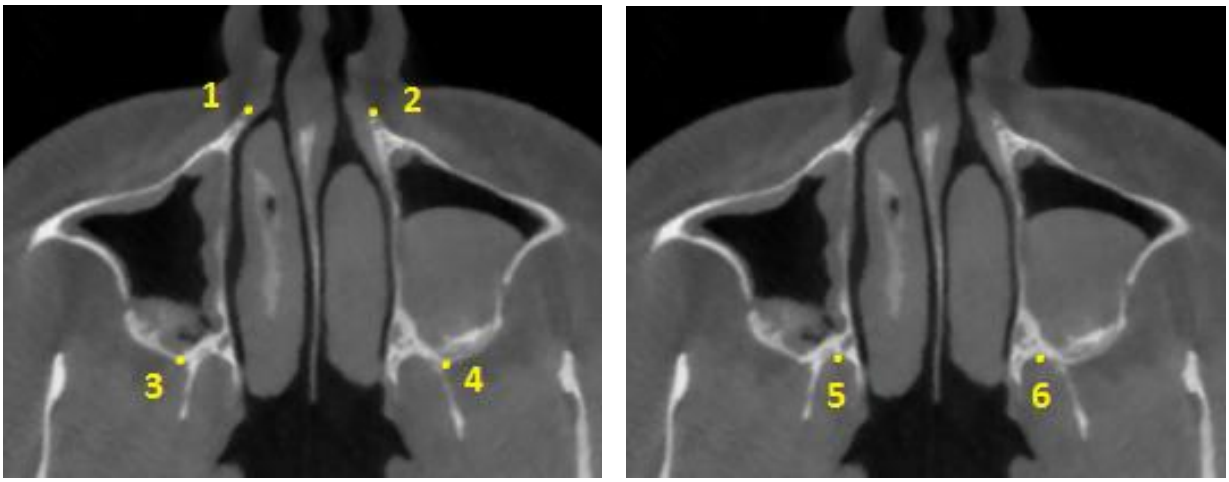

Fig 25. Landmarks identified in the lower nasal section (LNS). A: Landmarks in the maxillary bones. B: Landmarks in the pterygoid process of the sphenoid bone. 1: Most anterior point of right maxilla (Rt Lo Ant Mx); 2: Most anterior point of left maxilla (Lt Lo Ant Mx); 3: Most posterior point of right maxilla (Rt Lo Post Mx); 4: Most posterior point of left posterior maxilla (Lt Lo Post Mx); 5: Most anterior point of right pterygoid fossa (Rt Lo Pter); 6: Most anterior point of left pterygoid fossa (Lt Lo Pter).

The parameters measured in the lower nasal section (LNS) are listed in table 2.

Table 2. Parameters evaluated in the lower nasal section (LNS)

Transverse distances	
1	Distance of Rt Lo Ant Mx from maxillary sagittal plane
2	Distance of Lt Lo Ant Mx from maxillary sagittal plane
3	Distance of Rt Lo Post Mx from maxillary sagittal plane
4	Distance of Lt Lo post Mx from maxillary sagittal plane
5	Distance of Rt Lo Pter from maxillary sagittal plane
6	Distance of Lt Lo Pter from maxillary sagittal plane
7	Lateral slide in Rt pterygomaxillary fissure
8	Lateral slide in Lt pterygomaxillary fissure
Sagittal distance of lower posterior maxilla	
9	Distance of Rt Lo Po Mx from V-coronal plane
10	Distance of Lt Lo Po Mx from V-coronal plane
Sagittal distance of the pterygoid process	
11	Distance of Rt Lo Pter from V-coronal plane
12	Distance of Lt Lo Pter from V-coronal plane

The post-expansion CBCT of the patient was superimposed on the pre-expansion CBCT, the MSP, APP and VCP were identified in the pre-expansion CBCT and the slice through the lower nasal section was selected (Fig 26).

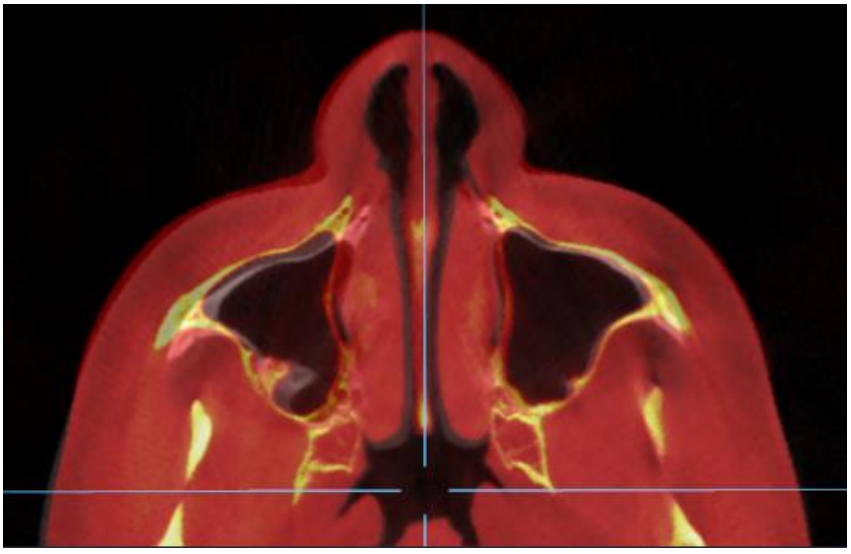

Fig 26. Lower nasal section (LNS): example of superimposed image of a MSE patient. The blue lines are MSP and VCP determined from the pre-expansion CBCT.

Both transverse measurements and sagittal measurements were performed in the lower nasal section (LNS).

Transverse measurements in the lower nasal section (LNS)

The distance from MSP to the landmarks were measured in the pre- and post-expansion CBCT as shown in Fig 27-28.

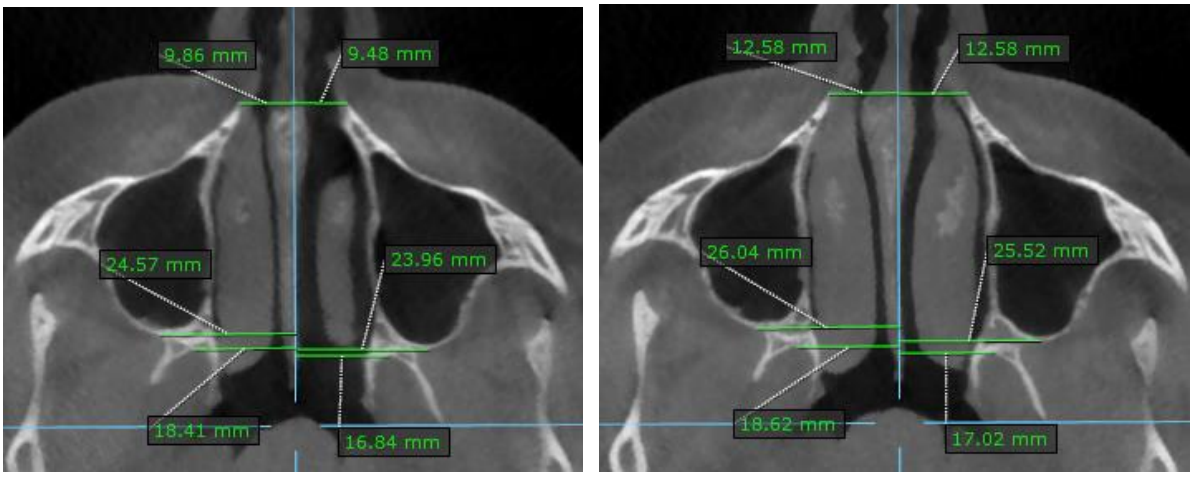

Fig 27. Transverse measurements on lower nasal section (LNS) in a MSE patient. A: pre-expansion. B: post-expansion. Blue lines: maxillary sagittal plane (MSP) and V-coronal plane (VCP).

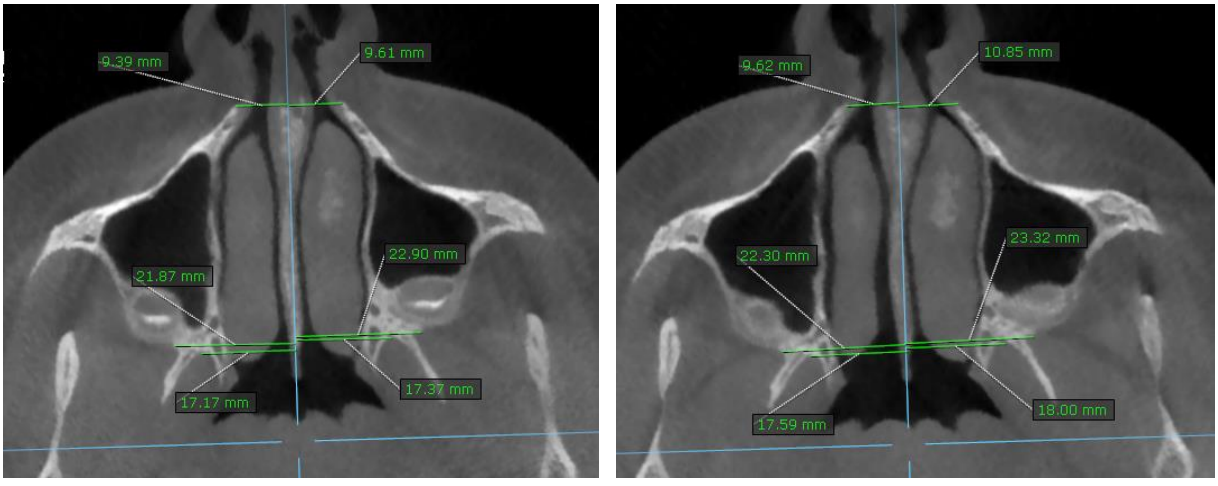

Fig 28. Transverse measurements on lower nasal section (LNS) in a Hyrax patient. A: pre-expansion. B: post-expansion. Blue lines: maxillary sagittal plane (MSP) and V-coronal plane (VCP).

The distance measurements from the pre-treatment CBCT was subtracted from the corresponding measurements from the post-treatment CBCT, and these differences represented the treatment changes. The treatment change is equivalent to the lateral movement of these landmarks during the maxillary expansion. The distance measurements for each landmark were averaged, and a paired T-test was used for statistical significance.

The lateral slide in the pterygomaxillary fissure was calculated by subtracting the lateral movement (treatment change) of the most anterior point of the pterygoid fossa (Lo Pter) from the lateral movement (treatment change) of the most posterior point of the maxilla (Lo Post Mx). This was done for each side separately. The lateral slide in the pterygomaxillary fissure represents the difference in the lateral movement between the posterior maxilla and the pterygoid process, hence it is an indicator for the loosening of the pterygopalatine suture. The higher slide indicates more loosening of the pterygopalatine suture. The lateral slide measurements were averaged, and a paired T-test was used for statistical significance.

Sagittal measurements on the lower nasal section (LNS)

The distance from the V-coronal plane (VCP) to the most posterior point of the right and left maxilla (Rt Lo Po Mx and Lt Lo Po Mx) was measured on the CBCTs before and after the expansion as shown in Fig 29-30.

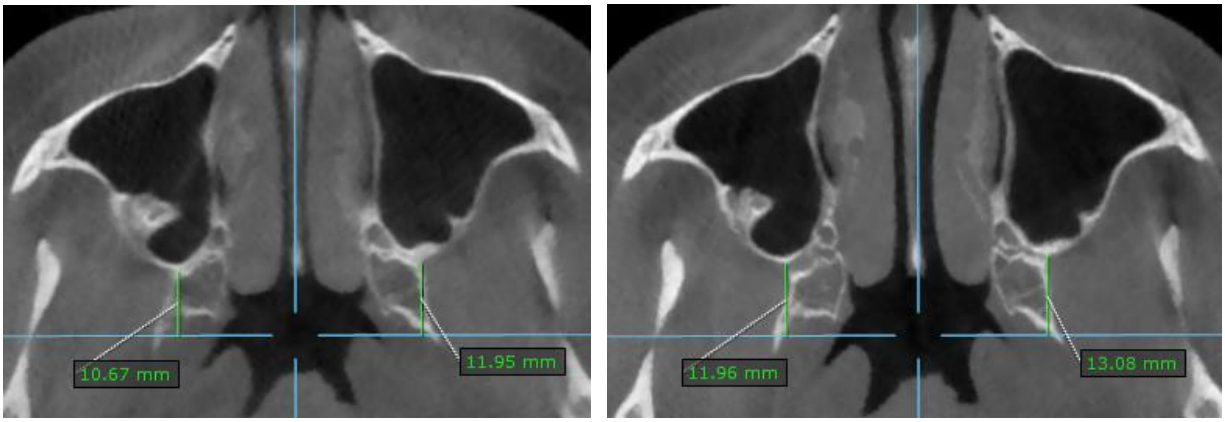

Fig 29. Sagittal measurements on the lower nasal section (LNS) in a MSE patient. A: pre-expansion. B: post-expansion. In blue the maxillary sagittal plane (MSP) and the V-coronal plane (VCP).

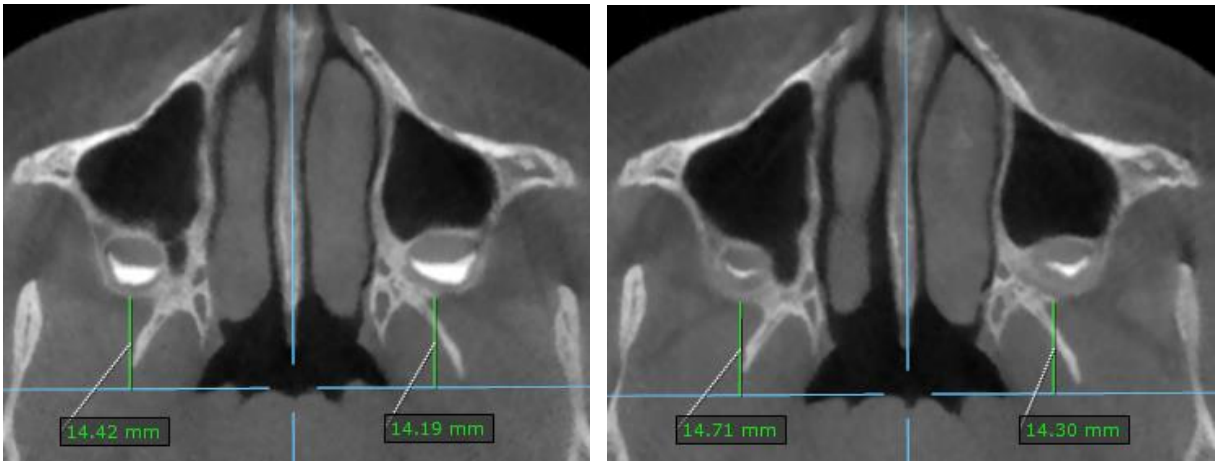

Fig 30. Sagittal measurements on the lower nasal section (LNS) in a Hyrax patient. A: pre-expansion. B: post-expansion. In blue the maxillary sagittal plane (MSP) and the V-coronal plane (VCP).

The distance before expansion was subtracted from the distance after expansion for calculating the treatment change. The treatment change is equivalent to the forward movement of the maxilla. The distances were averaged, and a paired T-test was used for statistical significance.

The distance from the V-coronal plane (VCP) to the most anterior point of the pterygoid fossa (Lo Pter) was measured in the pre- and post-expansion CBCT (Fig. 31).

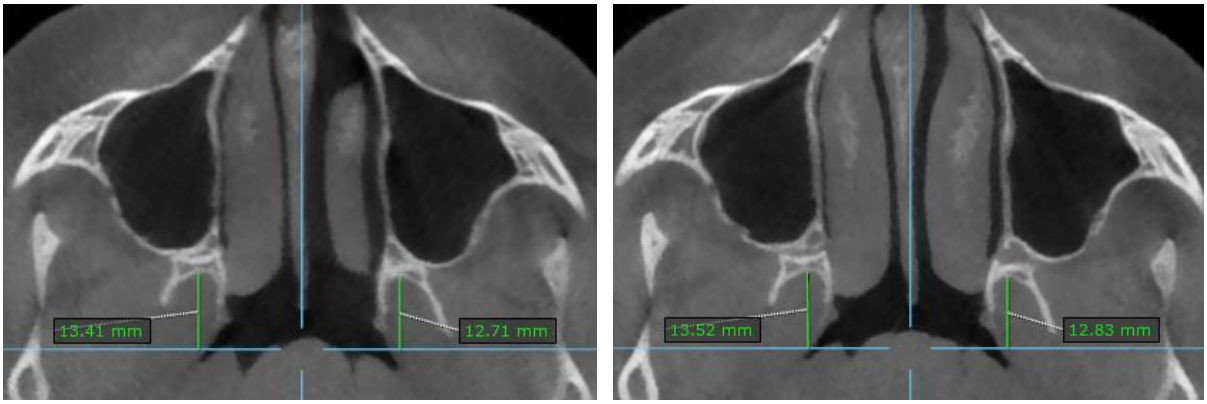

Fig 31. Distance measurement from the V-coronal plane (VCP) to the most anterior point of the pterygoid fossa In a MSE patient. A: pre-expansion. B: post-expansion.

The distance before expansion was subtracted from the distance after expansion to assess the treatment change. The treatment change is equivalent to the forward movement of the pterygoid process. The distance measurements were averaged, and a paired T-test was used for statistical significance.

Measurements in the upper nasal section

The upper nasal section was also used to evaluate the changes in the maxilla and the pterygoid processes of the sphenoid bone in the transverse and sagittal directions. The landmarks analyzed were the most anterior point of the right and left maxilla (Rt Up Ant Mx and Lt Up Ant Mx), the posterior-medial point of the right and left maxilla (Rt Post-med Mx and Lt Post-med Mx), the most posterior point of the right and left maxilla (Rt Up Po Mx and Lt Up Po Mx), the anterior-medial point of the right and left pterygoid process and the anterior-lateral point of the right and left pterygoid process as shown in Fig 32.

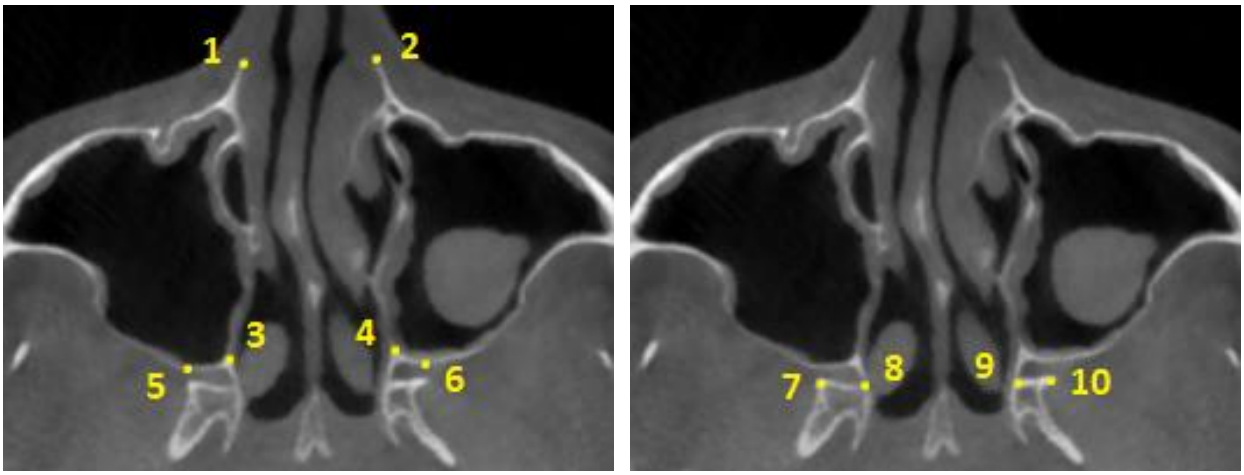

Fig 32. Landmarks identified in the upper nasal section (UNS). A: Landmarks in the maxillary bones. B: Landmarks in the pterygoid process of the sphenoid bone. 1: Most anterior point of the right maxilla (Rt Up Ant Mx); 2: Most anterior point of the left maxilla (Lt Up Ant Mx); 3: Posterior-medial point of the right maxilla (Rt Post-med Mx); 4: Posterior-medial point of the left maxilla (Lt Post-med Mx); 5: Most posterior point of the right maxilla (Rt Up Po Mx); 6: Most posterior point of the left maxilla (Lt Up Po Mx); 7: Anterior-lateral point of the right pterygoid process (Rt Up Lat Pter); 8: Anterior-medial point of the right pterygoid process (Rt Up Pter); 9: Anterior-medial point of the left pterygoid process (Lt Up Pter); 10: Anterior-lateral point of the left pterygoid process (Lt Up Lat Pter).

The parameters evaluated in the upper nasal section (UNS) are summarized in table 3.

Table 3. Parameters evaluated in the upper nasal section (UNS)

Transverse distances	
1	Distance of Rt Up Ant Mx from maxillary sagittal plane
2	Distance of Lt Up Ant Mx from maxillary sagittal plane
3	Distance of Rt Post-med Mx from maxillary sagittal plane
4	Distance of Lt Post-med Mx from maxillary sagittal plane
5	Distance of Rt Up Pter from maxillary sagittal plane
6	Distance of Lt Up Pter from maxillary sagittal plane
Sagittal distance of upper posterior maxilla	
7	Distance of Rt Up Po Mx from V-coronal plane
8	Distance of Lt Up Po Mx from V-coronal plane
Angular measurements	
9	Angle of Rt palatine bone
10	Angle of Lt palatine bone

The post-expansion CBCT of the patient was superimposed on the pre-expansion CBCT, the MSP, APP and VCP were traced in the pre-expansion CBCT, and the upper nasal section was selected (Fig 33).

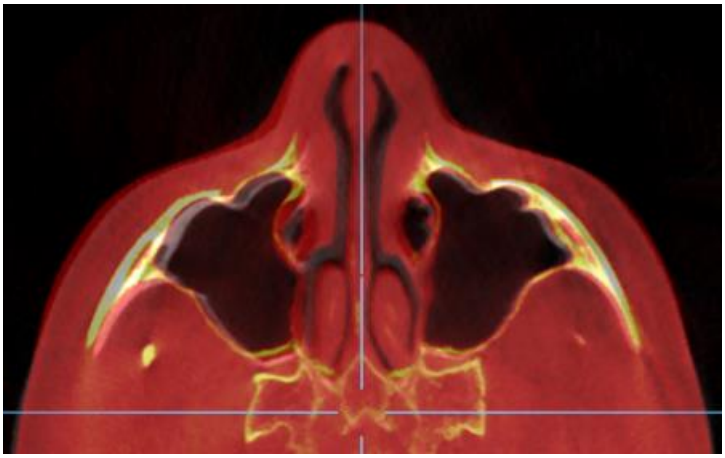

Fig 33. Upper nasal section (UNS): example of superimposed image of a MSE patient. The blue lines are MSP and VCP determined from the pre-expansion CBCT.

Transverse, sagittal and angular measurements were performed in the upper nasal section (UNS).

Transverse measurements in the upper nasal section (UNS)

The distance from the maxillary sagittal plane to the landmarks were measured in the pre- and post-expansion CBCTs as shown in Fig 34-35.

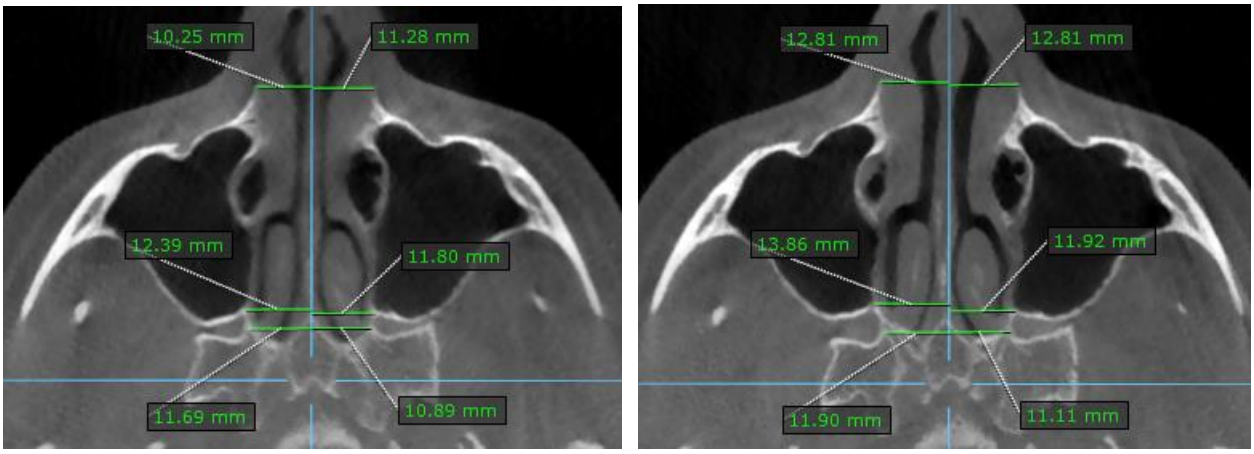

Fig 34. Transverse measurements on the upper nasal section (UNS) in a MSE patient. A: pre-expansion. B: post-expansion.

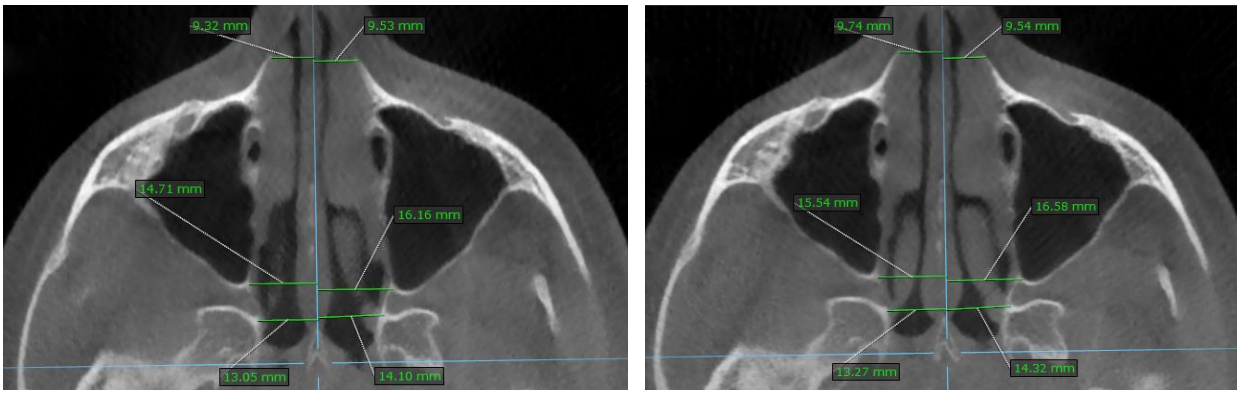

Fig 35. Transverse measurements on the upper nasal section (UNS) in a Hyrax patient. A: pre-expansion. B: post-expansion.

The distances from the maxillary sagittal plane (MSP) to these landmarks were measured in the pre- and post-expansion CBCTs. The distance measurements before

treatment were subtracted from those after treatment to assess the treatment changes. The treatment change is equivalent to the lateral movement of these landmarks. The distance measurements were averaged, and a paired T-test was used for statistical significance.

Angular changes in the perpendicular plate of the palatine bone

In the upper part of the pterygopalatine suture the sphenoidal process of the perpendicular plate of the palatine bone articulates with the anterior-medial surface of the pterygoid process of the sphenoid bone. During maxillary expansion the perpendicular plate of the palatine bone is pulled laterally by the maxilla. However the sphenoidal process of the perpendicular plate of the palatine bone cannot move laterally because it articulates with the anterior-medial surface of the pterygoid process of the sphenoid, and subsequently it is forced to bend in a medial direction. The bending of the perpendicular plate of palatine bone was measured by an angle formed by the posterior-medial point of the maxilla, the anterior-medial point of the pterygoid process and the anterior-lateral point of the pterygoid process as shown in Fig 36-37.

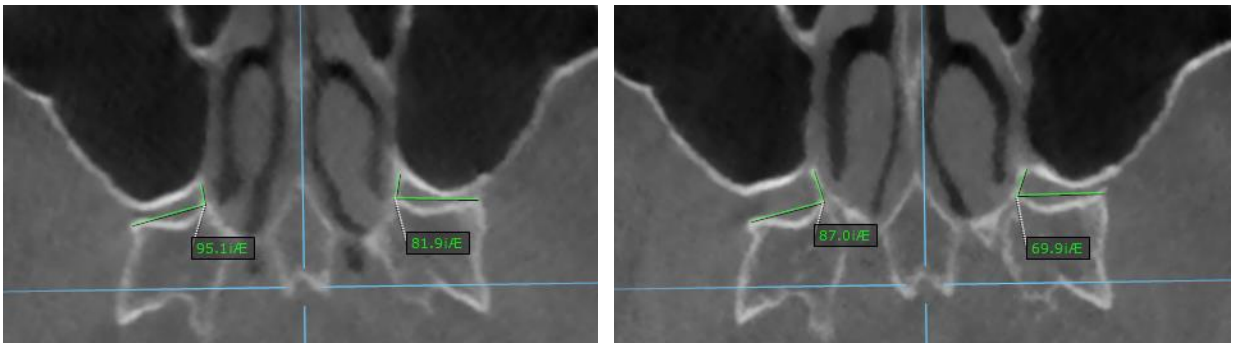

Fig 36. Angle that represents the inclination of the perpendicular plate of palatine bone in the upper nasal section (UNS) of a MSE patient. A: pre-expansion. B: post-expansion.

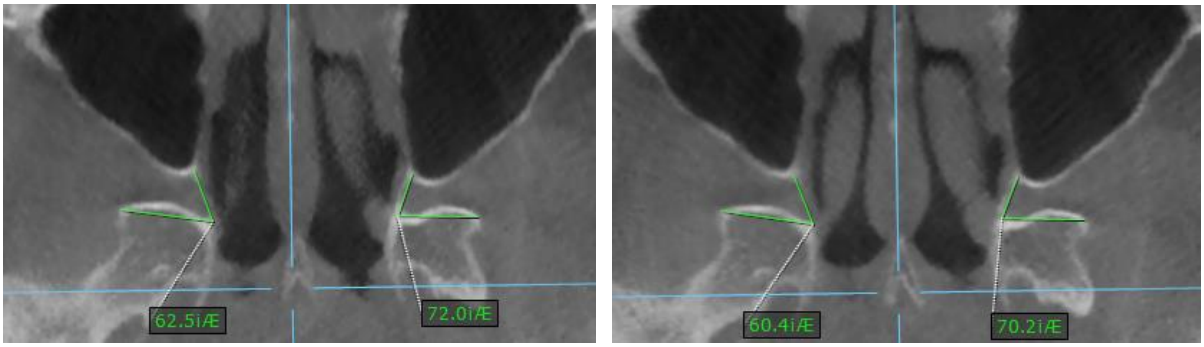

Fig 37. Angle that represents the inclination of the perpendicular plate of palatine bone in the upper nasal section (UNS) of a Hyrax patient. A: pre-expansion. B: post-expansion.

The value found in the pre-expansion CBCT was subtracted from the value found in the post-expansion CBCT to assess the treatment change that is equivalent to the amount of bone bending. The values were averaged, and a paired T-test was used for statistical significance.

Sagittal measurements on the upper nasal section (UNS): posterior maxilla

The distances from the V-coronal plane (VCP) to the most posterior point of the right and left maxilla (Rt Up Po Mx and Lt Up Po Mx) were measured on the CBCT before and after the expansion (Fig 38-39).

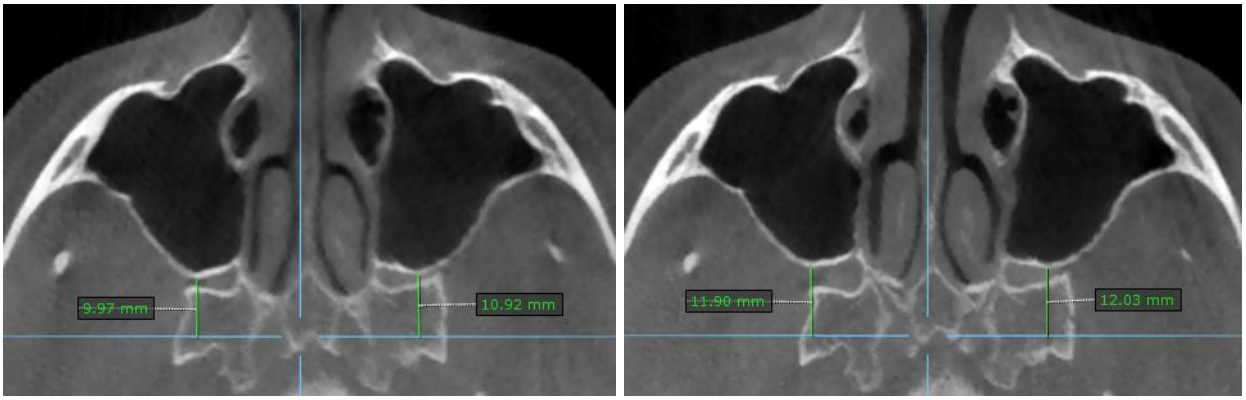

Fig 38. Sagittal measurements on the upper nasal section (UNS) in a MSE patient. A: pre-expansion. B: post-expansion.

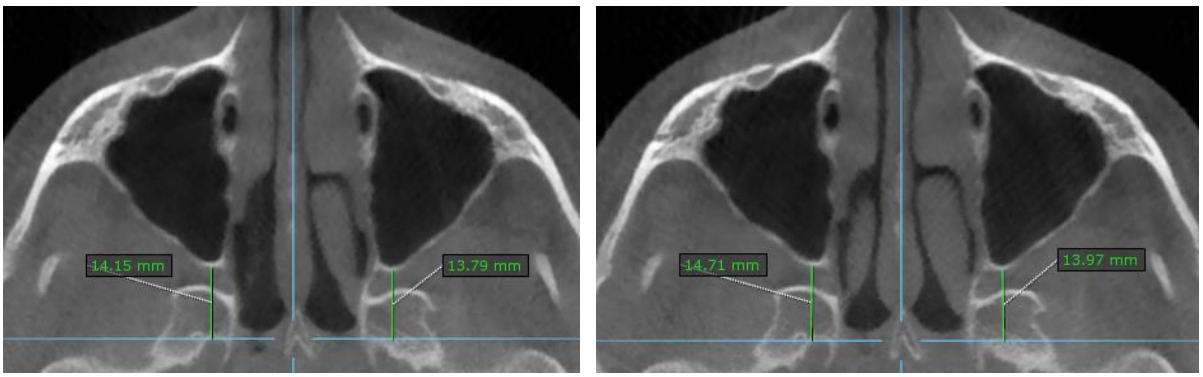

Fig 39. Sagittal measurements on the upper nasal section (UNS) in a Hyrax patient. A: pre-expansion. B: post-expansion.

The distance measurements before the expansion were subtracted from the measurements after the expansion to assess the treatment change which is equivalent to the forward movement of maxilla in the upper nasal section (UNS). The distance measurements were averaged, and a paired T-test was used for statistical significance.

Measurements on the coronal zygomatic section (CZS)

In order to analyze the skeletal changes of the frontal bone, zygomatic bone and maxilla in the coronal plane, a slice was selected on the CBCT.

The **coronal zygomatic section (CZS)** passes through the uppermost point of the right and left frontozygomatic suture, through the lowest point of the right and left zygomaticomaxillary suture, and through Crista galli of the ethmoid bone (Fig 40).

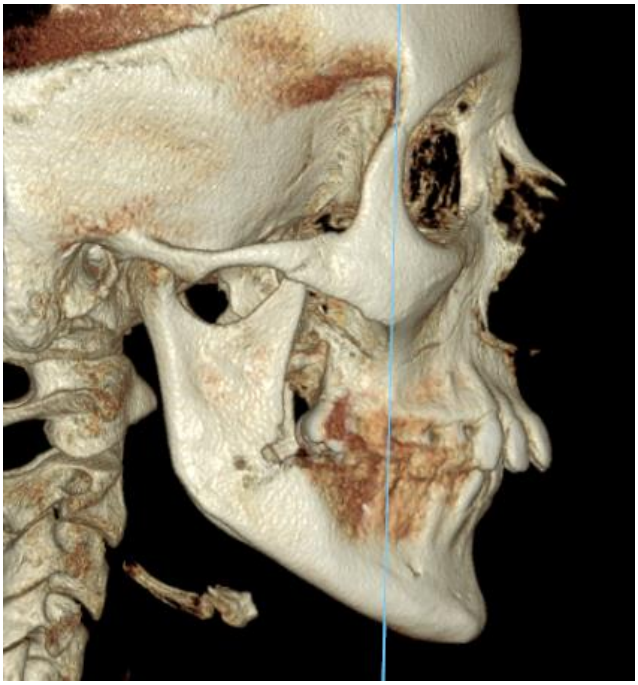

Fig 40. 3D rendering showing the coronal zygomatic section (CZS) traced with a blue line

The post-expansion CBCT was superimposed on the pre-expansion CBCT, the coronal zygomatic section (CZS) was selected (Fig. 41), and then linear and angular measurements were taken from the pre- and post-expansion CBCTs.

Fig 41. Coronal zygomatic section (CZS): example of the superimposed image of a MSE patient.

Parameters evaluated in the coronal zygomatic section (CZS) are listed in table 4.

Table 4. Parameters evaluated in the coronal zygomatic section (CZS)

Linear distances	
1	Upper inter-zygomatic distance
2	Lower inter-zygomatic distance
3	Inter-molar distance
Angular measurements	
4	Right frontozygomatic angle (Rt FZA)
5	Left frontozygomatic angle (Lt FZA)
6	Right zygomaticomaxillary angle (Rt ZMA)
7	Left zygomaticomaxillary angle (Lt ZMA)
8	Right maxillary inclination (Rt Mx incl)
9	Left maxillary inclination (Lt Mx Incl)
10	Right molar basal bone angle (Rt MBBA)
11	Left molar basal bone angle (Lt MBBA)

Linear distances

Linear distances include the upper inter-zygomatic distance, the lower inter-zygomatic distance and the inter-molar distance.

The upper inter-zygomatic distance extends from the most external point of the right frontozygomatic suture to the most external point of the left frontozygomatic suture.

The lower inter-zygomatic distance extends from the most external point of the right zygomaticomaxillary suture to the most external point of the left zygomaticomaxillary suture (Fig 42-43).

The inter-molar distance extends from the most occlusal point of the right upper first molar to the most occlusal point of the left upper first molar (Fig 44-45).

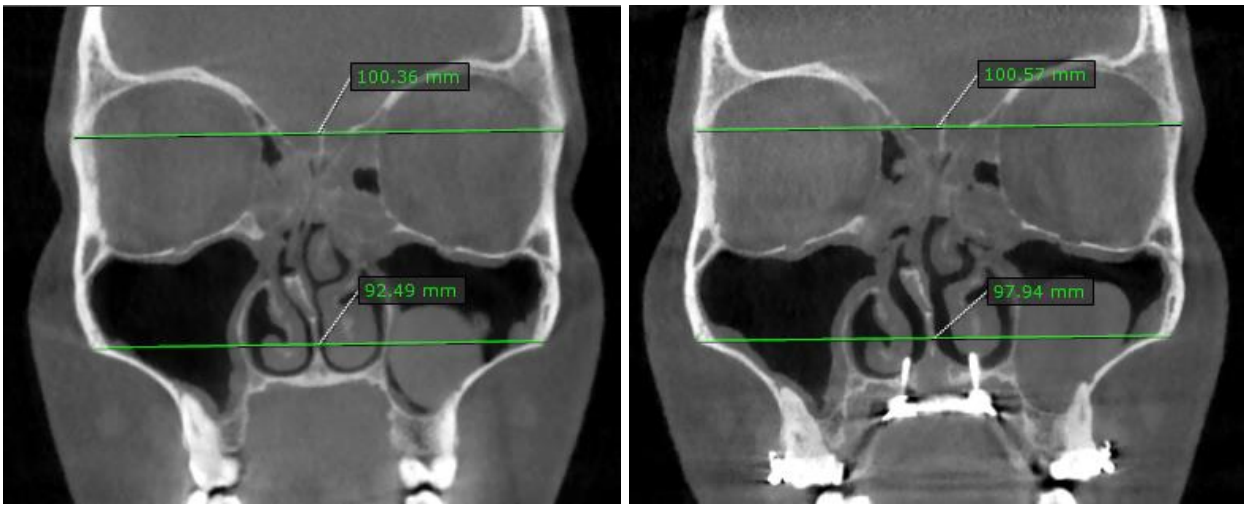

Fig 42. Coronal zygomatic section (CZS) in a MSE patient. A: pre-expansion. B: post-expansion. Linear measurements: upper inter-zygomatic distance and lower inter-zygomatic distance.

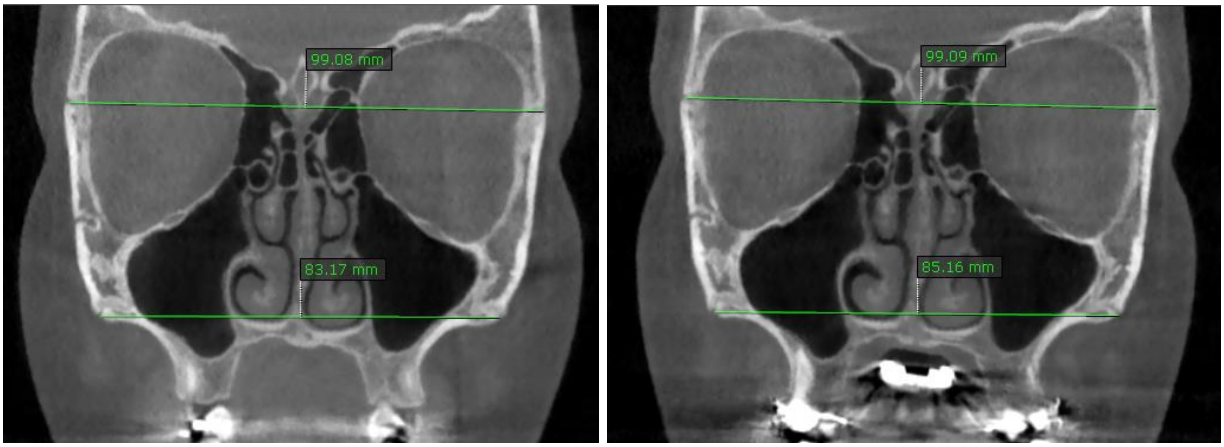

Fig 43. Coronal zygomatic section (CZS) in a Hyrax patient. A: pre-expansion. B: post-expansion. Linear measurements: upper inter-zygomatic distance and lower inter-zygomatic distance.

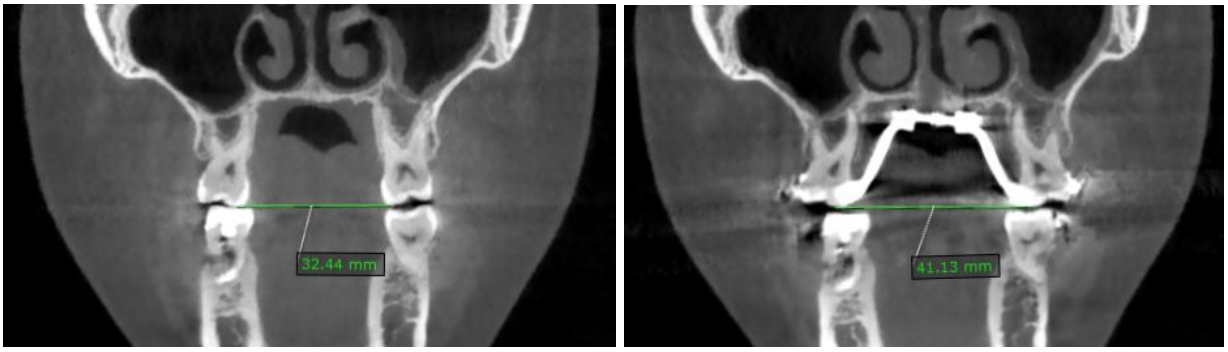

Fig 44. Coronal zygomatic section (CZS) in a MSE patient. A: pre-expansion. B: post-expansion. Linear measurements: inter-molar distance.

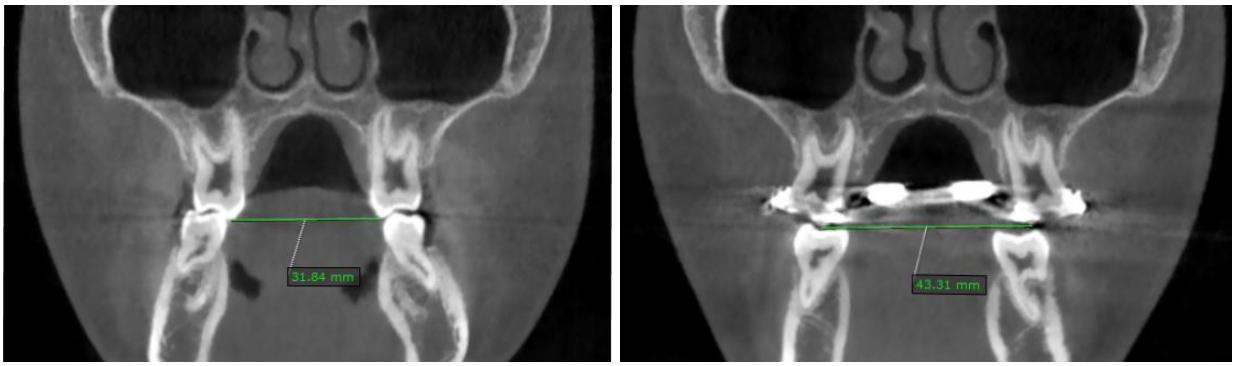

Fig 45. Coronal zygomatic section (CZS) in a Hyrax patient. A: pre-expansion. B: post-expansion. Linear measurements: inter-molar distance.

For the upper inter-zygomatic distance, the pre-expansion value was subtracted from the post-expansion value in order to calculate the treatment change. The distance measurements were averaged, and a paired T-test was used for statistical significance. The same procedure was done to compare the pre- and post-expansion lower inter-zygomatic distance and inter-molar distance.

Angular measurements

In order to analyze the rotation of the zygomaticomaxillary complex in the coronal plane, the following angles were evaluated: frontozygomatic angle, zygomaticomaxillary angle, maxillary inclination angle, molar basal bone angle.

The frontozygomatic angle (FZA) is formed by the Crista galli of the ethmoid bone, the most external point of the frontozygomatic suture and the most external point of the zygomaticomaxillary suture, shown in Fig 46-47.

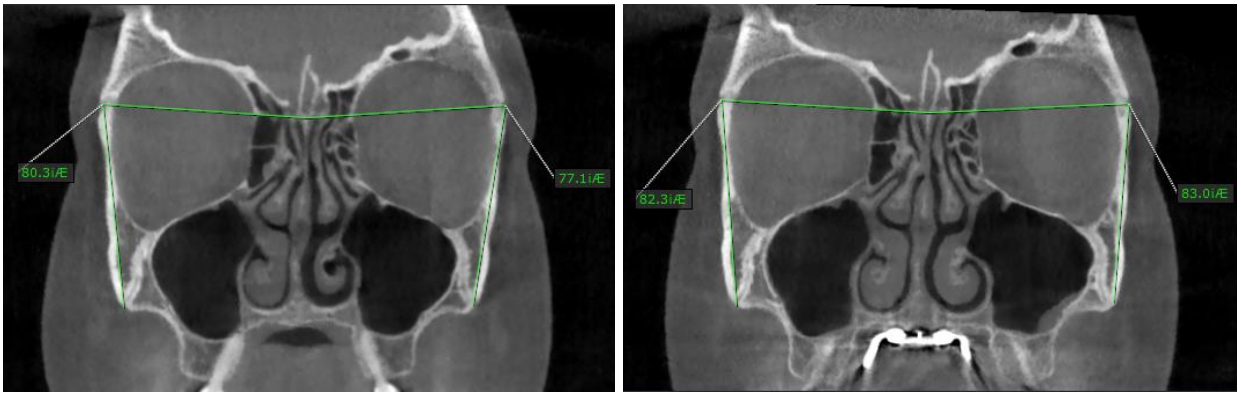

Fig 46. Coronal zygomatic section (CZS) in a MSE patient. A: pre-expansion. B: post-expansion. Angular measurements: right and left frontozygomatic angle (FZA).

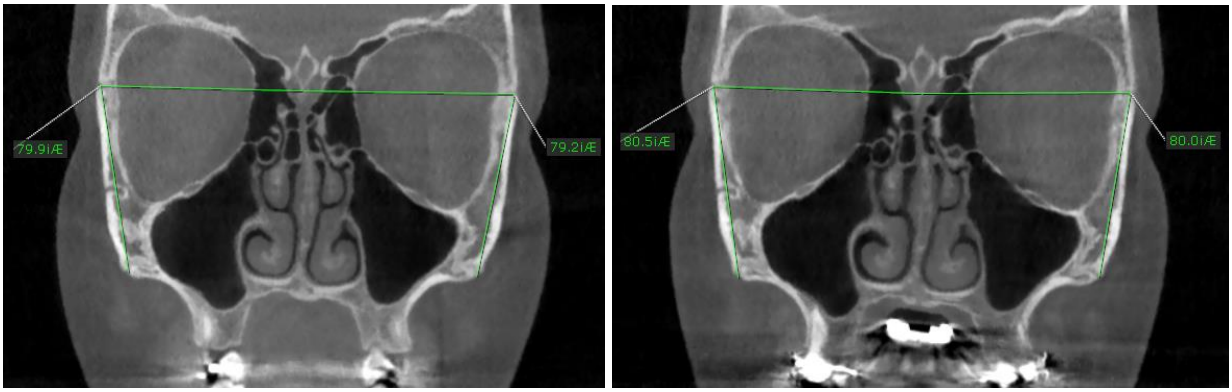

Fig 47. Coronal zygomatic section (CZS) in a Hyrax patient. A: pre-expansion. B: post-expansion. Angular measurements: right and left frontozygomatic angle (FZA).

The pre-expansion value of the FZA was subtracted from the post-expansion value to assess the treatment change. These values were averaged, and a paired T-test was used for statistical significance.

The zygomaticomaxillary angle (ZMA) is formed by the most external point of the frontozygomatic suture, the most external point of the zygomaticomaxillary suture, and the point where the cortical bone that forms the floor of the maxillary sinus and the cortical bone that forms the floor of the nose merge as shown in Fig 48-49.

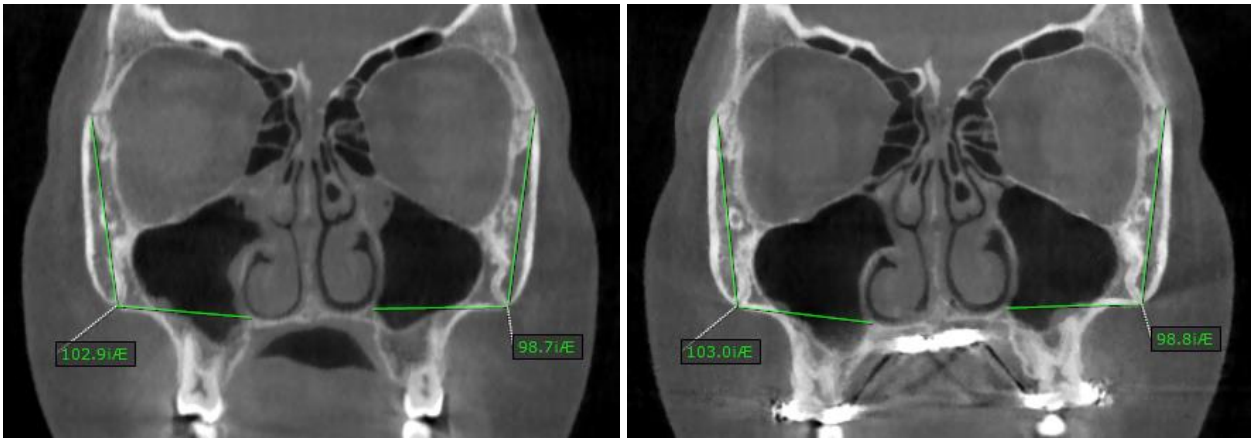

Fig 48. Coronal zygomatic section (CZS) in a MSE patient. A: pre-expansion. B: post-expansion. Angular measurements: right and left zygomaticomaxillary angle (ZMA).

Fig 49. Coronal zygomatic section (CZS) in a Hyrax patient. A: pre-expansion. B: post-expansion. Angular measurements: right and left zygomaticomaxillary angle (ZMA).

The pre-expansion value of the zygomaticomaxillary angle (ZMA) was subtracted from the post-expansion value to calculate the treatment change. These values were averaged, and a paired T-test was used for statistical significance.

The maxillary inclination (Mx Incl) was measured as follows. A line was drawn to connect the most lateral point of the maxilla to the point where the cortical bone that forms the floor of the maxillary sinus and the cortical bone that forms the floor of the nose merge as shown in Fig 50-51. The angulation of this line relative to the maxillary sagittal plane (MSP) was named “maxillary inclination” (Mx Incl).

The pre-expansion value of the maxillary inclination (Mx Incl) was subtracted from the post-expansion value to calculate the treatment change. The values were averaged, and a paired T-test was used for statistical significance.

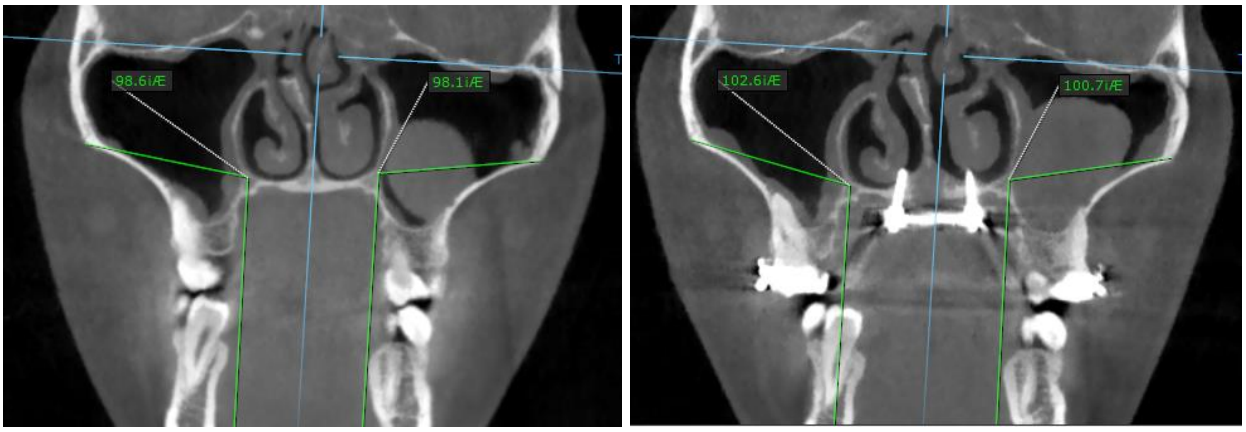

Fig 50. Coronal zygomatic section (CZS) in a MSE patient. A: pre-expansion. B: post-expansion. Angular measurements: right and left maxillary inclination (Mx Incl).

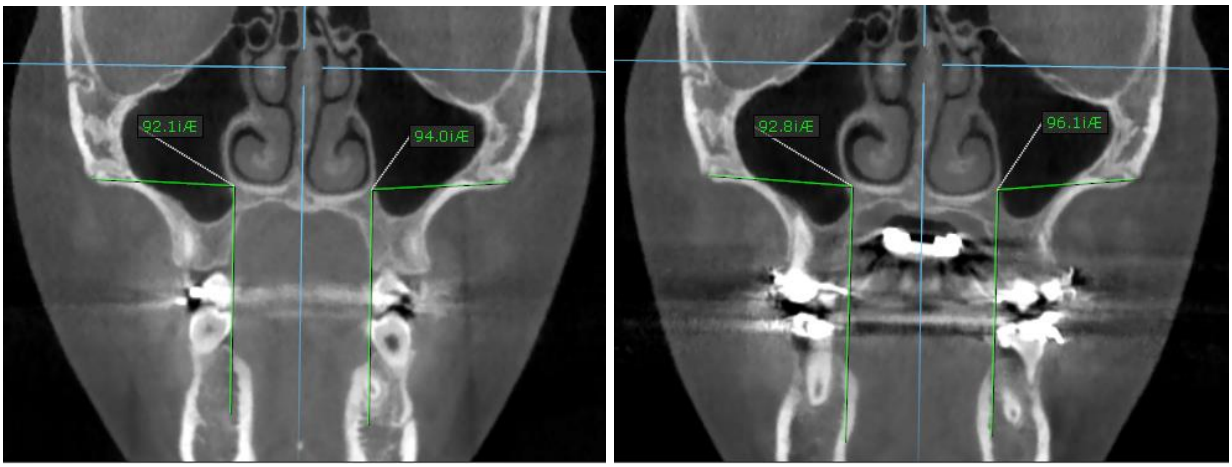

Fig 51. Coronal zygomatic section (CZS) in a Hyrax patient. A: pre-expansion. B: post-expansion. Angular measurements: right and left maxillary inclination (Mx Incl).

Finally the molar basal bone angle (MBBA) was calculated as follows. A line was drawn to connect the most lateral point of the maxilla to the point where the cortical bone that forms the floor of the maxillary sinus and the cortical bone that forms the floor of the nose merge. A second line was drawn to connect the central pit of the molar crown to the furcation of the root. The angle formed between the two lines (Fig 52-53) was named molar basal bone angle (MBBA).

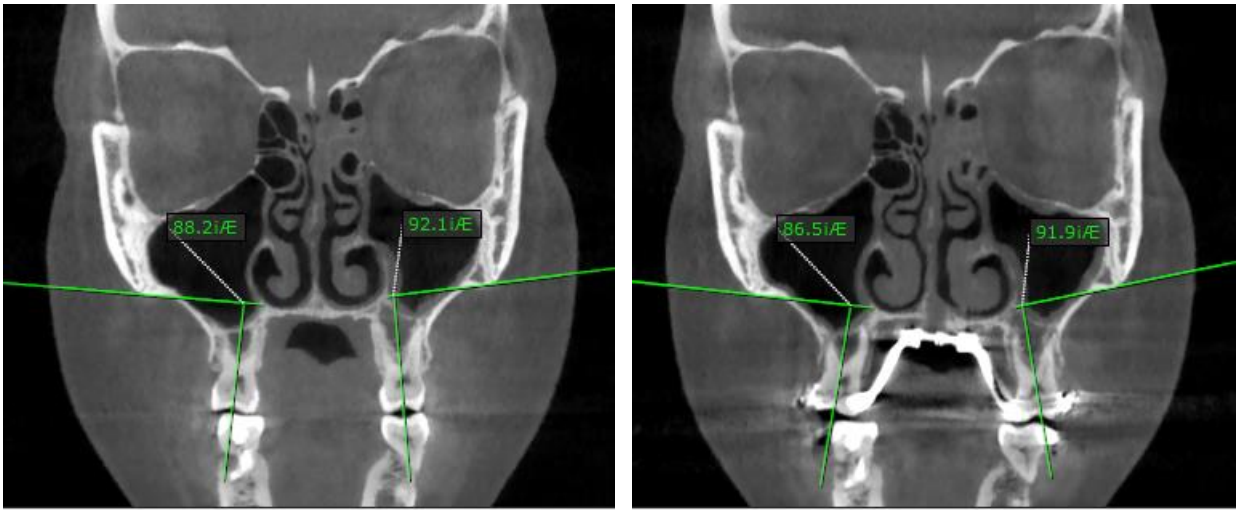

Fig 52. Coronal zygomatic section (CZS) in a MSE patient. A: pre-expansion. B: post-expansion. Angular measurements: right and left molar basal bone angle (MBBA).

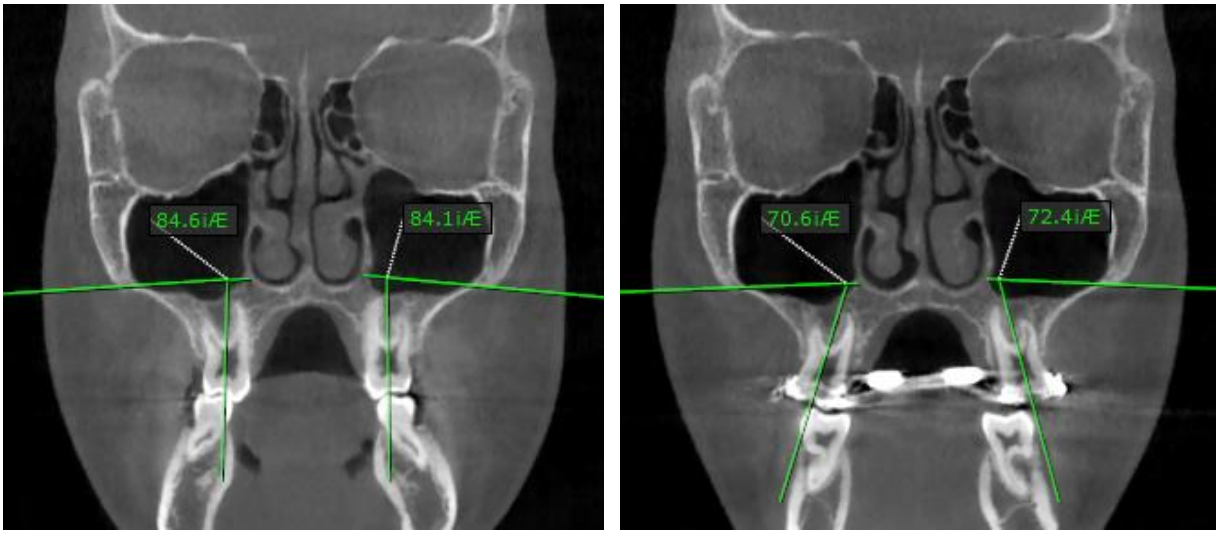

Fig 53. Coronal zygomatic section (CZS) in a Hyrax patient. A: pre-expansion. B: post-expansion. Angular measurements: right and left molar basal bone angle (MBBA).

The pre-expansion MBBA value was subtracted from the post-expansion value for the treatment change. The values were averaged, and a paired T-test was used for statistical significance.

Measurements on the axial zygomatic section (AZS)

In order to analyze the skeletal changes of the temporal bone, zygomatic bone and maxilla in the horizontal plane, a slice was selected on the CBCT.

The **axial zygomatic section (AZS)** passes through the upper part of the glenoid fossa of the right and left temporo-mandibular joint, through the right and left zygomatic process of the temporal bone and through the zygomaticomaxillary suture as shown in Fig 54.

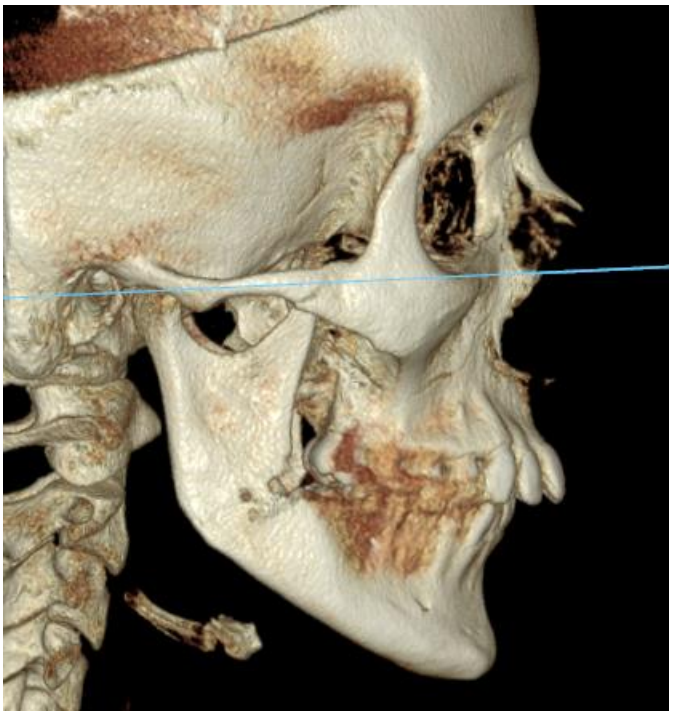

Fig 54. 3D rendering showing the axial zygomatic section (AZS) traced in blue.

The post-expansion CBCT was superimposed on the pre-expansion CBCT, the axial zygomatic section (AZS) was produced (Fig. 55), and then the linear and angular measurements were taken from the pre-expansion and post-expansion CBCT.

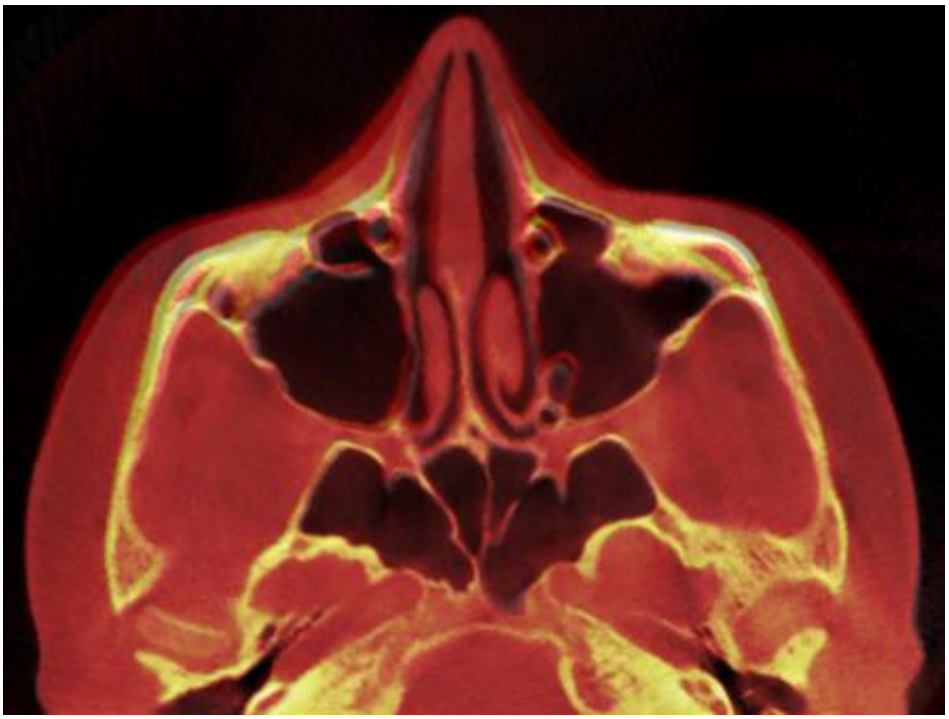

Fig 55. Axial zygomatic section (AZS): example of the superimposed image of a MSE patient.

Table 5 lists the parameters evaluated in the axial zygomatic section (AZS).

Table 5. Parameters evaluated in the axial zygomatic section (AZS)

Linear distances	
1	Anterior inter-maxillary distance
2	Posterior inter-zygomatic distance
Angular measurements	
3	Right zygomaticotemporal angle (Rt ZTA)
4	Left zygomaticotemporal angle (Lt ZTA)
5	Right angle of the zygomatic process of the temporal bone (Rt ZPA)
6	Left angle of the zygomatic process of the temporal bone (Lt ZPA)

Linear measurements on the axial zygomatic section (AZS)

The anterior inter-maxillary distance was measured from the most anterior point of the right maxilla to the most anterior point of the left maxilla as shown in Fig 56-57.

The posterior inter-zygomatic distance was measured from the most external point of the right zygomaticomaxillary suture to the most external point of the left zygomaticomaxillary suture as shown in Fig 56-57.

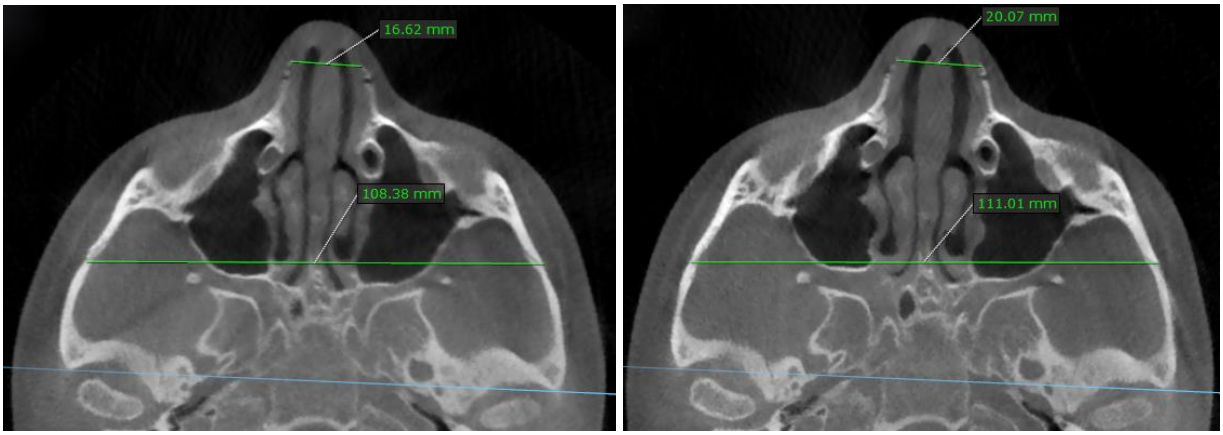

Fig 56. Axial zygomatic section (AZS) in a MSE patient. A: pre-expansion. B: post-expansion. Linear measurements: anterior inter-maxillary distance and posterior inter-zygomatic distance.

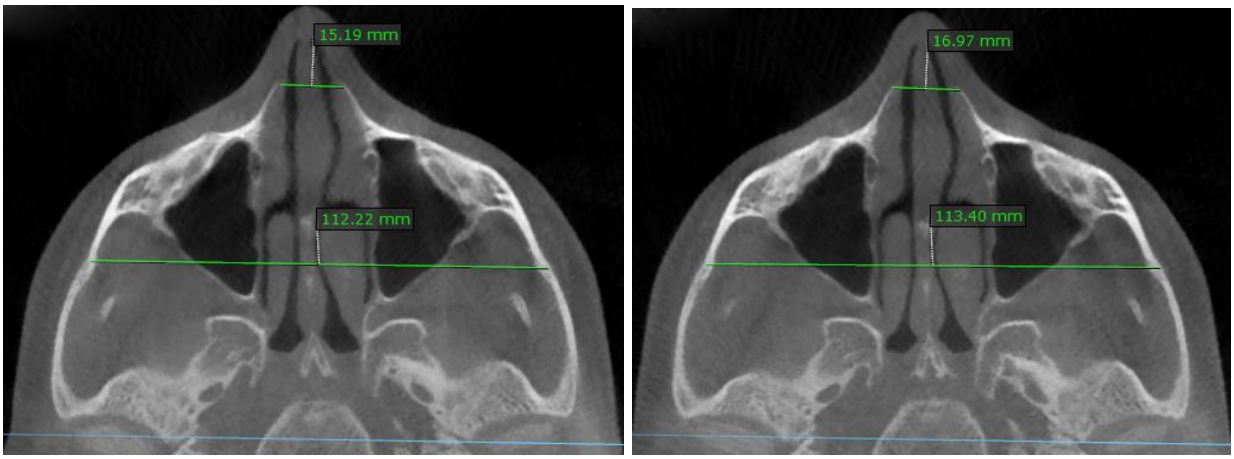

Fig 57. Axial zygomatic section (AZS) in a Hyrax patient. A: pre-expansion. B: post-expansion. Linear measurements: anterior inter-maxillary distance and posterior inter-zygomatic distance.

For the anterior inter-maxillary distance, the pre-expansion value was subtracted from the post-expansion value in order to calculate the treatment change. The values were averaged, and a paired T-test was used for statistical significance.

The same procedure was done for the pre- and post-expansion posterior inter-zygomatic distances.

Angular measurements

In order to further analyze the rotation of the zygomaticomaxillary complex in the horizontal plane, the zygomaticotemporal angle (ZTA) and the zygomatic process angle (ZPA) were evaluated.

The zygomaticotemporal angle (ZTA) is formed by the most anterior point of the maxilla, the most external point of the zygomaticotemporal suture and the most posterior-lateral point of the eminence of the glenoid fossa as shown in Fig 58-59.

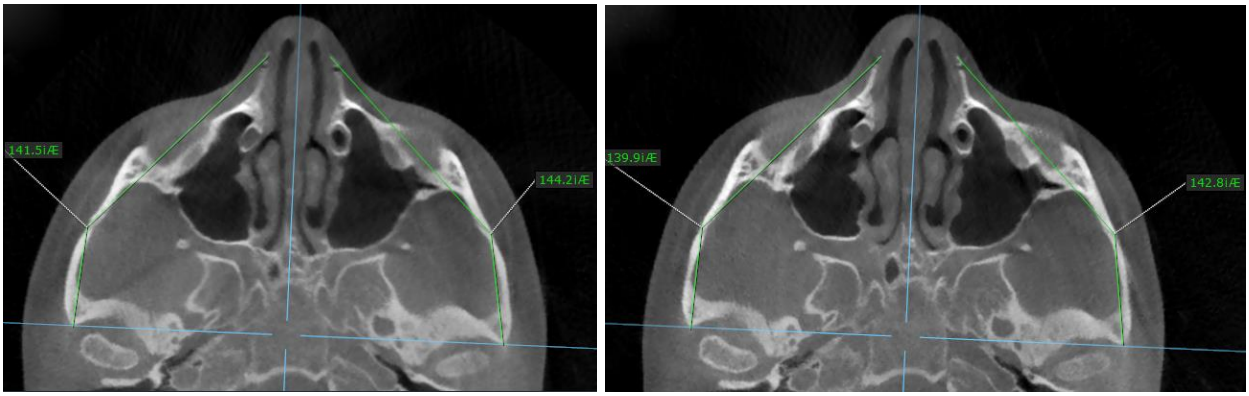

Fig 58. Axial zygomatic section (AZS) in a MSE patient. A: pre-expansion. B: post-expansion. Angular measurements: right and left zygomaticotemporal angle (ZTA).

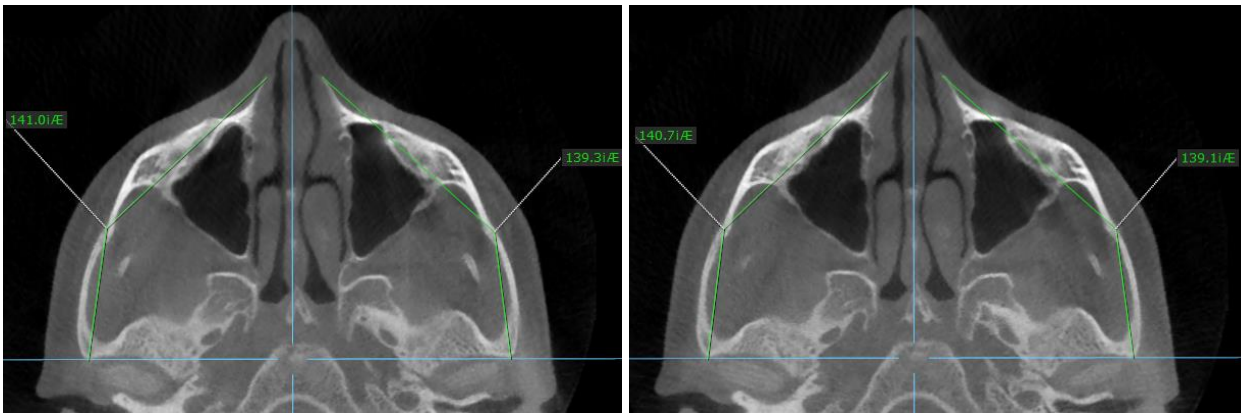

Fig 59. Axial zygomatic section (AZS) in a Hyrax patient. A: pre-expansion. B: post-expansion. Angular measurements: right and left zygomaticotemporal angle (ZTA).

The pre-expansion value of the zygomaticotemporal angle (ZTA) was subtracted from the post-expansion value to calculate the treatment change. The values were averaged, and a paired T-test was used for statistical significance.

In order to evaluate a possible bone bending of the zygomatic process of the temporal bone, the angle of the zygomatic process of the temporal bone (zygomatic process angle or ZPA) was measured as follows.

A line was drawn to connect the most posterior-lateral point of the eminence of the glenoid fossa on the right and left the temporo-mandibular joint. Then a line was drawn to connect the most posterior-lateral point of the eminence of the glenoid fossa of the temporo-mandibular joint to the most external point of the zygomaticotemporal suture. The angle formed between the two lines is the zygomatic process angle (ZPA) of the temporal bone as shown in Fig 60-61.

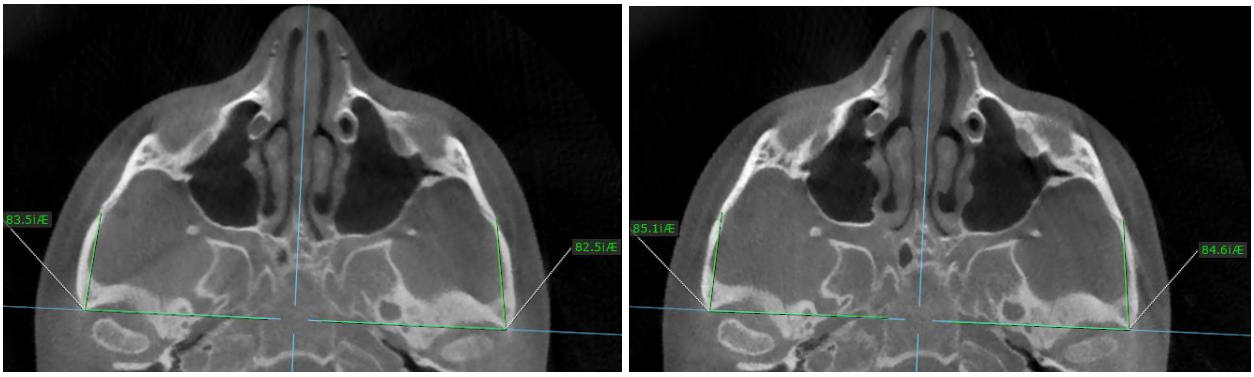

Fig 60. Axial zygomatic section (AZS) in a MSE patient. A: pre-expansion. B: post-expansion. Angular measurements: right and left angle of the zygomatic process of the temporal bone (Zygomatic Process Angle or ZPA)

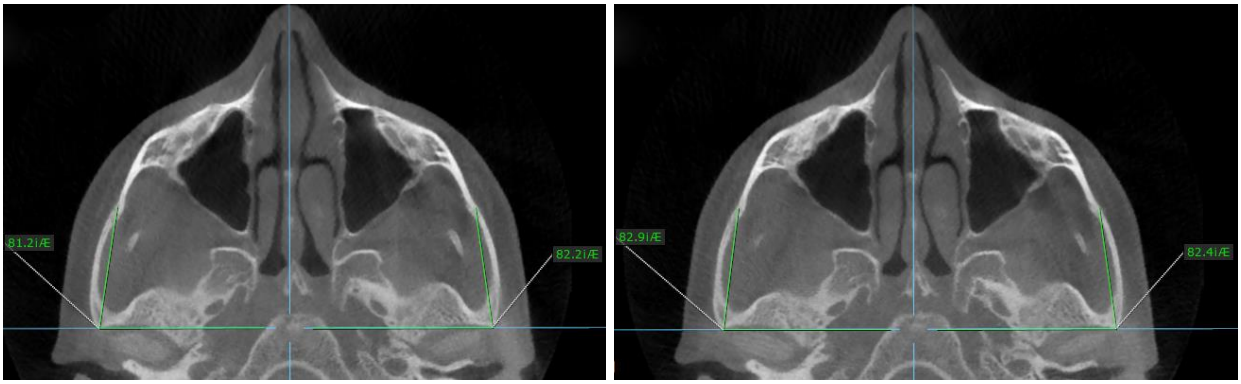

Fig 61. Axial zygomatic section (AZS) in a Hyrax patient. A: pre-expansion. B: post-expansion. Angular measurements: right and left angle of the zygomatic process of the temporal bone (Zygomatic Process Angle or ZPA).

The pre-expansion zygomatic process angle of the temporal bone (ZPA) was subtracted from the post-expansion value for the treatment change calculation. The values were averaged, and a paired T-test was used for statistical significance.

Statistical Analysis

Assessments of variables within and between groups - Variables were compared from pre- to post-treatment within each group parametrically using the paired T-test or non-parametrically using the Wilcoxon sign rank test as appropriate. In addition, pre- to post-changes in each variable were compared between groups parametrically using the t-test or non-parametrically using the Wilcoxon sign sum test as appropriate.

The frequency of openings in the lower part of the pterygopalatine suture were compared from pre- to post-treatment within each group and between groups using the Fisher's exact test.

Reliability assessments – Measurements were obtained for all variables (24) on the right side of the skull of 2 different patients. There were 4 measurements per patient corresponding to 2 different raters with 2 measurements per rater.

Reliability was evaluated in two ways: 1) by computing the coefficient of variation (CV) and 2) by computing the intra-class correlation coefficient (ICC).

The coefficient of variation (CV) - The variation across and/or within raters within patients is called the error SD (SD_{error}) or measurement error SD. For a given measure, the CV is defined as the ratio of the error SD to the overall mean. Therefore, the CV is the variability due to measurement error as a percent of the overall mean. If the measurements are the same between raters and within raters, then CV = 0 (perfect reliability) and error SD = 0. If reliability is high, the CV should be small (ideally not more than 2%).

The intraclass correlation coefficient (ICC) – In general, the variation in a given measure is due to 1) differences between patients (between patient SD) and 2) differences between and/or within raters within patients (error SD). The ICC is the proportion of the total variation due to patient variation. When the error SD is zero, all of the variation is due to patient (perfect reliability). For excellent reliability, the ICC should be near 100%.

RESULTS

Analysis of variables in the axial palatal section (APS)

The results of variables analyzed in the axial palatal section are shown in table 6-10.

Table 6. Results for axial palatal section (APS): MSE group

		Before Expansion		After Expansion		Treatment Change		P Value	
		mean	sd	mean	sd	mean	sd	p-value	
1	Rt ANS to maxillary sagittal plane	0.00	0.00	2.59	1.70	2.59	1.70	<.0001	**
2	Lt ANS to maxillary sagittal plane	0.00	0.00	2.16	1.27	2.16	1.27	<.0001	**
3	Rt PNS to maxillary sagittal plane	0.00	0.00	2.34	1.32	2.34	1.32	<.0001	**
4	Lt PNS to maxillary sagittal plane	0.00	0.00	1.99	0.90	1.99	0.90	<.0001	**
5	Lateral displacement of Rt ANS + Lt ANS	0.00	0.00	4.75	2.59	4.75	2.59	<.0001	**
6	Lateral displacement of Rt PNS + Lt PNS	0.00	0.00	4.33	1.74	4.33	1.74	<.0001	**
7	Width of opening in Rt pterygoid process	0.00	0.00	1.35	1.79	1.35	1.79	0.011	*
8	Width of opening in Lt pterygoid process	0.00	0.00	2.17	2.45	2.17	2.45	0.004	**

** p<0.01 * p<0.05

Table 7. Results for axial palatal section (APS): Hyrax group

		Before Expansion		After Expansion		Treatment Change		P Value	
		mean	sd	mean	sd	mean	sd	p-value	
1	Rt ANS to maxillary sagittal plane	0.00	0.00	1.40	1.01	1.40	1.01	0.019	*
2	Lt ANS to maxillary sagittal plane	0.00	0.00	1.72	1.46	1.72	1.46	0.035	*
3	Rt PNS to maxillary sagittal plane	0.00	0.00	1.21	0.98	1.21	0.98	0.029	*
4	Lt PNS to maxillary sagittal plane	0.00	0.00	1.38	0.97	1.38	0.97	0.018	*
5	Lateral displacement of Rt ANS + Lt ANS	0.00	0.00	3.12	2.04	3.12	2.04	0.032	*
6	Lateral displacement of Rt PNS + Lt PNS	0.00	0.00	2.59	1.68	2.59	1.68	0.031	*
7	Width of opening in Rt pterygoid process	0.00	0.00	0.22	0.54	0.22	0.54	0.363	
8	Width of opening in Lt pterygoid process	0.00	0.00	0.16	0.40	0.16	0.40	0.363	

** p<0.01 * p<0.05

Table 8. Axial Palatal Section (APS): Non parametric Wilcoxon rank sum test, difference between MSE and Hyrax groups

Parameter		**P Value**	
		p-value	
1	Rt ANS to maxillary sagittal plane	0.127	
2	Lt ANS to maxillary sagittal plane	0.500	
3	Rt PNS to maxillary sagittal plane	0.074	
4	Lt PNS to maxillary sagittal plane	0.183	
5	Lateral displacement of Rt ANS + Lt ANS	0.235	
6	Lateral displacement of Rt PNS + Lt PNS	0.045	*
7	Width of opening in Rt pterygoid process	0.151	
8	Width of opening in Lt pterygoid process	0.064	

** p<0.01 * p<0.05

Table 9. Statistical analysis of the frequency of openings in the lower part of the pterygopalatine suture: Fisher's exact test, within group change

	Before Expansion	After Expansion	P Value	
MSE				
Sutures with openings	0	16	0.0001	**
Sutures without openings	30	14		
Hyrax				
Sutures with openings	0	2	0.48	
Sutures without openings	12	10		

** p<0.01 * p<0.05

Table 10. Statistical analysis of the frequency of openings in the lower part of the pterygopalatine suture: Fisher's exact test, difference between MSE and Hyrax groups

	MSE After Expansion	Hyrax After Expansion	P Value	* p < 0.05	Odds ratio
Sutures with openings	16	2	0.042	*	5.49
Sutures without openings	14	10			

** p<0.01 * p<0.05

MSE patients: On average, ANS moved laterally by 2.6 mm and 2.2 mm (Rt and Lt side), and PNS moved laterally by 2.3 and 2.0 mm (Rt and Lt side). These lateral movements were highly significant for all landmarks (p<0.01).

The split of the midpalatal suture at ANS was symmetrical in 27% of the cases, asymmetrical with more movement on the right side in 40% of the cases, and asymmetrical with more movement on the left side in 33% of the cases.

On average, one half of the ANS moved more than the contralateral side by 1.1 ($\pm$ 1.0) mm.

Openings between the lateral and medial plates of the pterygoid process (Fig 62) were detectable in 9 out of 15 patients (60%): 7 patients with openings in both pterygopalatine sutures, 1 patient with opening only in the right suture and 1 patient with opening only in the left suture. If we count the number of opened sutures, a sum of 16 sutures (8 right and 8 left) from 9 patients exhibited positive opening out of 30 sutures (from 15 patients) evaluated. That means 53% of all sutures opened ($p<0.01$). The mean size of the opening was 1.3 mm for the right pterygopalatine suture and 2.2 mm for the left pterygopalatine suture ($p<0.05$).

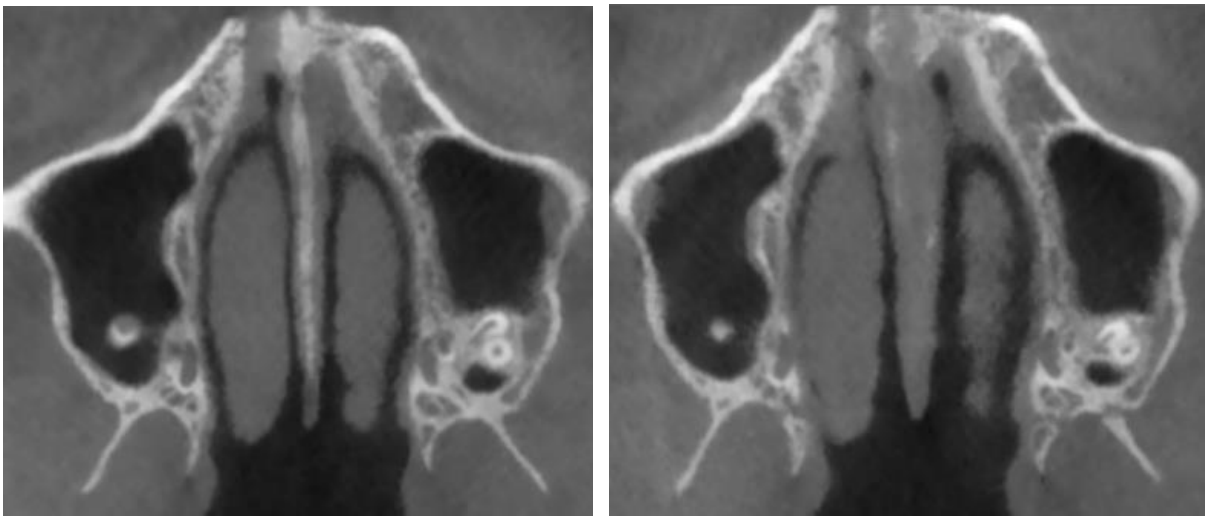

Fig 62. Openings between the lateral and medial plates of the pterygoid process detectable in the post-expansion CBCT in MSE patient. A: pre-expansion. B: post-expansion.

Hyrax patients: On average, ANS moved laterally by 1.4 mm and 1.7 mm (Rt and Lt side) and PNS moved laterally by 1.2 mm and 1.4 mm (Rt and Lt side). These lateral movements were statistically significant for all landmarks ($p<0.05$).

The split of the midpalatal suture at ANS was symmetrical in 33% of the cases, asymmetrical with more movement on the right side in 17% of the cases, and asymmetrical with more movement on the left side in 50% of the cases.

On average, one half of the ANS moved more than the contralateral side by 1.3 ($\pm$ 0.7) mm.

Openings between the lateral and the medial plate of the pterygoid process was observed in 1 out of 6 patients (17%). Suture openings were observed in 2 (1 right and 1 left from a patient) out of 12 total sutures examined. That means 17% of the sutures opened without statistical significance (Fisher's exact test). The mean size of the opening was 0.2 mm for the right pterygopalatine suture and 0.2 mm for the left pterygopalatine suture, without statistical significance.

All parameters measured for lateral movement were greater for MSE than Hyrax, even though not all values were statistical significant.

However, the sum of the lateral displacement at PNS was significantly larger in MSE ($p<0.05$).

The frequency and width of openings observed in post-expansion CBCTs were statistically significant in MSE patients ($p<0.01$) while they were not significant in Hyrax patients, indicating that the lower part of pterygopalatine suture was opened with MSE but not with Hyrax appliance ($p<0.05$) in comparison.

Analysis of variables in the lower nasal section (LNS)

The results of variables analyzed in the lower nasal section are shown in table 11-13.

Table 11. Results for lower nasal section (LNS): MSE group

		Before Expansion		After Expansion		Treatment Change		P Value	
		mean	sd	mean	sd	mean	sd	p-value	
Transverse distances									
1	Rt Lo Ant Mx to maxillary sagittal plane	10.14	1.81	12.85	2.02	2.72	1.44	<.0001	**
2	Lt Lo Ant Mx to maxillary sagittal plane	9.64	1.47	12.24	1.31	2.60	1.12	<.0001	**
3	Rt Lo Po Mx to maxillary sagittal plane	21.81	2.33	23.07	2.53	1.26	0.69	<.0001	**
4	Lt Lo Po Mx to maxillary sagittal plane	21.46	2.17	22.85	2.22	1.39	0.67	<.0001	**
5	Rt Lo Pter to maxillary sagittal plane	17.63	1.76	18.33	1.73	0.70	0.49	<.0001	**
6	Lt Lo Pter to maxillary sagittal plane	17.01	1.59	17.69	1.72	0.68	0.55	0.000	**
7	Lateral slide in Rt pterygomaxillary fissure	--	--	--	--	0.56	0.46	0.000	**
8	Lateral slide in Lt pterygomaxillary fissure	--	--	--	--	0.71	0.51	<.0001	**
Sagittal distance of lower posterior maxilla									
9	Rt Lo Po Mx to V-coronal plane	13.48	2.15	14.27	2.16	0.79	0.49	<.0001	**
10	Lt Lo Po Mx to V-coronal plane	13.17	2.19	14.18	2.13	1.02	0.55	<.0001	**
Sagittal distance of the pterygoid process									
11	Rt Lo Pter to V-coronal plane	12.29	2.67	12.42	2.69	0.13	0.24	0.064	
12	Lt Lo Pter to V-coronal plane	12.32	2.15	12.40	2.13	0.08	0.18	0.120	

** p<0.01 * p<0.05

Table 12. Results for lower nasal section (LNS): Hyrax group

		Before Expansion		After Expansion		Treatment Change		P Value	
		mean	sd	mean	sd	mean	sd	p-value	
Transverse distances									
1	Rt Lo Ant Mx to maxillary sagittal plane	10.08	1.13	11.18	1.54	1.10	0.78	0.018	*
2	Lt Lo Ant Mx to maxillary sagittal plane	9.93	0.91	11.17	1.41	1.24	0.88	0.018	*
3	Rt Lo Po Mx to maxillary sagittal plane	20.68	2.10	21.08	2.02	0.39	0.23	0.009	**
4	Lt Lo Po Mx to maxillary sagittal plane	21.41	2.59	21.96	2.65	0.55	0.29	0.005	**
5	Rt Lo Pter to maxillary sagittal plane	16.82	1.47	17.07	1.44	0.26	0.17	0.015	*
6	Lt Lo Pter to maxillary sagittal plane	16.61	1.54	16.86	1.55	0.25	0.17	0.017	*
7	Lateral slide in Rt pterygomaxillary fissure	--	--	--	--	0.14	0.18	0.120	
8	Lateral slide in Lt pterygomaxillary fissure	--	--	--	--	0.30	0.24	0.029	*
Sagittal distance of lower posterior maxilla									
9	Rt Lo Po Mx to V-coronal plane	13.81	2.66	14.26	2.70	0.46	0.48	0.067	
10	Lt Lo Po Mx to V-coronal plane	14.05	3.27	14.34	3.23	0.29	0.18	0.011	*
Sagittal distance of the pterygoid process									
11	Rt Lo Pter to V-coronal plane	12.61	2.66	12.71	2.55	0.10	0.14	0.152	
12	Lt Lo Pter to V-coronal plane	12.76	4.05	12.83	3.98	0.07	0.16	0.317	

** p<0.01 * p<0.05

Table 13. Lower Nasal Section (LNS): T-test, difference between MSE and Hyrax groups

Parameter		P Value		Parameter		P Value	
		p-value				p-value	
Transverse distances				**Sagittal distance of lower posterior maxilla**			
1	Rt Lo Ant Mx to maxillary sagittal plane	0.019	*	9	Rt Lo Po Mx to V-coronal plane	0.171	
2	Lt Lo Ant Mx to maxillary sagittal plane	0.016	*	10	Lt Lo Po Mx to V-coronal plane	0.006	**
3	Rt Lo Po Mx to maxillary sagittal plane	0.008	**				
4	Lt Lo Po Mx to maxillary sagittal plane	0.008	**				
5	Rt Lo Pter to maxillary sagittal plane	0.044	*				
6	Lt Lo Pter to maxillary sagittal plane	0.083					
7	Lateral slide in Rt pterygomaxillary fissure	0.041	*				
8	Lateral slide in Lt pterygomaxillary fissure	0.046	*				

** p<0.01 * p<0.05

The most anterior point of the maxilla moved laterally by 2.7 mm and 2.6 mm (Rt and Lt side) in MSE patients (p<0.01), and by 1.1 mm and 1.2 mm (Rt and Lt side) in Hyrax patients (p<0.05). The differences between the two groups were statistically significant (p<0.05).

The most posterior point of the maxilla moved laterally by 1.3 mm and 1.4 mm (Rt and Lt side) in MSE patients (p<0.01), and by 0.4 mm and 0.5 mm (Rt and Lt side) in Hyrax patients (p<0.05). The difference between the two groups were highly significant (p<0.01).

The most anterior point of the pterygoid fossa moved laterally by 0.7 mm (Rt and Lt side) in MSE patients (p<0.01), and by 0.3 and 0.2 mm (Rt and Lt side) in

Hyrax patients ($p<0.05$). The difference between the two groups on the Rt was statistically significant ($p<0.05$).

The lateral slide in the pterygomaxillary fissure is the difference between the lateral movement (treatment change) of the most posterior point of maxilla and the lateral movement (treatment change) of the most anterior point of the pterygoid fossa. For example, on average, the right posterior point of the maxilla (Rt Lo Po Mx) moved laterally by 1.3 mm and the right pterygoid process (Rt Lo Pter) moved laterally by 0.7 mm in MSE patients. This means that the right tuberosity of the maxilla, on average, moved 0.6 mm (1.3 mm – 0.7 mm) laterally relative to the pterygoid process. The left posterior point of the maxilla (Lt Lo Po Mx) moved laterally by 1.4 mm, and the left pterygoid process (Lt Lo Pter) moved laterally by 0.7 mm. This means that the left tuberosity of the maxilla on average moved 0.7 mm (1.4 mm – 0.7 mm) laterally relative to the pterygoid process.

The lateral slide in the pterygomaxillary fissure was 0.6 mm and 0.7 mm (Rt and Lt side) in MSE patients ($p<0.01$), and 0.1 mm and 0.3 mm (Rt and Lt side) in Hyrax patients ($p<0.05$ for Lt side). These differences between the two groups were statistically significant ($p<0.05$).

Sometimes a clear separation between the tuberosity of maxilla and the pterygoid process was visible in the post-expansion CBCTs of MSE patients as shown in Fig 29 and 63. On the other hand, this separation was not visible in Hyrax patients.

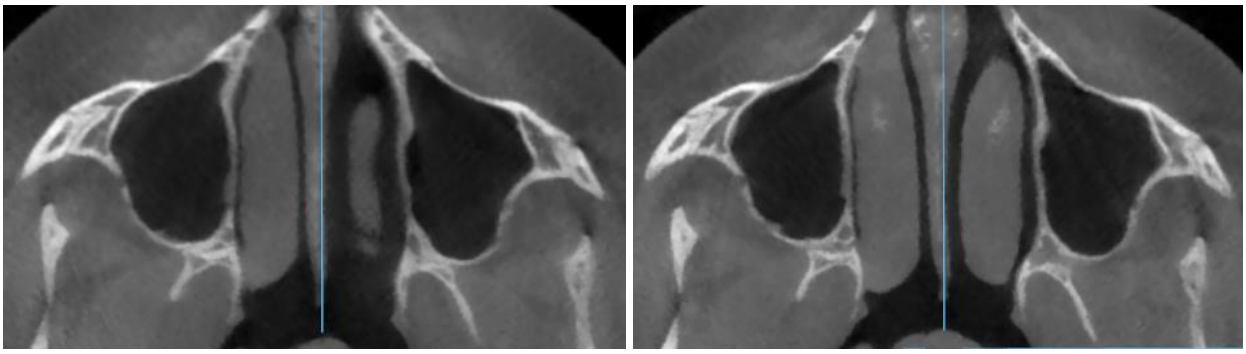

Fig 63. Lower nasal section of a MSE patient. A: pre-expansion. B: post-expansion. The maxilla moving laterally and anteriorly relatively to pterygoid process is visible in Fig 63B. A gap is visible between the tuberosity of maxilla and the pterygoid process, especially in the left pterygomaxillary fissure. This lateral movement of the most posterior point of maxilla relatively to the pterygoid process was named “lateral slide in the pterygomaxillary fissure”.

The lateral movements of the most anterior and posterior points of the maxilla were both larger in MSE patients than in Hyrax patients ($p<0.05$ for anterior and $p<0.01$ for posterior), indicating a larger increase of nasal cavity in transverse dimension with MSE patients than with Hyrax patients.

Also, the lateral slide in the pterygomaxillary fissure was significantly larger in MSE group than in Hyrax group ($p<0.05$), indicating a significantly greater loosening of the pterygopalatine suture in MSE patients than in Hyrax patients.

Regarding sagittal dislocations, the most posterior point of the maxilla moved forward by 0.8 mm and 1.0 mm (Rt and Lt side) in MSE patients ($p<0.01$), and by 0.5 mm and 0.3 mm (Rt and Lt side) in Hyrax patients with statistical significance only on the left side ($p<0.05$).

The forward movement of the pterygoid process was negligible without statistical significance in both MSE and Hyrax patients.

Analysis of variables in the upper nasal section (UNS)

The results of variables analyzed in the upper nasal section are shown in table 14-16.

Table 14. Results for upper nasal section (UNS): MSE group

		Before Expansion		After Expansion		Treatment Change		P Value	
		mean	sd	mean	sd	mean	sd	p-value	
Transverse distance									
1	Rt Up Ant Mx to maxillary sagittal plane	9.32	1.59	11.14	2.22	1.82	0.97	<.0001	**
2	Lt Up Ant Mx to maxillary sagittal plane	9.30	1.21	10.83	1.82	1.53	0.99	<.0001	**
3	Rt Po-med Mx to maxillary sagittal plane	13.94	2.19	14.85	2.28	0.91	0.36	<.0001	**
4	Lt Po-med Mx to maxillary sagittal plane	14.30	2.68	15.24	3.06	0.95	0.60	<.0001	**
5	Rt Up Pter to maxillary sagittal plane	13.11	2.02	13.47	2.05	0.36	0.32	0.001	**
6	Lt Up Pter to maxillary sagittal plane	12.64	1.98	13.09	2.01	0.45	0.42	0.001	**
Sagittal distance of upper posterior maxilla									
7	Rt Up Po Mx to V-coronal plane	13.36	2.28	14.28	2.08	0.92	0.64	<.0001	**
8	Lt Up Po Mx to V-coronal plane	13.17	2.20	14.13	2.24	0.96	0.48	<.0001	**
Angular measurements									
9	Angle of right palatine bone	76.69	26.40	71.59	23.48	-5.10	4.35	0.001	**
10	Angle of left palatine bone	82.60	23.40	76.21	23.89	-6.39	5.24	0.000	**

** p<0.01 * p<0.05

Table 15. Results for upper nasal section (UNS): Hyrax group

		Before Expansion		After Expansion		Treatment Change		P Value	
		mean	sd	mean	sd	mean	sd	p-value	
Transverse distance									
1	Rt Up Ant Mx to maxillary sagittal plane	8.57	1.10	9.24	0.93	0.67	0.86	0.115	
2	Lt Up Ant Mx to maxillary sagittal plane	8.99	0.74	9.61	0.40	0.62	0.47	0.024	*
3	Rt Po-med Mx to maxillary sagittal plane	13.35	0.71	13.71	0.95	0.36	0.30	0.033	*
4	Lt Po-med Mx to maxillary sagittal plane	13.60	1.55	13.91	1.65	0.31	0.25	0.027	*
5	Rt Up Pter to maxillary sagittal plane	11.62	1.09	11.87	1.08	0.26	0.18	0.016	*
6	Lt Up Pter to maxillary sagittal plane	12.37	1.19	12.62	1.22	0.25	0.14	0.007	**
Sagittal distance of upper posterior maxilla									
7	Rt Up Po Mx to V-coronal plane	14.95	1.73	15.27	1.85	0.32	0.25	0.026	*
8	Lt Up Po Mx to V-coronal plane	14.62	2.53	14.86	2.37	0.24	0.25	0.065	
Angular measurements									
9	Angle of right palatine bone	60.78	10.98	59.07	10.18	-1.72	1.19	0.017	*
10	Angle of left palatine bone	70.50	9.24	68.72	9.28	-1.78	0.76	0.002	**

** p<0.01 * p<0.05

Table 16. Upper Nasal Section (UNS): T-test, difference between MSE and Hyrax groups

Parameter		P Value		Parameter		P Value	
		p-value	**p <0.05			p-value	
Transverse distances				**Sagittal distance of upper posterior maxilla**			
1	Rt Up Ant Mx to maxillary sagittal plane	0.021	*	7	Rt Up Po Mx to V-coronal plane	0.040	*
2	Lt Up Ant Mx to maxillary sagittal plane	0.046	*	8	Lt Up Po Mx to V-coronal plane	0.002	**
3	Rt Po-med Mx to maxillary sagittal plane	0.004	**	**Angular measurements**			
4	Lt Po-med Mx to maxillary sagittal plane	0.022	*	9	Angle of right palatine bone	0.080	
5	Rt Up Pter to maxillary sagittal plane	0.453		10	Angle of left palatine bone	0.048	*
6	Lt Up Pter to maxillary sagittal plane	0.274					

** p<0.01 * p<0.05

The most anterior point of the maxilla moved laterally by 1.8 mm and 1.5 mm (Rt and Lt side) in MSE patients (p<0.01), and by 0.7 mm and 0.6 mm (Rt and Lt side) in Hyrax patients (p<0.05 for Lt side). The difference between the two groups were statistically significant (p<0.05).

The posterior-medial point of the maxilla moved laterally by 0.9 mm and 1.0 mm (Rt and Lt side) in MSE patients (p<0.01), and by 0.4 mm and 0.3 mm (Rt and Lt side) in Hyrax patients (p<0.05). The difference between the two groups were statistically significant (p<0.01 for Rt side and p<0.05 for Lt side).

The anterior-medial point of the pterygoid process moved laterally by 0.4 mm and 0.5 mm (Rt and Lt side) in MSE patients (p<0.01), and by 0.3 mm (Rt and Lt side) in Hyrax patients (p<0.05 for Rt side and p<0.01 for Lt side). The difference between the two groups were not statistically significant.

Regarding sagittal dislocations, the most posterior point of the maxilla moved forward by 0.9 mm and 1.0 mm (Rt and Lt side) in MSE patients ($p<0.01$), and by 0.3 mm and 0.2 mm (Rt and Lt side) in Hyrax patients ($p<0.05$ for Rt side). The difference between the two groups were statistically significant ($p<0.05$ for Rt side and $p<0.01$ for Lt side).

During maxillary expansion the posterior aspect of perpendicular plate of the palatine bone bent in a medial direction (Fig 64-65), by 5.1° and 6.4° (Rt and Lt side) in MSE patients ($p<0.01$), and by 1.7° and 1.8° (Rt and Lt side) in Hyrax patients ($p<0.05$ for Rt side and $p<0.01$ for Lt side). Bone bending was larger for MSE compared to Hyrax patients in both right and left sides ($p<0.05$ for Lt side).

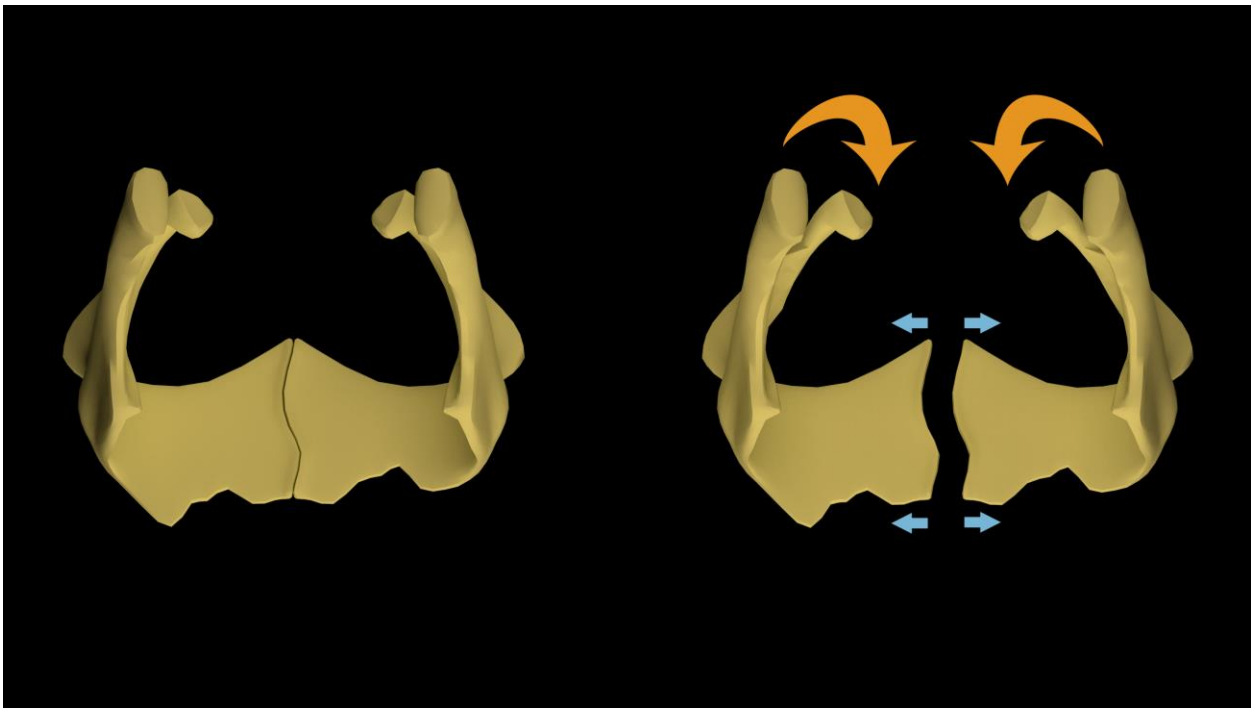

Fig. 64. Illustration showing the right and left palatine bone, anterior view. A: pre-expansion. B: post-expansion. During maxillary expansion the posterior aspect of perpendicular plate of the palatine bone (sphenoidal process) bent medially.

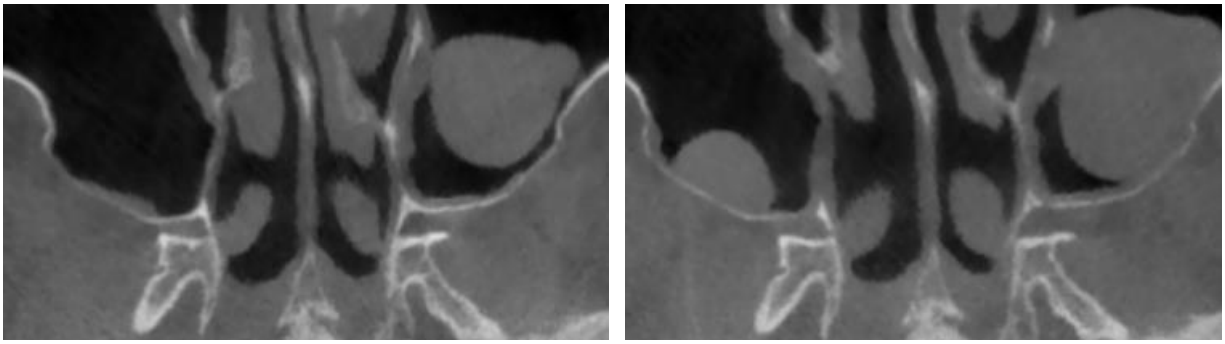

Fig. 65. Upper nasal section (UNS) of a MSE patient showing medial bending of the posterior aspect of perpendicular plate of the palatine bone. A: pre-expansion. B: post-expansion.

Pattern of lateral movement of the maxilla in the horizontal plane

If we consider the axial palatal section (APS) for MSE group, the lateral dislocation of Rt ANS and Lt ANS together was 4.8 mm, and the lateral dislocation of Rt PNS and Lt PNS together was 4.3 mm. The magnitude of expansion at PNS was 90% (4.3 / 4.8) of the expansion at ANS, indicating that the right and left borders of the midpalatal suture were nearly parallel to each other at the end of the expansion.

If we consider the upper nasal section (UNS) for MSE group, the average movement of the most anterior point of the maxilla (Rt side + Lt side) was 3.3 mm while the average movement of the most posterior point of the maxilla (Rt side + Lt side) was 1.8 mm. The average lateral movement of the posterior maxilla was 54% (1.8 / 3.3) of the expansion at the anterior maxilla, illustrating more “V-shaped” expansion than at the APS level, with more movement anteriorly than posteriorly. Fig 66 is a schematic illustration of the movement of maxilla in MSE patients.

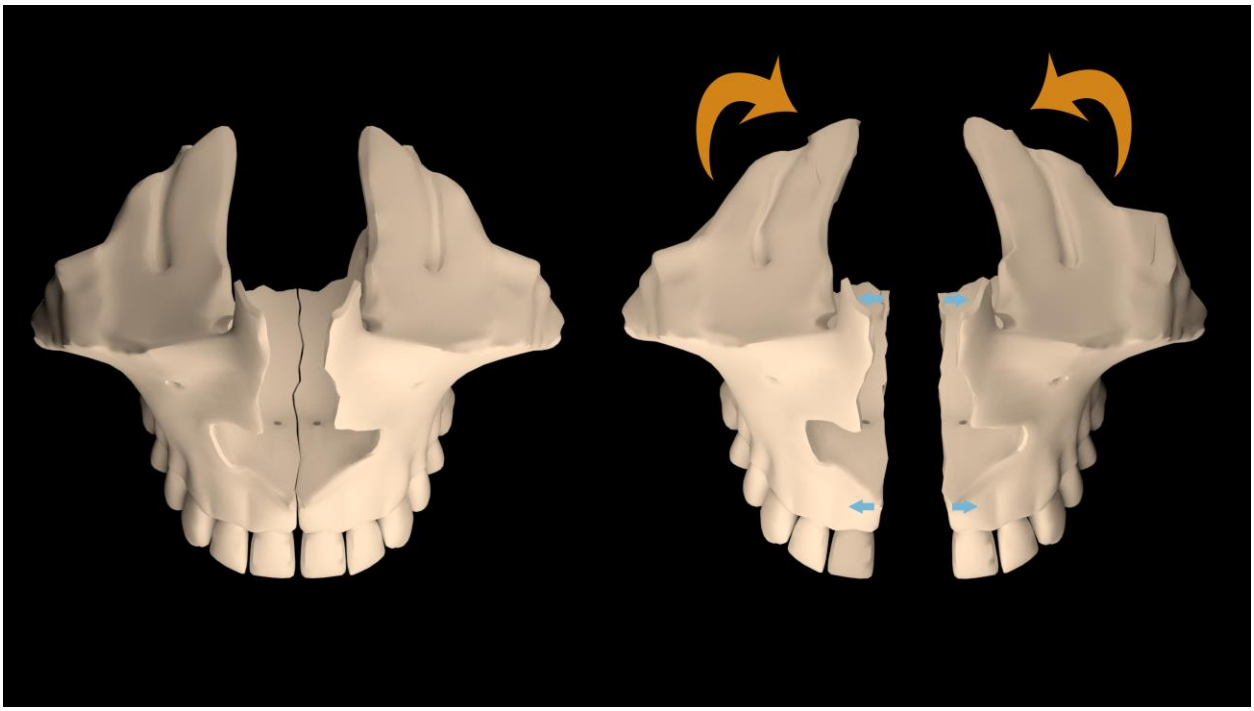

Fig. 66. Illustration of the right and left maxillary halves in MSE patients, anterior view. A: pre-expansion. B: post-expansion. In MSE patients, as the maxilla moves laterally, the borders of the midpalatal suture move almost perfectly parallel to each other, while the upper part of the maxilla moves in a “V-shape” fashion with more movement anteriorly than posteriorly. A torsion takes place within each maxillary bone, as the posterior and superior aspect of the maxilla is forced to bend medially, probably as a consequence of the articulation with circummaxillary bones.

If we do the same calculations for Hyrax patients, the magnitude of expansion at PNS (2.6 mm) was 83% of the one at ANS (3.1 mm) in the axial palatal section (APS), while the lateral movement of the posterior point of maxilla (0.7 mm) was 53% of the one at anterior point of the maxilla (1.3 mm) in the upper nasal section (UNS). Fig 67 is a schematic illustration of the movement of maxilla in Hyrax patients.

Fig. 67. Illustration of the right and left maxillary halves in Hyrax patients, anterior view. A: pre-expansion. B: post-expansion.

The split at PNS was 90% as large as the split at ANS for MSE patients, and it was 83% for Hyrax patients, indicating that the pattern of maxillary expansion in the horizontal plane is more parallel with MSE than with Hyrax appliance at APS level.

Lateral displacement of the pterygoid processes of the sphenoid bone

The lateral movement of the pterygoid processes was larger in LNS (0.7 mm for both Rt and Lt sides) than in UNS (0.4 mm for both Rt and Lt sides) in MSE patients. This indicated that the pterygoid process bent more in its lower level and less in its upper level in closer proximity to the cranial base (Fig 68).

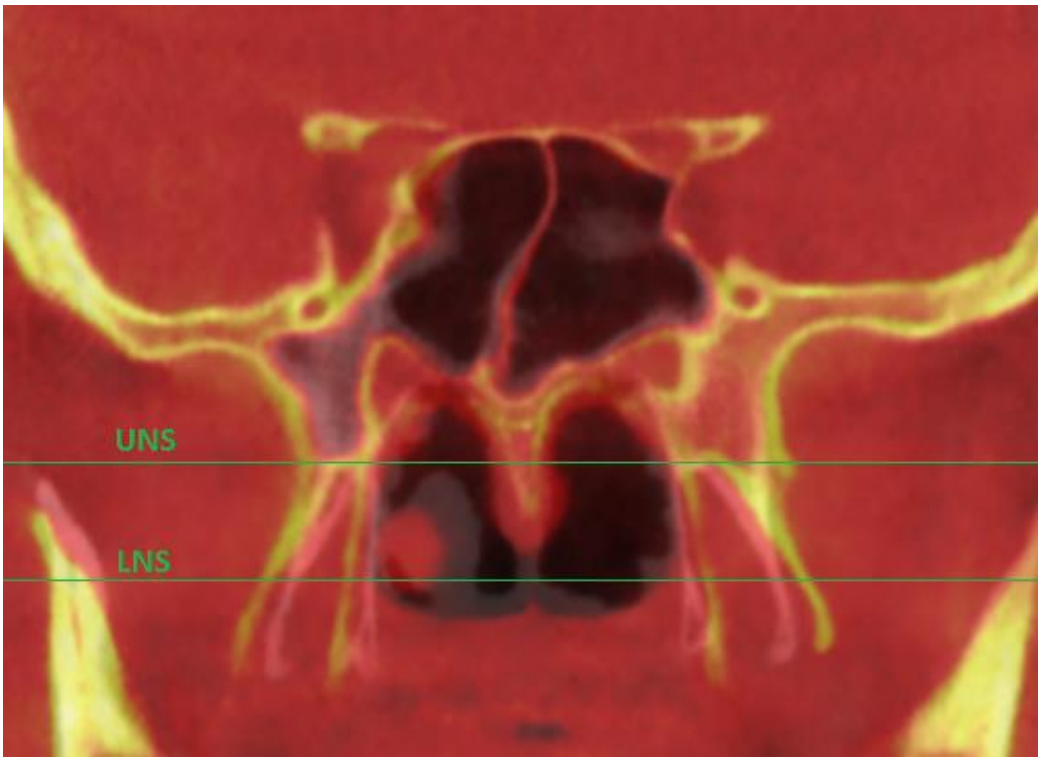

Fig 68. Superimposed images of a MSE patient (coronal view) showing the lateral bending of the pterygoid processes of sphenoid bone. White: pre-expansion. Yellow: post-expansion. The lateral movement is larger at the bottom, and smaller at the top of the processes. The green lines are the upper nasal section (UNS) and lower nasal section (LNS) where the distances from the maxillary sagittal plane to the pterygoid landmarks have been measured in the study.

In Hyrax patients, the lateral movement of the pterygoid processes was uniform and of small entity in both LNS and UNS (0.3 mm in both Rt and Lt side).

Analysis of variables in the coronal zygomatic section (CZS)

The results of variables analyzed in the coronal zygomatic section (CZS) are shown in table 17-19.

Table 17. Results for coronal zygomatic section (CZS): MSE group

		Before Expansion		After Expansion		Treatment Change		P Value	
		mean	sd	mean	sd	mean	sd	p-value	
Linear distances									
1	Upper inter-zygomatic distance	98.18	2.93	98.70	3.09	0.52	0.37	<.0001	**
2	Lower inter-zygomatic distance	86.14	4.88	90.76	5.66	4.62	1.33	<.0001	**
3	Inter-molar distance	38.58	3.53	46.91	3.46	8.33	2.29	<.0001	**
Angular measurements									
4	Right frontozygomatic angle (Rt FZA)	79.36	4.09	81.81	3.81	2.45	1.26	<.0001	**
5	Left frontozygomatic angle (Lt FZA)	77.94	2.64	80.85	2.79	2.91	1.39	<.0001	**
6	Right zygomaticomaxillary angle (Rt ZMA)	103.80	5.52	103.50	5.68	-0.23	0.88	0.324	
7	Left zygomaticomaxillary angle (Lt ZMA)	105.80	5.51	105.50	5.29	-0.35	0.96	0.175	
8	Right maxillary inclination (Rt Mx Incl)	96.61	4.85	98.63	5.31	2.01	1.03	<.0001	**
9	Left maxillary inclination (Lt Mx Incl)	97.25	4.42	99.74	4.64	2.49	1.81	0,000	**
10	Right molar basal bone angle (Rt MBBA)	90.21	8.36	88.17	10.24	-2.04	3.31	0.076	
11	Left molar basal bone angle (Lt MBBA)	89.67	8.45	87.85	11.50	-1.83	4.26	0.144	

** p<0.01 * p<0.05

Table 18. Results for coronal zygomatic section (CZS): Hyrax group

		Before Expansion		After Expansion		Treatment Change		P Value	
		mean	sd	mean	sd	mean	sd	p-value	
Linear distances									
1	Upper inter-zygomatic distance	100.00	3.21	100.20	3,15	0.21	0.17	0.029	*
2	Lower inter-zygomatic distance	86.56	6.67	88.89	7,75	2.33	1.14	0.004	**
3	Inter-molar distance	33.95	2.56	42.70	3.15	8.74	2.22	<.0001	**
Angular measurements									
4	Right frontozygomatic angle (Rt FZA)	78.43	3.27	79.78	3,37	1.35	0.46	0.001	**
5	Left frontozygomatic angle (Lt FZA)	78.13	4.30	79.03	4,19	0.90	0.57	0.012	*
6	Right zygomaticomaxillary angle (Rt ZMA)	97.30	3.67	97.15	3,18	-0.15	0.95	0.716	
7	Left zygomaticomaxillary angle (Lt ZMA)	98.10	4.54	98.30	4,18	0.20	0.69	0.508	
8	Right maxillary inclination (Rt Mx Incl)	88.75	6.71	90.22	6,86	1.47	0.86	0.009	**
9	Left maxillary inclination (Lt Mx Incl)	90.32	5.69	91.63	6,18	1.32	0.79	0.010	**
10	Right molar basal bone angle (Rt MBBA)	87.00	7.47	78.00	10.58	-9	4.68	0.005	**
11	Left molar basal bone angle (Lt MBBA)	84.23	11.52	75.88	11.37	-8.35	4.30	0.005	**

** p<0.01 * p<0.05

Table 19. Coronal zygomatic section (CZS):
T-test, difference between MSE and Hyrax groups

Parameter		P Value	
		p-value	
Linear distances			
1	Upper inter-zygomatic distance	0.067	
2	Lower inter-zygomatic distance	0.002	**
3	Inter-molar distance	0.712	
Angular measurements			
4	Right frontozygomatic angle (Rt FZA)	0.048	*
5	Left frontozygomatic angle (Lt FZA)	0.003	**
6	Right zygomaticomaxillary angle (Rt ZMA)	0.851	
7	Left zygomaticomaxillary angle (Lt ZMA)	0.215	
8	Right maxillary inclination (Rt Mx Incl)	0.266	
9	Left maxillary inclination (Lt Mx Incl)	0.148	
10	Right molar basal bone angle (Rt MBBA)	0.012	*
11	Left molar basal bone angle (Lt MBBA)	0.011	*

** $p<0.01$ * $p<0.05$

The upper inter-zygomatic distance increased by 0.5 mm in MSE patients ($p<0.01$) and by 0.2 mm in Hyrax patients ($p<0.05$). The inter-group difference was not statistically significant.

The lower inter-zygomatic distance increased by 4.6 mm in MSE patients ($p<0.01$) and by 2.3 mm in Hyrax patients ($p<0.05$). The inter-group difference was highly significant ($p<0.01$).

The inter-molar distance increased by 8.3 mm in MSE patients ($p<0.01$) and by 8.7 mm in Hyrax patients ($p<0.01$), and there was no statistically significant difference between the two groups.

The frontozygomatic angle (FZA) increased by 2.5° and 2.9° (Rt and Lt side) in MSE patients ($p<0.01$) and by 1.4° and 0.9° (Rt and Lt side) in Hyrax patients ($p<0.05$ for Lt side and $p<0.01$ for Rt side). The inter-group difference was statistically significant ($p<0.01$ for Lt side and $p<0.05$ for Rt side).

The zygomaticomaxillary angle (ZMA) changed by - 0.2° and - 0.4° (Rt and Lt side) in MSE patients and by - 0.2° and + 0.2° (Rt and Lt side) in Hyrax patients. The changes were not statistically significant in both groups.

The maxillary inclination (Mx Incl) increased by 2.0° and 2.5° (Rt and Lt side) in MSE patients ($p<0.01$) and by 1.5° and 1.3° (Rt and Lt side) in Hyrax patients ($p<0.01$). However, there was no statistically significant difference between the two groups.

The molar basal bone angle (MBBA) changes show that molars tipped buccally by 9.0° and 8.4° (Rt and Lt side) in Hyrax patients ($p<0.01$), while they tipped only by 2.0° and 1.8° (Rt and Lt side) in MSE patients without statistical significance.

Figure 69 and 70 illustrate the center of rotation for the zygomaticomaxillary complex in the coronal plane and the changes in the midface structures.

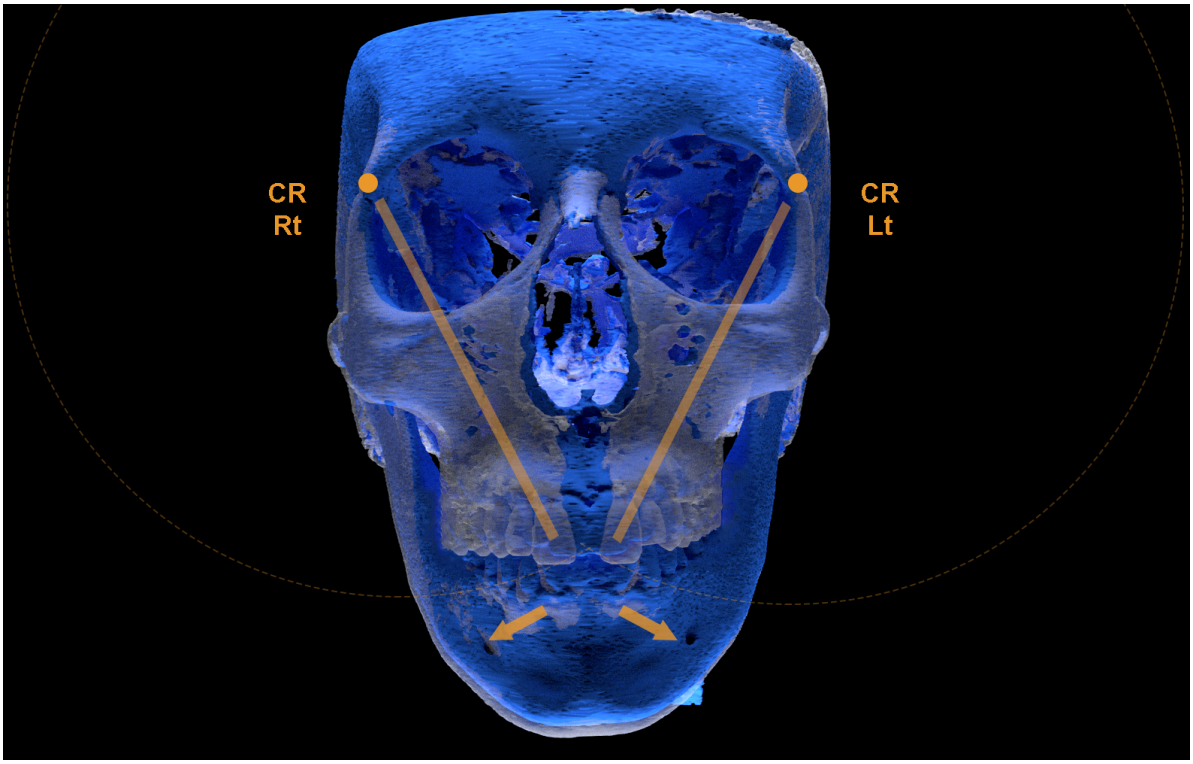

Fig. 69. Superimposed 3D images of a MSE patient showing the rotation of the zygomaticomaxillary complex with a center of rotation (CR) located near the frontozygomatic suture. Blue: pre-expansion. White: post-expansion.

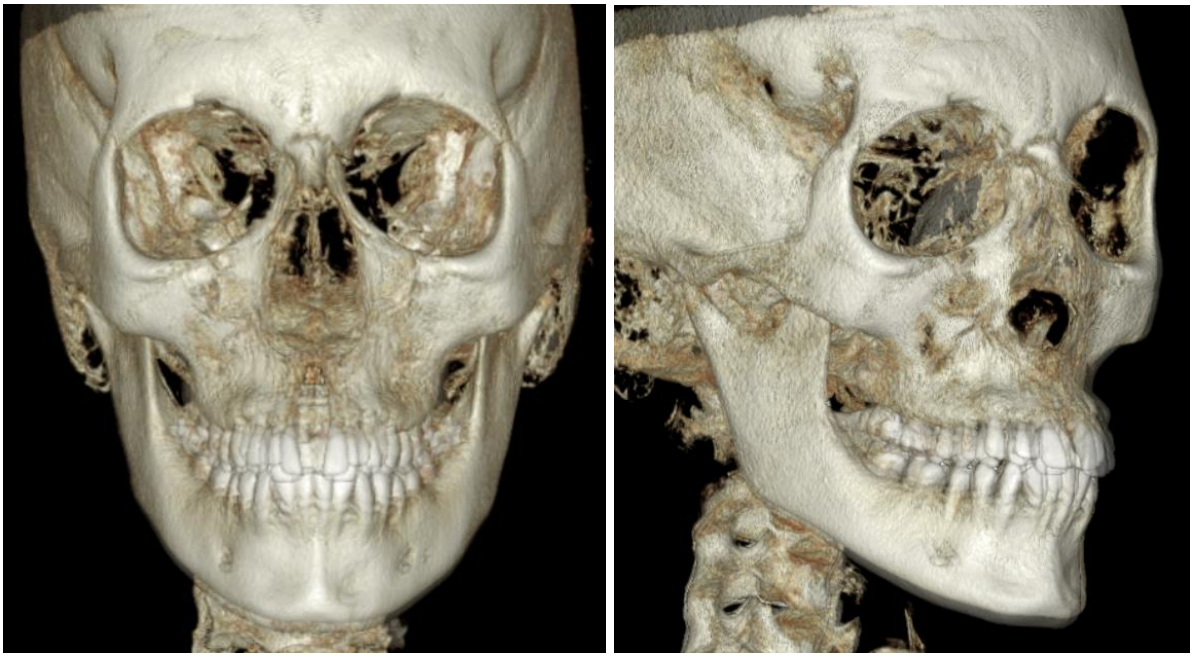

Fig 70. Superimposed 3D renderings of a MSE patient showing the midfacial changes in the coronal plane. A: frontal view. B: 3/4 view.

Pattern of lateral movement of the maxillary bone in the coronal plane

The pattern of lateral movement of the maxilla is described by the ratio between the increase of the maxillary inclination (average of right and left side) and the increase of the lower inter-zygomatic distance.

The parameter maxillary inclination (Mx incl) represents the inclination of the maxilla relatively to the maxillary sagittal plane (MSP). In MSE patients, the maxillary inclination increased by 2.25° (average of right and left side) after the expansion.

In Hyrax patients, the maxillary inclination increased by 1.4° (average of right and left side).

Maxillary inclination increased during the expansion because the lateral displacement of the maxilla is not a translational movement, but rather a rotatory movement displacing the zygomaticomaxillary point laterally and superiorly. The more the maxilla and zygomatic bone move laterally, the most lateral points of the maxilla will move laterally and superiorly while medial points will move laterally and inferiorly, causing the maxillary inclination measurements to increase.

The increase in the lower inter-zygomatic distance expresses the lateral displacement of the right and left zygomaticomaxillary complex at the level of the lowest point of the zygomaticomaxillary suture.

The ratio between the increase in maxillary inclination and the increase in the lower inter-zygomatic distance was 0.5°/mm (2.25°/4.62mm) for MSE and 0.6°/mm (1.4°/2.33mm) for Hyrax patients. This indicates that for each mm of increase in the lower inter-zygomatic distance the rotation of the maxilla was approximately 0.5° in

MSE and 0.6° in Hyrax patients, as shown in Fig 71-72. In the coronal plane, the pattern of lateral movement of the maxilla was more parallel with MSE than with Hyrax.

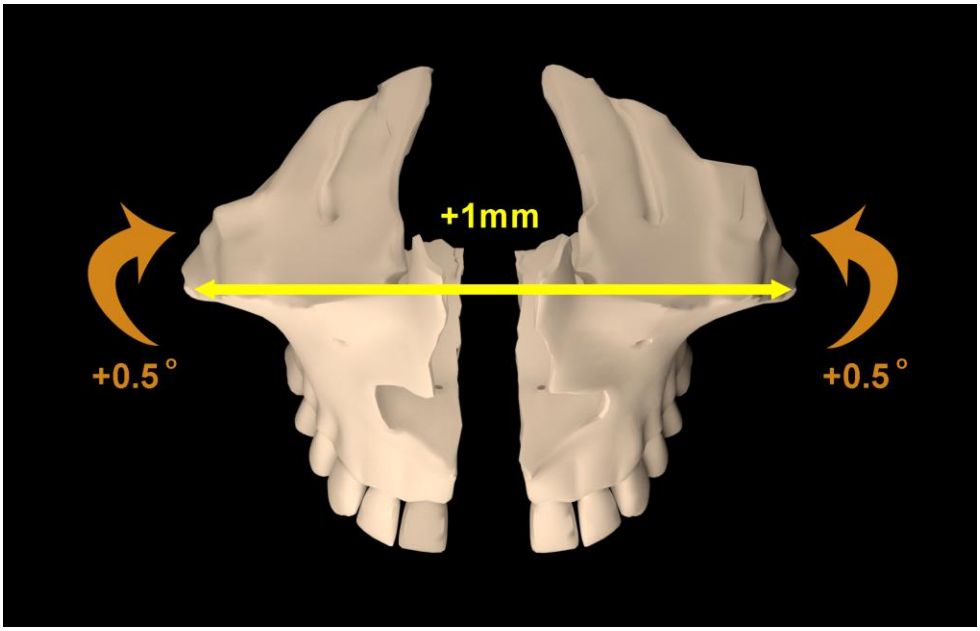

Fig 71. Pattern of lateral movement of the maxilla in the coronal plane for MSE group. For each mm of increase in the lower inter-zygomatic distance, the maxilla rotated 0.5°.

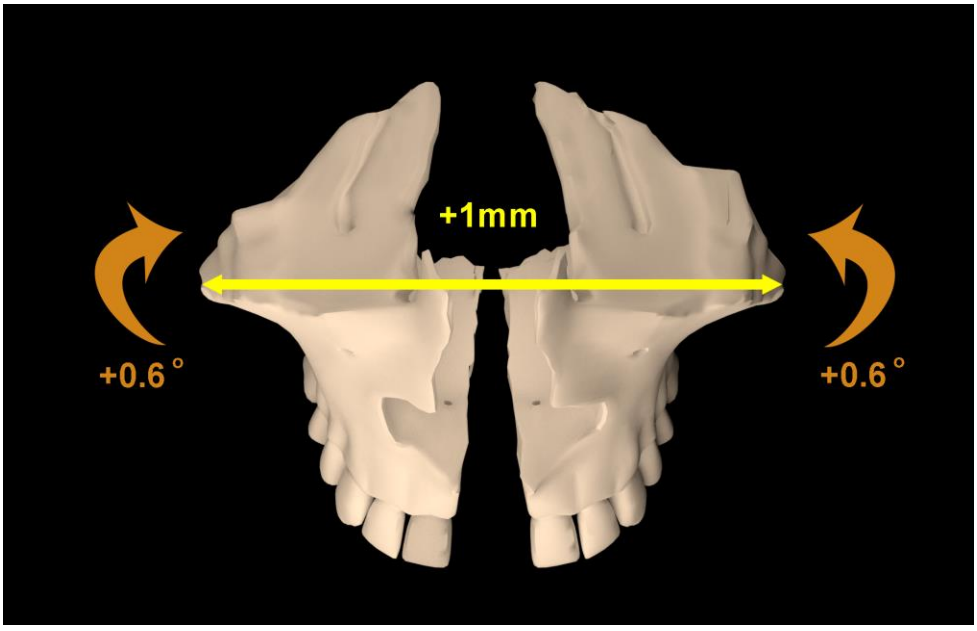

Fig 72. Pattern of lateral movement of the maxilla in the coronal plane for Hyrax group. For each mm of increase in the lower inter-zygomatic distance, the maxilla rotated 0.6°.

Analysis of variables in the axial zygomatic section (AZS)

The results of variables analyzed in the axial zygomatic section (AZS) are shown in table 20-22.

Table 20. Results for axial zygomatic section (AZS): MSE group

		Before Expansion		After Expansion		Treatment Change		P Value	
		mean	sd	mean	sd	mean	sd	p-value	
Linear distances									
1	Anterior inter-maxillary distance	17.05	3.06	19.81	3.11	2.76	1.51	<.0001	**
2	Posterior inter-zygomatic distance	111.80	4.99	114.20	5.34	2.35	0.58	<.0001	**
Angular measurements									
3	Right zygomaticotemporal angle (Rt ZTA)	134.20	5.81	134.10	6.08	-0.15	1.09	0.612	
4	Left zygomaticotemporal angle (Lt ZTA)	134.30	6.05	134.30	5.63	-0.06	1.53	0.882	
5	Right angle of the zygomatic process (Rt ZPA)	87.16	4.71	88.90	5.18	1.74	1.07	<.0001	**
6	Left angle of the zygomatic process (Lt ZPA)	86.62	5.29	88.75	6.00	2.13	1.57	0.000	**

** p<0.01 * p<0.05

Table 21. Results for axial zygomatic section (AZS): Hyrax group

		Before Expansion		After Expansion		Treatment Change		P Value	
		mean	sd	mean	sd	mean	sd	p-value	
Linear distances									
1	Anterior inter-maxillary distance	16.51	2.51	18.28	2.40	1.77	1.32	0.022	*
2	Posterior inter-zygomatic distance	113.50	6.59	114.60	6.87	1.17	0.60	0.005	**
Angular measurements									
3	Right zygomaticotemporal angle (Rt ZTA)	136.40	5.83	136.50	5.37	0.08	0.69	0.780	
4	Left zygomaticotemporal angle (Lt ZTA)	135.30	3.53	135.50	3.75	0.23	0.52	0.322	
5	Right angle of the zygomatic process (Rt ZPA)	87.37	6.02	88.25	6.01	0.88	0.88	0.057	
6	Left angle of the zygomatic process (Lt ZPA)	86.07	3.76	86.90	3.79	0.83	0.91	0.074	

** p<0.01 * p<0.05

Table 22. Axial zygomatic section (AZS):
T-test, difference between MSE and Hyrax groups

Parameter		P Value	
		p-value	
Linear distances			
1	Anterior inter-maxillary distance	0.179	
2	Posterior inter-zygomatic distance	0.001	**
Angular measurements			
3	Right zygomaticomaxillary angle (Rt ZTA)	0.641	
4	Left zygomaticomaxillary angle (Lt ZTA)	0.656	
5	Right angle of the zygomatic process (Rt ZPA)	0.099	
6	Left angle of the zygomatic process (Lt ZPA)	0.074	

** p<0.01 * p<0.05

The anterior inter-maxillary distance increased by 2.8 mm in MSE patients ($p<0.01$) and by 1.8 mm in Hyrax patients ($p<0.05$). The inter-group difference was not statistically significant.

The posterior inter-zygomatic distance increased by 2.4 mm in MSE patients ($p<0.01$) and by 1.2 in Hyrax patients ($p<0.01$). The increase in MSE was significantly more than in Hyrax group ($p<0.01$).

The zygomaticotemporal angle (ZTA) underwent changes by -0.2° and -0.1° (Rt and Lt sides) in MSE patients and by 0.1° and 0.2° (Rt and Lt sides) in Hyrax patients. The changes were not statistically significant in both groups.

The angle of the zygomatic process of the temporal bone (ZPA) increased by 1.7° and 2.1° (Rt and Lt sides) in MSE patients and by 0.9° and 0.8° (Rt and Lt sides) in Hyrax patients. The increase was statistically significant in MSE patients ($p<0.01$) but not in Hyrax patients.

Figure 73 and 74 illustrate the center of rotation for the zygomaticomaxillary complex and the changes in the midface structures in the horizontal plane for the MSE group. Fig. 75 shows the center of rotation for the maxilla in Hyrax patients.

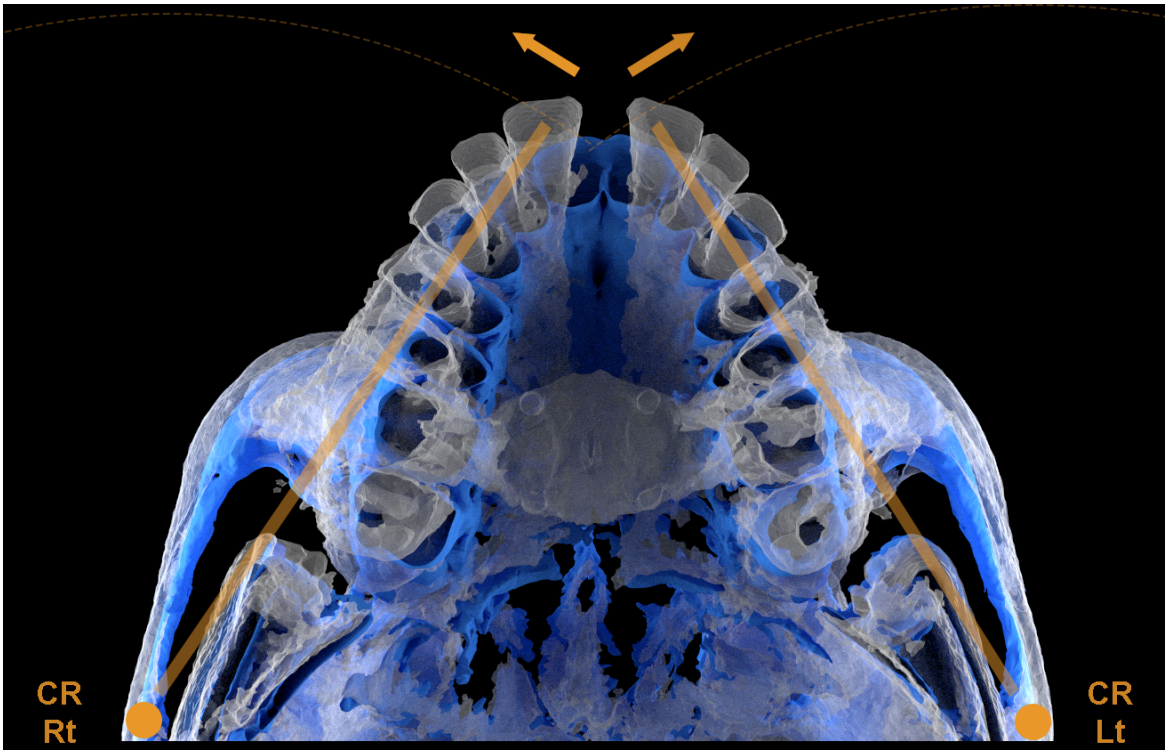

Fig 73. Superimposed 3D images of a MSE patient showing the rotation of the zygomaticomaxillary complex with a center of rotation (CR) located near the proximal aspect of the zygomatic process of the temporal bone. Blue: pre-expansion. White: post-expansion.

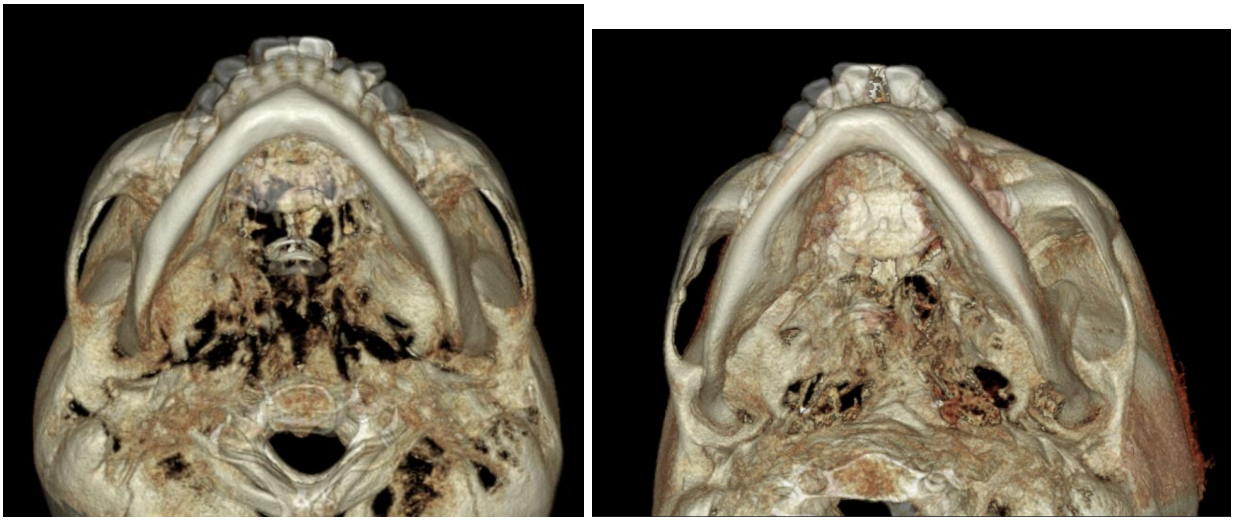

Fig 74. Superimposed 3D renderings of a MSE patient showing the changes in the midface in a horizontal plane. A: lower view. B: lower 3/4 view.

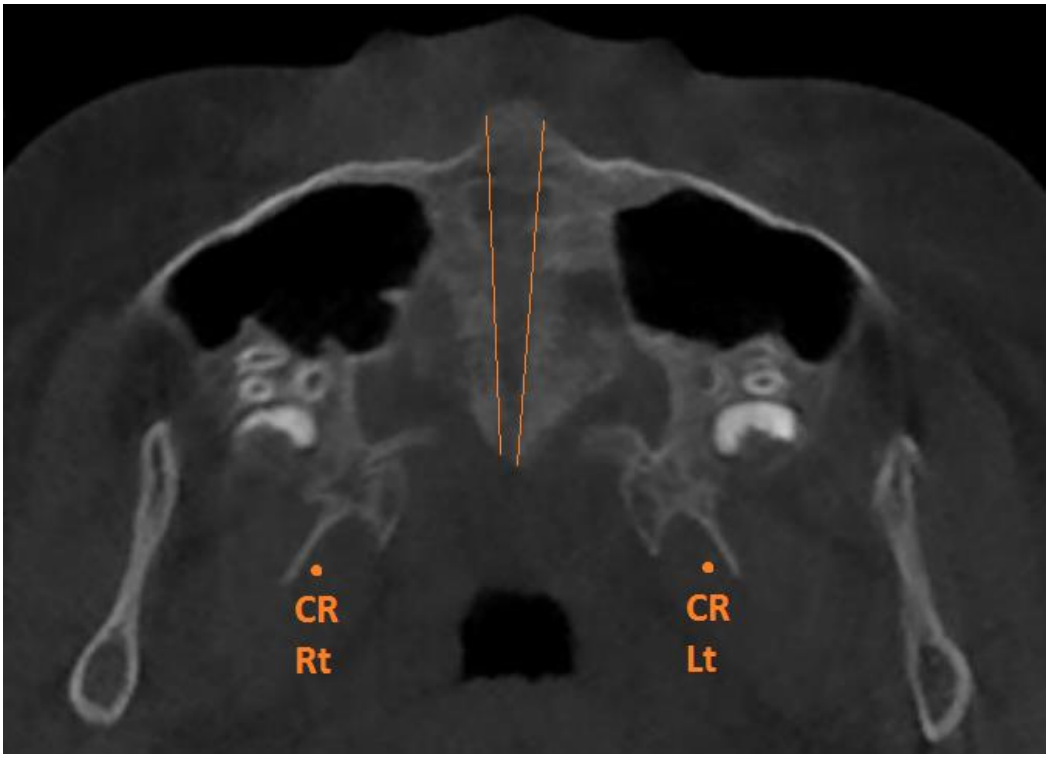

Fig 75. Axial palatal section showing the center of rotation for the maxilla in Hyrax patients.

In order to better visualize the displacements of the maxillary and zygomatic bones, illustrations have been made to demonstrate the treatment change of the maxillary and zygomatic landmarks (Fig 76-83). The illustrations display the quantity of landmark displacement in proper scale maintaining correct proportion of the movements.

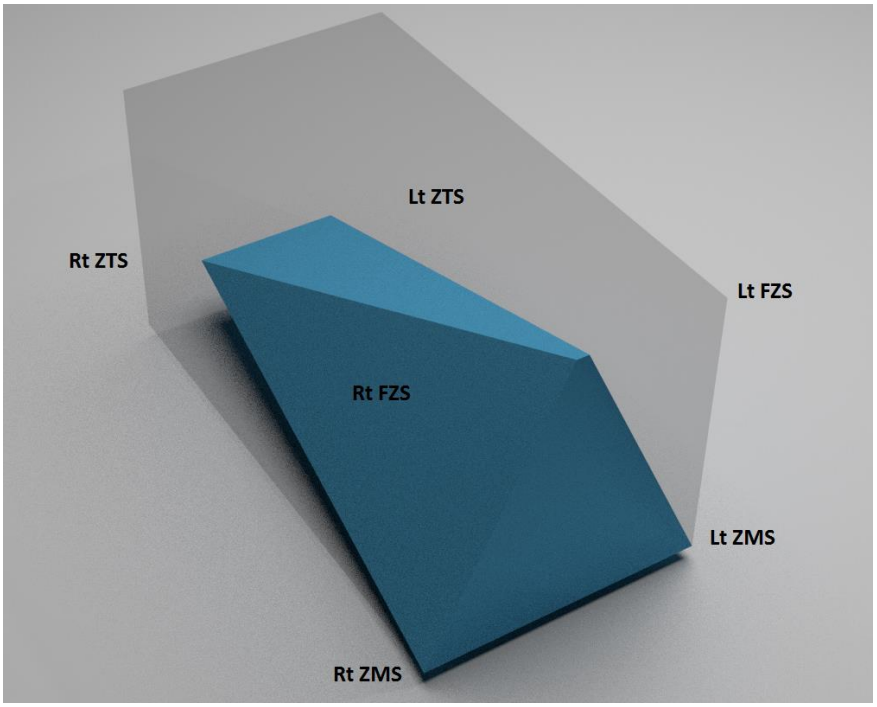

Fig 76. Illustration showing the treatment change in zygomatic landmarks for MSE patients. ZMS: zygomaticomaxillary suture; ZTS: zygomaticotemporal suture; FZS: frontozygomatic suture.

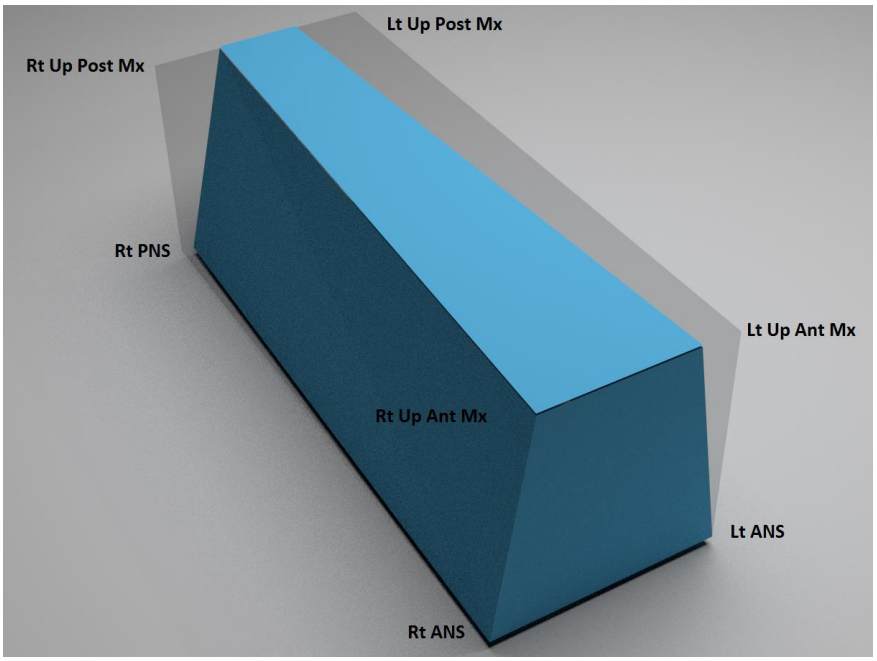

Fig 77. Illustration showing the treatment change in maxillary landmarks for MSE patients. ANS: anterior nasal spine; PNS: posterior nasal spine; Up Ant Mx: most anterior point of maxilla in UNS; Up Post Mx: most posterior point of maxilla in UNS.

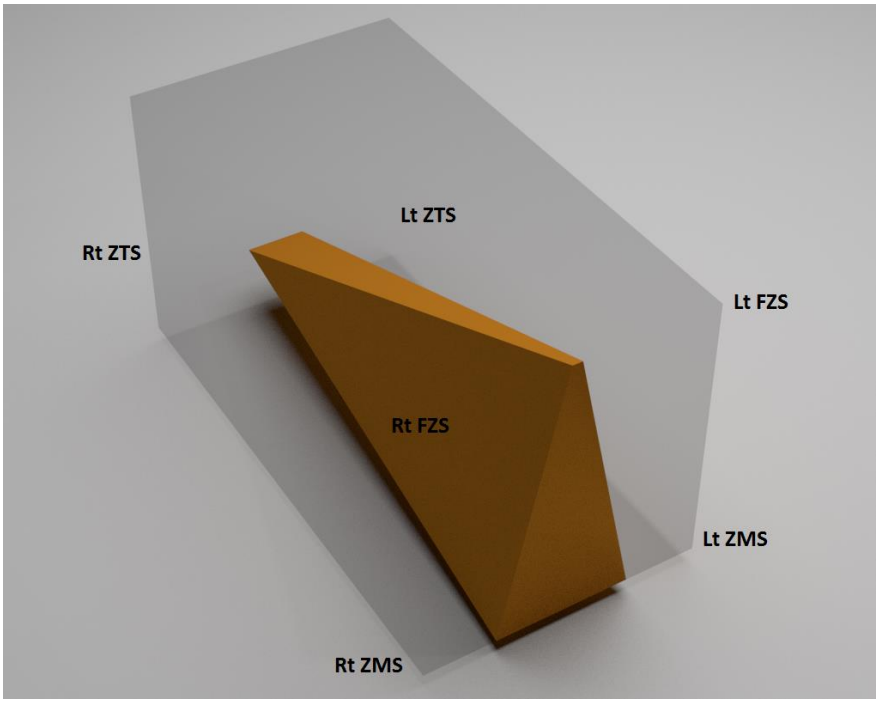

Fig 78. Illustration showing the treatment change in zygomatic landmarks for Hyrax patients. ZMS: zygomaticomaxillary suture; ZTS: zygomaticotemporal suture; FZS: frontozygomatic suture.

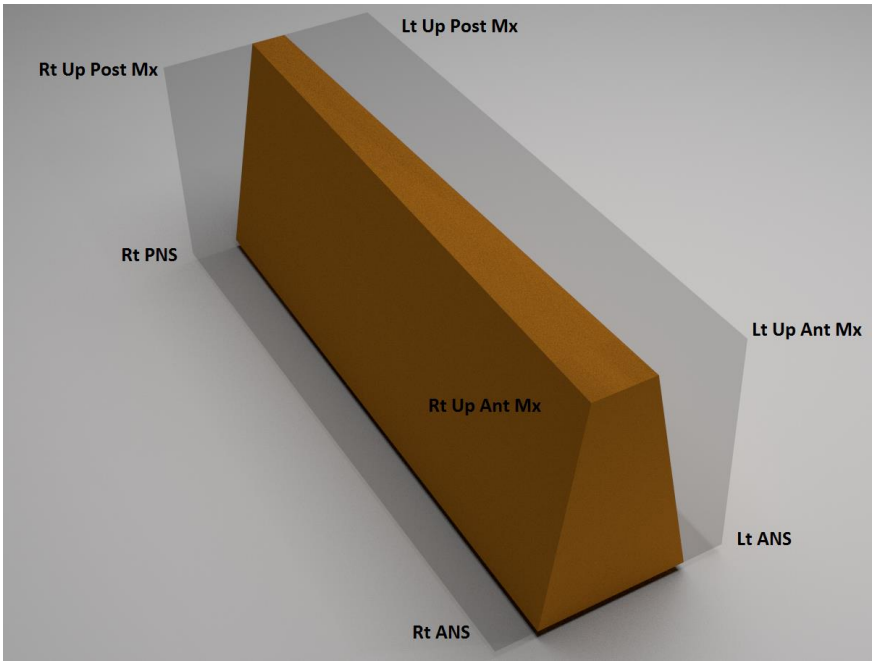

Fig 79. Illustration showing the treatment change in maxillary landmarks for Hyrax patients. ANS: anterior nasal spine; PNS: posterior nasal spine; Up Ant Mx: most anterior point of maxilla in UNS; Up Post Mx: most posterior point of maxilla in UNS.

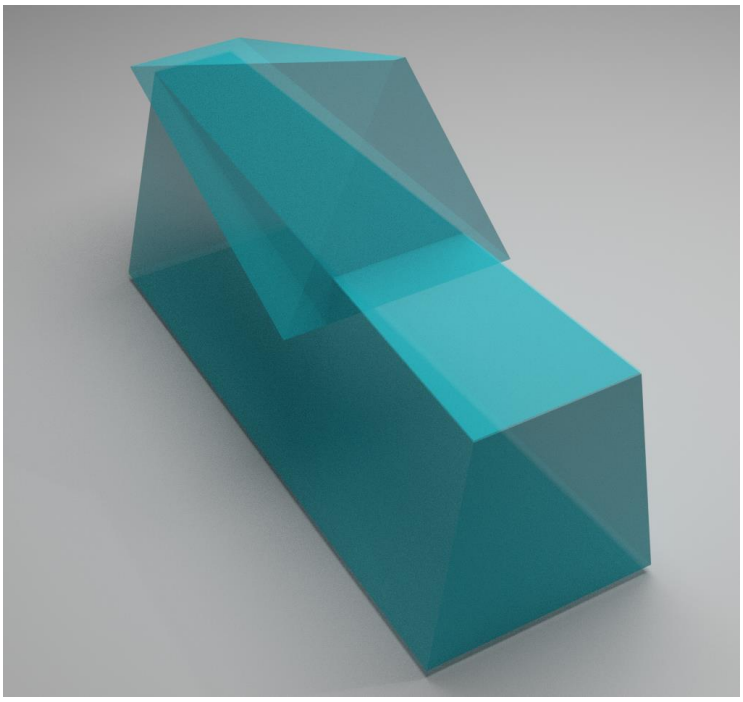

Fig 80. Illustration showing the treatment change in the zygomatic and maxillary landmarks for MSE patients.

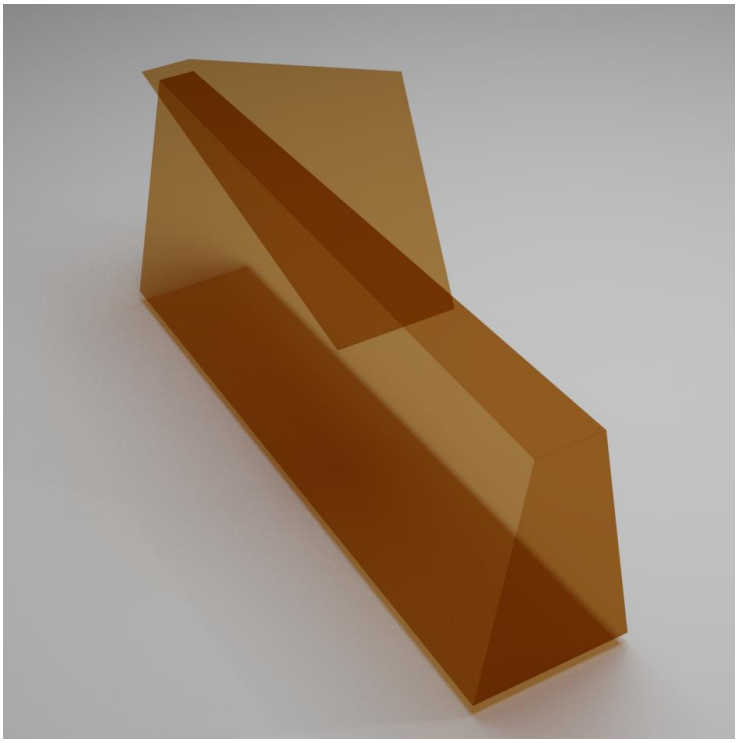

Fig 81 Illustration showing the treatment change in the zygomatic and maxillary landmarks for Hyrax patients.

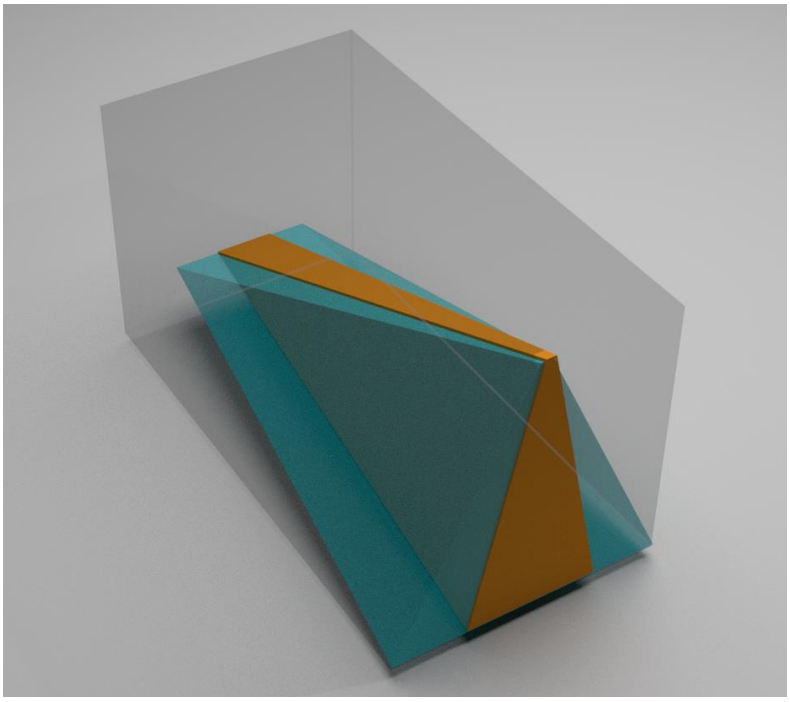

Fig 82. Illustration showing a comparison of the treatment change in the zygomatic landmarks: MSE (light blue) versus Hyrax (brown) patients.

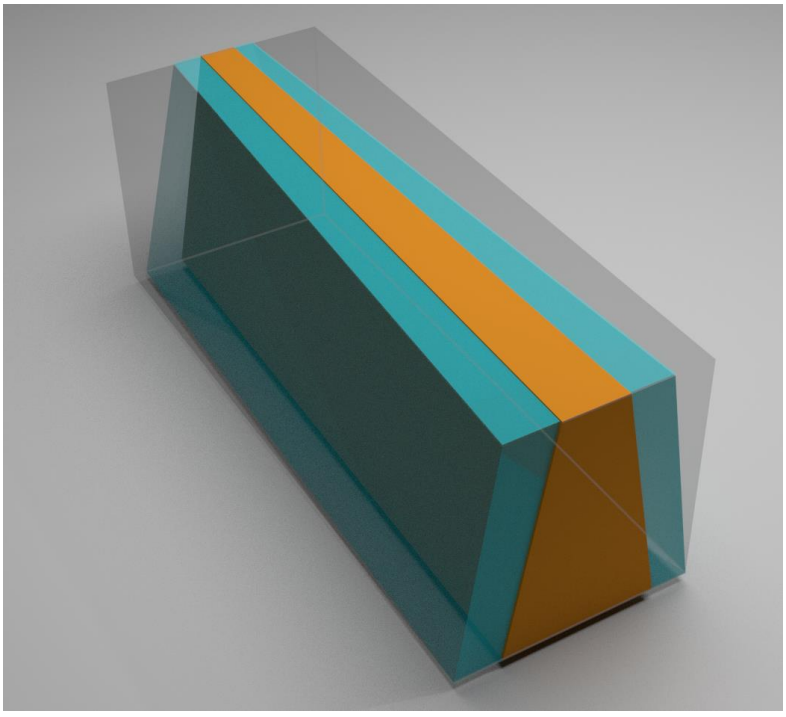

Fig 83. Illustration showing a comparison of the treatment change in the maxillary landmarks: MSE (light blue) versus Hyrax (brown) patients.

Statistical Analysis: Reliability

The coefficient of variation (CV) was at least 1.4% or less for linear parameters and at least 1.3% or less for angular parameters.

The intraclass correlation coefficient (ICC) was at least 98.5% or more for linear parameters and at least 94.4% or more for angular parameters.

DISCUSSION

3D measurements

Traditionally, cephalometric superimpositions were most widely used and considered to be the best way to quantitatively assess the skeletal and dental changes associated with orthodontics. Stable structures described by Bjork [107], Bjork and Skieller [108-110] and Doppel [111], are used as registration and orientation landmarks. Dislocations of bones can be described relative to those reference structures [112]. However, with the advent of cone beam computed tomography (CBCT) and the development of novel computer software in modern days, it is possible to optimally align and therefore superimpose 3D CBCT data sets at different time points with subvoxel accuracy after identification of the cranial base structures [100]. The analysis of changes due to treatment, growth, aging, and post-treatment relapse in all three dimensions of the space is possible by using this technology [113]. The superimposition method used in the present study is fully automated with voxel-wise rigid registration of the entire surface of the cranial base for adults and of the anterior cranial fossae for growing children. The superimposition is automated in order to avoid observer-dependent techniques based on overlap of anatomic landmarks. This automated method compares the grey level intensity of each voxel in the cranial base to establish the best fit for the superimposition of the pre- and post-treatment CBCTs, allowing the image analysis to become largely independent of the observer errors [98,99,113] . OnDemand3D™ Software by Cybermed Inc. allows visual and quantitative assessment of the landmark locations and magnitude of location changes over time via graphic overlays, and calculation of the distance and angular measurements between two or three time points.

Reference planes

In the present study three novel reference planes were produced: the maxillary sagittal plane (MSP), axial palatal plane (APP) and V-coronal plane (VCP). A novel quantitative methodology was developed in order to establish a procedure that enables analysis of the movements of various skeletal structures induced by rapid palatal expansion. Landmarks were tested for inter-rater reliability with Intraclass Correlation Coefficient (ICC). ICC has been at least 98.5% and higher for linear parameters and at least 94.4% and higher for angular parameters, showing a high reliability. Furthermore, this methodology can be used for analyzing patients with severe skeletal asymmetry. The main reference plane is the maxillary sagittal plane (MSP), which passes through the anterior nasal spine, posterior nasal spine and Nasion. This plane crosses the "center of the face" and the center of the midpalatal suture, where the movement of the bones in midface originate during the maxillary expansion. During the expansion, the bones move away from the maxillary sagittal plane, and using this reference point to describe the linear and angular changes of the maxillary and circummaxillary bones makes the analysis more clear than the traditional planes related to the structures in cranial base. The use of the maxillary sagittal plane combined with the superimposition technique utilizing the gray scales of the anterior cranial base allowed accurate superimposition of pre- and post-expansion CBCTs and detailed description of how the midpalatal sutures split (symmetric versus asymmetric expansion) for the first time.

Split of the midpalatal suture and movement of maxillary bones in the coronal and horizontal planes

We analyzed the split of the midpalatal suture in the axial palatal section (APS). Interestingly, we found that the midpalatal suture splits in a symmetrical way only in 27% of the cases in MSE patients and in 33% of the cases in Hyrax patients if we consider 0.5 mm as a parameter to distinguish between the symmetrical and asymmetrical expansion. We also found that, on average, one half of ANS moves more than the contralateral one by 1.1 mm in MSE patients and 1.3 mm in Hyrax patients. The reason why the midpalatal suture splits in an asymmetrical way is unknown. One reason could be that external forces, for example due to the occlusion in the presence of a unilateral cross bite, can hamper the movement of one side of the maxilla. Another contributing factor can be the surrounding structures. In order for the maxillary bones to move, several circummaxillary sutures must be disarticulated and other perimaxillary structures must be displaced on both sides of the skull. More movement of the maxilla can take place on the side of the skull with less challenging circummaxillary resistance.

We also found that the midpalatal suture always split both in MSE and Hyrax group. This is important if we consider that MSE patients were in their post-pubertal age, and there is no consensus in the literature regarding the possibility of splitting the midpalatal suture at this age with conventional RPE appliances. The use of four micro-implants in the MSE with bi-cortical engagement promotes the separation force to be concentrated directly against the maxillary bones, minimally loading on dentition, and this leads to the split of the interlocked sutures even in mature stage patients.

Several studies reported that the separation of the maxillary bones occur in a triangular manner (V-shaped) in the coronal plane, with the apex toward the nasal cavity and the base at the same level as the palatine processes [6,38,62-68]. In the horizontal plane, the greatest opening of the midpalatal suture has been found anteriorly, with progressively less separation towards its posterior part [1,2,6,69-71]. However, FEM studies analyzed the separation of maxillary bones also in more cranial sections (i.e. at the level of the frontal process of the maxilla) and found that more parallel expansion can be achievable [19,49,50]. Magnusson [114] recently reported a non-uniform transverse expansion with substantially larger expansion posteriorly than anteriorly.

In the present study we used three axial slices on the CBCTs (APS, LNS, UNS) in order to analyze the movement of the maxillary bones at the level of the midpalatal suture and beyond. Landmarks have been identified in the bones and their distance from the maxillary sagittal plane has been measured in the pre- and post-expansion CBCTs. The treatment change was equivalent to the lateral movement of each landmark.

Our results in the Hyrax group agree with the above mentioned literature, producing V-shaped expansion in both horizontal and coronal planes.

However, in the MSE group, the borders of the midpalatal suture moved almost perfectly parallel to each other in the axial palatal plane, and the movement of maxillary bones became progressively more “V-shaped’ with more movement anteriorly than posteriorly in the lower nasal section and upper nasal section. In MSE patients probably a torsion takes place along the vertical axis of the maxilla, as the posterior and superior aspect of the maxilla is forced to bend medially during the expansion as shown in

Fig 66. This is probably due to greater level of resistance against expansion offered by circummaxillary structures, particularly the sphenoid and the zygomatic bone. Such concepts were also offered by other authors [37,38], some even achieved a more parallel expansion of the midpalatal suture as well [18,19,49,115]. The fact that four micro-implants are utilized in the MSE, placed more posteriorly than other expansion devices, promotes these two halves to move parallel to each other in a translational manner during the maxillary expansion.

In the coronal plane, the pattern of lateral movement was evaluated by the ratio between the increase in maxillary inclination (the average of right and left side) and the increase of the inter-zygomatic distance. As the zygomaticomaxillary complex is laterally displaced, the maxilla rotates 0.5° in MSE and 0.6° in Hyrax patients for each mm of increase of the lower inter-zygomatic distance, indicating more parallel pattern of movement with MSE appliance (Fig 71-72).

Overall, MSE resulted in a more parallel movement of maxillary bones both in the horizontal and coronal planes in 3D space (Fig 77, 79, 83), compared to Hyrax appliance.

Changes in the pterygopalatine suture

As the maxilla is attached posteriorly to the sphenoid bone via the palatine bone, the pterygopalatine suture has been object of study by several authors during maxillary expansion [22,48,50,51,77,78]. The pterygopalatine suture can be divided in three parts (Fig 16 and 17). In the lower part, the pyramidal process of the palatine bone articulates with the pterygoid notch located between the lateral and medial plate of the

pterygoid process. The axial palatal section (APS) was designed to cut through this area in this study. In the middle part, the posterior border of the perpendicular plate of the palatine bone articulates with the anterior surface of the pterygoid process of the sphenoid. The lower nasal section (LNS) was designed to cut through this area for analysis in our study. In the upper part, the perpendicular plate of the palatine bone articulates with the medial surface of the pterygoid process of the sphenoid. This part was analyzed with the upper nasal section (UNS) in our study.

In the literature, some studies focused on the pterygopalatine suture only at the level of the approximation between the tuberosity of the maxilla and of the pterygoid process, and form their conclusions based on if the pterygopalatine suture can be separated or not [19,44,46,84]. Other studies also have analyzed the inclination change in the pterygoid processes of the sphenoid and illustrated a possible bending of these processes during maxillary expansion, in order to describe the process more accurately [22,48,50,51,63,76,77,82,83].

In the present study, we used three axial sections (APS, LNS, UNS) in order to thoroughly analyze what happened in these three levels of the pterygopalatine suture during maxillary expansion. In the axial palatal section, the frequency and width of openings detectable in the post-expansion CBCT were assessed and used as the indicators for the loosening of pterygopalatine suture. In the lower nasal section, the lateral slide of the tuberosity relative to the pterygoid process was used as an indicator for the loosening of the pterygopalatine suture; while in the upper nasal section, the medial bending of the perpendicular plate of palatine bone has been analyzed for the same purpose.

For the Hyrax group, the pterygopalatine openings were detectable only in 17% of the sutures and the width of the openings after expansion was negligible in the axial palatal section. Both the frequency and the width of openings were not statistically significant. In the lower nasal section, the lateral slide in the pterygomaxillary fissure was quite small (0.1 mm in Rt side and 0.3 mm in Lt side) and only the left side was statistically significant. In the upper nasal section, the medial bending of the perpendicular plate of the palatine bone was 1.7° and 1.8° (Rt and Lt side) with statistical significance.

In Hyrax group, the pterygoid processes of the sphenoid bone bent laterally by 0.3 mm and 0.2 mm (Rt and Lt side) in the lower nasal and upper nasal sections. Although these values were with statistical significance, the magnitude of the change was negligible.

From the results above, it appears that the significant changes in the pterygopalatine suture for the Hyrax group is the lateral bending of the pterygoid processes of the sphenoid bone and the medial bending of the perpendicular plate of the palatine bones, although their magnitudes were small. Other Authors also have found that the pterygoid processes of the sphenoid bone bend laterally during maxillary expansion [22,48,50,51,63,77]. Lione [77] and Timms [63] concluded that the width between the pterygoid processes of the sphenoid bone was significantly increased after RPE therapy in humans. These findings were recently supported by Gautam [50], Jarafi [48] and Baldawa [51] in their 3D FEM studies based on cone beam computed tomography (CBCT) of a 7, 12 and 20 years old human skull respectively. All of these studies agree that the pterygoid processes can be displaced laterally, but do not detach from the body of the sphenoid bone.

For MSE group, the openings between the lateral and the medial pterygoid plates were observed in 60% of the patients and in 53% of the sutures ($p<0.01$) in the axial palatal section. The mean size of the openings was 1.3 mm and 2.2 mm (Rt and Lt side), both with statistical significance. Openings are due to the fact that during maxillary expansion the pyramidal process of the palatine bone is pulled out of the pterygoid notch leaving the “openings” between the lateral and medial pterygoid plates of the pterygoid processes, detectable on the CBCTs. This indicates a loosening of the lower part of the pterygopalatine suture with MSE. The size of opening depends on the size of the pyramidal process of the palatine bone, which presents large variability in shape and size among the population [116]. If a partial disengagement of the pyramidal process from the pterygoid process occurs, such as in the case where only a minor movement of the maxilla was required, the opening does not become complete and hence presents a smaller size. In the case of a complete disengagement, the size of the opening becomes much larger. In the lower nasal section, the lateral slides between the posterior aspect of the tuberosity and pterygoid process were 0.6 mm on the right side and 0.7 mm on the left side, both with statistical significance, indicating that the sutures were loosened even at this level. Sometimes a clear separation was visible in the post-expansion CBCT of MSE patients as shown in Fig 29 and 63. This separation is also due to the fact that the posterior maxillary landmarks moved forward by 0.8 mm and 1.0 mm (Rt and Lt side) while the pterygoid process did not show a forward displacement. A clear separation between the tuberosity and pterygoid process was not visible in the CBCT of Hyrax patients, indicating suture disarticulation did not occur for this group unlike the MSE group.

Lastly, the posterior aspect of the perpendicular plate of the palatine bone was bent medially by 5.1° and 6.4° (Rt and Lt side) ($p<0.01$) in the upper nasal section. As the maxilla moves laterally during expansion, the palatine bone is pulled laterally by the expanding maxilla; however, the posterior aspect of perpendicular plate of the palatine bone (sphenoidal process) cannot move laterally because it articulates with the medial surface of perpendicular plate of the sphenoid bone. As a consequence, the sphenoidal process is forced to bend in a medial direction (Fig 64 and 65).

In MSE patients, the pterygoid processes of the sphenoid bone were bent laterally and this distortion was much larger than in Hyrax patients. The lateral movement of the pterygoid process was smaller in the upper nasal section (0.4 mm and 0.5 mm) than in the lower nasal section (0.7 mm) in the MSE group, as shown in Fig 68. The lateral movement of the pterygoid processes was larger in its lower part than the upper part. Bishara [22] reported that the pterygoid processes are subject to bending anteriorly during RPE; however, our study did not show a forward movement of the pterygoid process.

If we compare MSE with Hyrax patients, the size and frequency of the openings were statistically significant in the MSE group in the axial palatal section, but not with Hyrax patients; the lateral slide in the pterygomaxillary fissure was larger in MSE patients than in Hyrax patients in the lower nasal section; and the medial bending of the perpendicular plate of the palatine bone was larger in MSE than in Hyrax patients in the upper nasal section. The above findings indicate that the loosening of the pterygopalatine suture was substantially larger in the MSE group than in the Hyrax group. This can be due to the fact that the lateral force generated by the expansion screw is directed to the dentoalveolar bone via dentition with Hyrax appliance,

generating only a small effect at the circummaxillary skeletal level. With the MSE, the use of four micro-implants deeply embedded in the posterior aspect of the maxilla allows the force to be directly transmitted to the surrounding bone. This is reflected in the lesser tipping of the molars and larger lateral movement of the bony landmarks with MSE compared to Hyrax patients in all three axial sections analyzed in this study. As the maxilla is forced to move laterally by the MSE appliance, especially in its posterior part, the pterygopalatine suture gets disrupted more than with the conventional Hyrax appliance.

Moreover, for the first time, the present study clearly illustrated that the pterygopalatine suture can be separated by a bone-borne maxillary skeletal expander (MSE) as confirmed by the openings between the lateral and medial plates of the pterygoid processes (APS) and by the lateral slide in the pterygomaxillary fissure (LNS). This is remarkable considering the post-pubertal ages of MSE patients.

Conversely, the pterygopalatine suture did not split in Hyrax patients. This finding is in agreement with the studies by Melsen [82] and Baccetti [83] with dry human skulls, who affirm that a spontaneous opening of the pterygomaxillary connection is not expected during RPE with tooth-borne expanders because of the extensive interlocking of the corresponding bone surfaces. Acar and Wertz [96,97] on the other hand considered that the disjunction of the maxillopalatine complex from the pterygoid plates of the sphenoid could provide a possible answer to why point A and the entire maxilla moved forward significantly during RPE in few rare instances.

The loosening of the pterygopalatine suture is also enhanced by the forward movement of maxilla which was larger in MSE patients than in Hyrax patients. In MSE

patients, the forward movements of maxillary halves were 0.8 mm and 1.0 mm (Rt and Lt side) in the lower nasal section, and they were 0.9 mm and 1.0 mm (Rt and Lt side) in the upper nasal section. On the other hand, the forward movement of the pterygoid process of the sphenoid was negligible without statistical significance.

These findings can have important implications in the treatment of Class III patients when MSE is followed by facemask therapy: MSE loosens the pterygopalatine suture and can reduce its resistance to maxillary protraction. In fact, RPE is a procedure commonly utilized to enhance maxillary advancement [117] in the therapy of class III patients. This study clearly indicated that MSE can provide much more meaningful loosening of the perimaxillary sutures.

The reason why the maxilla moves forward during maxillary expansion is not clear yet. Garib [60] and Jafari [48] believe that the restraining effect of the pterygopalatine suture and the buttressing effect of the zygomatic bone could be the possible explanation for forward movement of the nasomaxillary complex. Gardner [40] believes that the forward and downward movement of the maxilla during RPE is correlated with the opening of the spheno-occipital synchondrosis (SOS), suggesting that the SOS can undergo bony remodeling in response to RPE therapy. On the other hand, the forward movement of the maxilla can be simply due to the disarticulation in the sutures located posteriorly to the maxilla, especially in the pterygomaxillary region. In MSE patients, this movement may be associated with the rotational effect that takes places in the horizontal plane during the maxillary expansion since the entire zygomaticomaxillary complex rotates laterally with a center of rotation located near the proximal portion of the zygomatic process of the temporal bone (Fig 73-74). This rotational movement can promote

forward displacement of maxillary halves as demonstrated in the present study.

Rotation of the zygomaticomaxillary complex in the coronal plane

In MSE patients, the upper inter-zygomatic distance increased by 0.5 mm and the lower inter-zygomatic distance increased by 4.6 mm in the coronal zygomatic section (CZS), indicating that the lower part of the zygomatic bone moved laterally more than its upper part. The frontozygomatic angle (FZA) increased by 2.5° and 2.9° (Rt and Lt side) illustrating the rotational movement of zygoma during the expansion. The zygomaticomaxillary angle (ZMA) underwent negligible changes, indicating that the zygomatic and the maxillary bone do not change their relative relationship during maxillary expansion, and they together rotate around a common center of rotation. The above data suggest that the maxilla rotates outwards together with the zygomatic bone, and that the center of rotation for the zygomaticomaxillary complex is located near the frontozygomatic suture (Fig 69-70). A similar conclusion was drawn also for the Hyrax group. In the literature, it is still debated where the rotational fulcrum of the maxilla is located. The majority of FEM studies affirm that the fulcrum is located at the frontomaxillary suture [19,48,49,51]. However, Gardner [40] in his study with rhesus monkeys and Gautam [50] in his FEM study found that the center of rotation of the maxilla is close to the superior orbital fissure. These results are more in agreement with the data obtained in our study. The downward movements of PNS and ANS induced by RPE, reported by some authors [60,97], can be a consequence of the rotation of the zygomaticomaxillary complex around the frontozygomatic suture, as found in the present study. Furthermore, the opening of the frontomaxillary and nasomaxillary

sutures reported by Leonardi et al. [42] can be explained by the rotation of the zygomaticomaxillary complex around the frontozygomatic suture, as shown in our study.

The increase in the frontozygomatic angle (FZA) was larger in MSE patients than in Hyrax patients ($p<0.05$). This can be due to the fact that, overall, Hyrax patients showed a smaller displacement of maxillary and circummaxillary bones in all CBCT sections of our study. In addition, since the pattern of lateral movement of the maxilla is more parallel in MSE than in Hyrax patients, the upper part of the maxilla underwent a larger lateral displacement in MSE patients, leading to a larger lateral movement in the lower part of the zygomatic bone.

Rotation of the zygomaticomaxillary complex in the horizontal plane

In the axial zygomatic plane (AZP), the anterior inter-maxillary distance increased by 2.7 mm and the posterior inter-zygomatic distance increased by 2.4 mm for the MSE group; and the anterior inter-maxillary distance increased by 1.8 mm and the posterior inter-zygomatic distance increased by 1.2 mm for the Hyrax group. These results show that the maxilla, zygomatic bone and zygomatic arch were displaced laterally, especially with MSE.

The zygomatic process angle of the temporal bone (ZPA) increased in both groups: 1.7° and 2.1° (Rt and Lt side) with statistical significance in MSE patients, and 0.9° and 0.8° (Rt and Lt side) without statistical significance in Hyrax patients. No significant changes were observed at the zygomaticotemporal suture indicated by negligible changes in the zygomaticotemporal angle (ZTA) for both groups. This is in

agreement with the study of Leonardi [42] who found insignificant opening at the zygomaticotemporal suture during maxillary expansion.

In Hyrax patients, the change at the angle of the zygomatic process of the temporal bone (ZPA) was not statistically significant. Gautam [50] , in a FEM study with conventional RPE, mentioned that the center of rotation of the maxilla in the horizontal plane was located between the lateral and the medial pterygoid plates. Our study also indicated that the center of rotation of maxillary bones is located close to the pterygoid process of the sphenoid (Fig 75) in the Hyrax group, since the changes in the zygomaticotemporal angle (ZTA) and in the angle of the zygomatic process of the temporal bone (ZPA) were not statistically significant. In addition, the lateral displacements of all posterior maxillary landmarks in the lower nasal section and upper nasal section were very small in Hyrax patients (0.4 mm and 0.6 mm for the LNS, and 0.4 mm and 0.3 mm for the UNS), suggesting that this part of the maxilla has not moved much and is therefore close to the center of rotation.

However, in MSE group, the palatal expansion in the axial palatal plane was almost perfectly parallel, and the posterior maxillary landmarks in the lower nasal section and upper nasal section moved considerably in lateral direction (1.3 mm and 1.4 mm in the LNS, and 0.9 mm and 1.0 mm in the UNS). In addition, the posterior inter-zygomatic distance and the angle of the zygomatic process of the temporal bone (ZPA) significantly increased during maxillary expansion. The above findings suggested that the center of rotation in the horizontal plane for MSE patients is probably more posteriorly placed than the Hyrax patients. This finding with MSE contradicts what was reported so far in the literature for conventional RPE. Our study indicates that the center

of rotation for the zygomaticomaxillary complex in MSE patients is close to the proximal portion of the zygomatic process of the temporal bone (Fig 73-74).

Maxillary expansion and its impact in the nasal cavity

Significant increases in the width of the circummaxillary sutures, such as the internasal, nasomaxillary, frontomaxillary and frontonasal sutures, are found in various studies demonstrating that these areas are affected by maxillary expansion appliances [16,18,26,44,72,89-93]. In the present study, we found that maxillary expansion affects the maxillary and several circummaxillary bones and sutures. The expansion produced in the lower nasal section and in the upper nasal section shows that the transverse dimension of the nasal cavity can be increased with maxillary expansion appliances. MSE produced substantially larger lateral displacement of the maxilla both in the lower nasal section and upper nasal section than the Hyrax appliance ($p<0.05$). This increase in the transverse dimension of the nasal cavity supports the studies that suggested that a reduction in the nasal airflow resistance is an orthopedic effect of RPE. These results are also confirmed in FEM studies [49] and in studies based on acoustic rhinometry measurements [118].

CONCLUSIONS

1) The novel reference planes and novel methodology allowed to quantify precisely the displacement of maxillary and circummaxillary bones induced by maxillary expansion; they also can be used to illustrate the asymmetrical expansion
2) Maxilla moved laterally and forward during the maxillary expansion
3) Both Hyrax and MSE appliances were able to split the midpalatal suture
4) The midpalatal suture can be split in post-pubertal age by MSE
5) In the horizontal plane, the split of the midpalatal suture was V-shaped in Hyrax patients and almost perfectly parallel in MSE patients
6) In the coronal plane, the pattern of lateral movement of maxillary bones was rotatory with more movement at the bottom and less movement at the top both in MSE and in Hyrax patients; however, the movement was more parallel in MSE than Hyrax patients
7) The pterygoid processes of the sphenoid bone bent laterally during the maxillary expansion following the lateral movement of the maxilla, and the movement was larger at the bottom of the processes than at the top in the MSE group. The pterygoid processes did not undergo anterior displacement
8) For the first time, the present study demonstrated that the pterygopalatine suture can be split by an orthopedic appliance without the need of surgery. MSE was able to split the pterygopalatine suture: the pyramidal process of the palatine bone was pulled out of the pterygoid notch of the pterygoid process in the axial palatal section; the tuberosity of the maxilla slid laterally relatively to the pterygoid process in the lower nasal section; the posterior portion of the

perpendicular plate of the palatine bone bent medially in the upper nasal section. Hyrax appliance induced mainly bone bending in the pterygopalatine suture (in the pterygoid processes of the sphenoid bone and in the perpendicular plate of the palatine bone) while no signs of split of the pterygopalatine suture was detected

9) Several circummaxillary bones and sutures were modified by the maxillary expansion both in MSE and Hyrax patients, even in post-pubertal age in the case of MSE
10) Rotations and openings occurred at maxillary and circummaxillary sutures
11) Bone remodeling (bone bending) played an important role in the skeletal effects induced by orthopedic appliances: large bone bending took place in the pterygoid process of the sphenoid, in the perpendicular plates of the palatine bone and in the zygomatic process of the temporal bone during the maxillary expansion
12) MSE and Hyrax appliance induced lateral dislocation of the maxillary bones (also at post-pubertal age in the case of MSE), increasing the transverse dimension of the nasal cavity, potentially improving the nasal airflow. This effect was significantly larger in MSE than in Hyrax patients
13) In the coronal plane, the center of rotation for the zygomaticomaxillary complex was located near the frontozygomatic suture in both MSE and Hyrax patients
14) In the horizontal plane, the center of rotation for the zygomaticomaxillary complex was located near the proximal portion of the zygomatic process of the temporal bone in MSE patients and close to the pterygoid processes of the sphenoid bone in Hyrax patients

15) MSE and Hyrax resulted in maxillary expansion of different pattern and magnitude: 1) skeletal changes were, in general, considerably larger in MSE than in Hyrax patients; 2) the movement of maxilla was more parallel with MSE than with Hyrax appliance in both the horizontal and vertical planes; 3) in MSE patients, the split of the midpalatal suture was almost perfectly parallel and the center of rotation of the zygomaticomaxillary complex was located near the proximal portion of the zygomatic process of the temporal bone in the horizontal plane; while in Hyrax patients, the split of the midpalatal suture was V-shaped and the center of rotation of the maxilla was located near the pterygoid process of the sphenoid bone; 4) MSE produced a considerable opening of the pterygopalatine suture whereas the Hyrax appliance did not; 5) the buccal tipping of the molars was large in Hyrax and negligible in MSE patients

REFERENCES

1. Haas AJ. The treatment of maxillary deficiency by opening of the midpalatal suture. Angle Orthod. 1965;35:200-17.

2. Haas AJ. Palatal expansion: just the beginning of dentofacial orthopedics. Am J Orthod. 1970;57:219-55.

3. Haas AJ. Long-term posttreatment evaluation of rapid palatal expansion. Angle Orthod. 1980;50:189-217.

4. Lagravere MO, Major PW, Flores-Mir C. Long-term dental arch changes after rapid maxillary expansion treatment: a systematic review. Angle Orthod. 2005;75:155-61.

5. Angell, E.C. Treatment of irregularities of the permanent or adult teeth. *Dent. Cosmos*. 1860;1:540–544.

6. Haas AJ. Rapid expansion of the maxillary dental arch and nasal cavity by opening the midpalatal suture. Angle Orthodontist. 1961;31:73-90.

7. Bench RW. The quad helix appliance. Semin Orthod. 1998;4:231-7

8. Mundstock KS, Barreto G, Meloti AF, Araújo MA, dos Santos-Pinto A, Raveli DB. Rapid maxillary expansion with the Hyrax appliance: an occlusal radiographic evaluation study. World J Orthod. 2007;8:277-84.

9. Handelman CS, Wang L, BeGole EA, Haas AJ. Nonsurgical rapid maxillary expansion in adults: report on 47 cases using the Haas expander. Angle Orthod. 2000;70:129-44.

10. Proffit, W.R., Fields, H.W. Jr., Sarver, D.M. Contemporary orthodontics. 4th ed. C.V. Mosby, St Louis; 2007.

11. Erverdi N, Okar I, Kucukkeles N, Arbak S. A comparison of two different rapid palatal expansion techniques from the point of root resorption. Am J Orthod Dentofacial Orthop. 1994;106:47-51.

12. Weissheimer A, de Menezes LM, Mezomo M, Dias DM, de Lima EM, Rizzatto SM. Immediate effects of rapid maxillary expansion with Haas-type and hyrax-

type expanders: a randomized clinical trial. Am J Orthod Dentofacial Orthop. 2011;140:366-376.

13. Schuster G, Borel-Scherf I, Schopf PM. Frequency of and complications in the use of RPE appliances--results of a survey in the Federal State of Hesse, Germany. J Orofac Orthop. 2005;66:148-61.

14. Garib DG, Henriques JF, Janson G, de Freitas MR, Fernandes AY. Periodontal effects of rapid maxillary expansion with tooth-tissue-borne and tooth-borne expanders: a computed tomography evaluation. Am J Orthod Dentofacial Orthop. 2006;129:749-58.

15. Gurel HG, Memili B, Erkan M, Sukurica Y. Long-term effects of rapid maxillary expansion followed by fixed appliances. Angle Orthod. 2010;80:5-9.

16. Baysal A, Uysala T, Velia I, et al. Evaluation of alveolar bone loss following rapid maxillary expansion using cone- beam computed tomography. Korean J Orthod. 2013;43: 83–95.

17. Lagravère MO, Carey J, Heo G, Toogood RW, Major PW. Transverse, vertical, and anteroposterior changes from bone-anchored maxillary expansion vs traditional rapid maxillary expansion: a randomized clinical trial. Am J Orthod Dentofacial Orthop. 2010;137:304-12.

18. Carlson C, Sung J, McComb RW, Machado AW, Moon W. Microimplant-assisted rapid palatal expansion appliance to orthopedically correct transverse maxillary deficiency in an adult. Am J Orthod Dentofacial Orthop. 2016;149:716-28.

19. MacGinnis M, Chu H, Youssef G, Wu KW, Machado AW, Moon W. The effects of micro-implant assisted rapid palatal expansion (MARPE) on the nasomaxillary complex--a finite element method (FEM) analysis. Prog Orthod. 2014;15:52.

20. Nienkemper M, Wilmes B, Pauls A, Drescher D. Maxillary protraction using a hybrid hyrax-facemask combination. Prog Orthod. 2013;14:5.

21. Starnbach H, Bayne D, Cleall J, Subtelny JD. Facioskeletal and dental changes resulting from rapid maxillary expansion. Angle Orthod. 1966;36:152-64.

22. Bishara SE, Staley RN. Maxillary expansion: clinical implications. Am J Orthod Dentofacial Orthop. 1987;91:3-14.

23. Epker, B. N. and C. Wolford . Dentofacial Deformity, Surgical-Orthodontic Correction. St Louis, Mo: CV Mosby; 1980.

24. McNamara, JA, Brudon WL. Treatment of tooth-size/arc-size discrepancy problems. In: McNarama JA Jr, Brudon WL, eds. Orthodontic and Orthopedic Treatment in the Mixed Dentition. Ann Arbor, Michigan: Needham Press; 1993:67-93.

25. Magnusson A, Bjerklin K, Nilsson P, Marcusson A. Surgically assisted rapid maxillary expansion: long-term stability. Eur J Orthod. 2009;31:142-9.

26. Glassman AS, Nahigian SJ, Medway JM, Aronowitz HI. Conservative surgical orthodontic adult rapid palatal expansion: sixteen cases. Am J Orthod. 1984;86:207-13.

27. Lehman JA Jr, Haas AJ, Haas DG. Surgical orthodontic correction of transverse maxillary deficiency: a simplified approach. Plast Reconstr Surg. 1984;73:62-8.

28. Pogrel MA, Kaban LB, Vargervik K, Baumrind S. Surgically assisted rapid maxillary expansion in adults. Int J Adult Orthodon Orthognath Surg. 1992;7:37-41.

29. Lines PA. Adult rapid maxillary expansion with corticotomy. Am J Orthod. 1975;67:44-56.

30. Koudstaal MJ, Poort LJ, van der Wal KG, Wolvius EB, Prahl-Andersen B, Schulten. AJ. Surgically assisted rapid maxillary expansion (SARME): a review of the literature. Int J Oral Maxillofac Surg. 2005;34:709-14.

31. Bell WH, Epker BN. Surgical-orthodontic expansion of the maxilla. Am J Orthod. 1976;70:517-28.

32. Han UA, Kim Y, Park JU. Three-dimensional finite element analysis of stress distribution and displacement of the maxilla following surgically assisted rapid maxillary expansion. J Craniomaxillofac Surg. 2009;37:145-54

33. Koudstaal MJ, Smeets JB, Kleinrensink GJ, Schulten AJ, van der Wal KG. Relapse and stability of surgically assisted rapid maxillary expansion: an anatomic biomechanical study. J Oral Maxillofac Surg. 2009;67:10-4.

34. Pinto PX, Mommaerts MY, Wreakes G, Jacobs WV. Immediate postexpansion changes following the use of the transpalatal distractor. J Oral Maxillofac Surg. 2001;59:994-1000

35. Fricke-Zech S, Gruber RM, Dullin C, Zapf A, Kramer FJ, Kubein-Meesenburg D, Hahn W. Measurement of the midpalatal suture width. Angle Orthod. 2012;82:145-50.

36. Handelman CS, Wang L, BeGole EA, Haas AJ. Nonsurgical rapid maxillary expansion in adults: report on 47 cases using the Haas expander. Angle Orthod. 2000;70:129-44.

37. Isaacson RJ, Wood JL, Ingram AH. Forces produced by rapid maxillary expansion. Part I. Design of the force measuring system. Angle Orthod 1964;34:256-60.

38. Isaacson RJ, Ingram AH. Forces produced by rapid maxillary expansion. Part II. Forces present during treatment. Angle Orthod 1964;34:261-70.

39. Chaconas SJ, Caputo AA. Observation of orthopedic force distribution produced by maxillary orthodontic appliances. Am J Orthod. 1982;82:492-501.

40. Gardner GE, Kronman JH. Cranioskeletal displacements caused by rapid palatal expansion in the rhesus monkey. Am J Orthod. 1971;59:146-55.

41. Arat ZM, Gökalp H, Atasever T, Türkkahraman H. 99mTechnetium-labeled methylene diphosphonate uptake in maxillary bone during and after rapid maxillary expansion. Angle Orthod. 2003;73:545-9.

42. Leonardi R, Sicurezza E, Cutrera A, Barbato E. Early post-treatment changes of circumaxillary sutures in young patients treated with rapid maxillary expansion. Angle Orthod. 2011;81:36-41.

43. Leonardi R, Cutrera A, Barbato E. Rapid maxillary expansion affects the spheno-occipital synchondrosis in youngsters. A study with low-dose computed tomography. Angle Orthod. 2010;80:106-10.

44. Ghoneima A, Abdel-Fattah E, Hartsfield J, El-Bedwehi A, Kamel A, Kula K. Effects of rapid maxillary expansion on the cranial and circummaxillary sutures. Am J Orthod Dentofacial Orthop. 2011;140:510-9.

45. Itoh T, Chaconas SJ, Caputo AA, Matyas J. Photoelastic effects of maxillary protraction on the craniofacial complex. Am J Orthod. 1985;88:117-24.

46. Shetty V, Caridad JM, Caputo AA, Chaconas SJ. Biomechanical rationale for surgical-orthodontic expansion of the adult maxilla. J Oral Maxillofac Surg. 1994;52:742-9.

47. Baydas B, Yavuz I, Uslu H, Dagsuyu IM, Ceylan I. Nonsurgical rapid maxillary expansion effects on craniofacial structures in young adult females. A bone scintigraphy study. Angle Orthod. 2006;76:759-67.

48. Jafari A, Shetty KS, Kumar M. Study of stress distribution and displacement of various craniofacial structures following application of transverse orthopedic forces--a three-dimensional FEM study. Angle Orthod. 2003;73:12-20.

49. Işeri H, Tekkaya AE, Oztan O, Bilgiç S. Biomechanical effects of rapid maxillary expansion on the craniofacial skeleton, studied by the finite element method. Eur J Orthod. 1998;20:347-56.

50. Gautam P, Valiathan A, Adhikari R. Stress and displacement patterns in the craniofacial skeleton with rapid maxillary expansion: a finite element method study. Am J Orthod Dentofacial Orthop. 2007;132:1-11

51. Baldawa RS, Bhad WA. Stress distribution analysis during an intermaxillary dysjunction: A 3-D FEM study of an adult human skull. Ann Maxillofac Surg. 2011;1:19-25.

52. Holberg C, Rudzki-Janson I. Stresses at the cranial base induced by rapid maxillary expansion. Angle Orthod. 2006;76:543-50.

53. Holberg C. Effects of rapid maxillary expansion on the cranial base—an FEM-analysis. J Orofac Orthop. 2005;66:54-66.

54. Yu HS, Baik HS, Sung SJ, Kim KD, Cho YS. Three-dimensional finite-element analysis of maxillary protraction with and without rapid palatal expansion. Eur J Orthod. 2007;29:118-25.

55. Provatidis C, Georgiopoulos B, Kotinas A, McDonald JP. On the FEM modeling of craniofacial changes during rapid maxillary expansion. Med Eng Phys. 2007 Jun;29(5):566-79. Erratum in: Med Eng Phys. 2008;30:402.

56. Boryor A, Geiger M, Hohmann A, Wunderlich A, Sander C, Martin Sander F, Sander FG. Stress distribution and displacement analysis during an intermaxillary disjunction--a three-dimensional FEM study of a human skull. J Biomech 2008;41:376-82.

57. Provatidis CG, Georgiopoulos B, Kotinas A, McDonald JP. Evaluation of craniofacial effects during rapid maxillary expansion through combined in vivo/in vitro and finite element studies. Eur J Orthod. 2008;30:437-48.

58. Lee H, Ting K, Nelson M, Sun N, Sung SJ. Maxillary expansion in customized finite element method models. Am J Orthod Dentofacial Orthop. 2009;136:367-74.

59. Bell WH, Epker BN. Surgical-orthodontic expansion of the maxilla. Am J Orthod. 1976;70:517-28.

60. Garib DG, Henriques JF, Janson G, Freitas MR, Coelho RA. Rapid maxillary expansion--tooth tissue-borne versus tooth-borne expanders: a computed tomography evaluation of dentoskeletal effects. Angle Orthod. 2005;75:548-57.

61. Babacan H, Sokucu O, Doruk C, Ay S. Rapid maxillary expansion and surgically assisted rapid maxillary expansion effects on nasal volume. Angle Orthod. 2006;76:66-71.

62. Storey, E. Bone changes associated with tooth movement. A histological study of the effect of force in the rabbit, guinea pig and rat. Aust. J. Dent. 1955;59:147-61.

63. Timms DJ. A study of basal movement with rapid maxillary expansion. Am J Orthod. 1980;77:500-7.

64. Storey E. Tissue response to the movement of bones. Am J Orthod. 1973;64:229-47.

65. Wieslander L. The effect of force on craniofacial development. Am J Orthod. 1974;65:531-8.

66. Brossman RE, Bennett CG, Merow WW. Facioskeletal remodelling resulting from rapid palatal expansion in the monkey (Macaca cynomolgus). Arch Oral Biol. 1973;18:987-94.

67. Rune B, Sarnäs KV, Selvik G, Jacobsson S. Movement of maxillary segments after expansion and/or secondary bone grafting in cleft lip and palate: a roentgen stereophotogrammetric study with the aid of metallic implants. Am J Orthod. 1980;77:643-53.

68. Enoki C, Valera FC, Lessa FC, Elias AM, Matsumoto MA, Anselmo-Lima WT. Effect of rapid maxillary expansion on the dimension of the nasal cavity and on nasal air resistance. Int J Pediatr Otorhinolaryngol. 2006;70:1225–30.

69. Ekström C, Henrikson CO, Jensen R. Mineralization in the midpalatal suture after orthodontic expansion. Am J Orthod. 1977;71:449-55.

70. Wertz RA. Skeletal and dental changes accompanying rapid midpalatal suture opening. Am J Orthod. 1970;58:41-66.

71. Debbane, E.F. A cephalometric and histologic study on the effect of orthodontic expansion of the midpalatal suture of the cat. Am. J. Orthod. 1958;44:187.

72. Ballanti F, Lione R, Baccetti T, Franchi L, Cozza P. Treatment and posttreatment skeletal effects of rapid maxillary expansion investigated with low-dose computed tomography in growing subjects. Am J Orthod Dentofacial Orthop. 2010;138:311-7.

73. Lione R, Franchi L, Cozza P. Does rapid maxillary expansion induce adverse effects in growing subjects? Angle Orthod. 2013;83:172-82.

74. Liu S, Xu T, Zou W. Effects of rapid maxillary expansion on the midpalatal suture: a systematic review. Eur J Orthod. 2015;37:651-5.

75. Bazargani F, Feldmann I, Bondemark L. Three-dimensional analysis of effects of rapid maxillary expansion on facial sutures and bones. Angle Orthod. 2013;83:1074-82.

76. Stepanko LS, Lagravère MO. Sphenoid bone changes in rapid maxillary expansion assessed with cone-beam computed tomography. Korean J Orthod. 2016;46:269-79.

77. Lione R, Ballanti F, Franchi L, Baccetti T, Cozza P. Treatment and posttreatment skeletal effects of rapid maxillary expansion studied with low-dose computed tomography in growing subjects. Am J Orthod Dentofacial Orthop. 2008;134:389-92.

78. Huynh T, Kennedy DB, Joondeph DR, Bollen AM. Treatment response and stability of slow maxillary expansion using Haas, hyrax, and quad-helix appliances: a retrospective study. Am J Orthod Dentofacial Orthop. 2009;136:331-9.

79. Silvestrini-Biavati A, Angiero F, Gambino A, Ugolini A. Do changes in spheno-occipital synchondrosis after rapid maxillary expansion affect the maxillomandibular complex?. Eur J Paediatr Dent. 2013;14:63-7.

80. Rukkulchon BK, Wong RW. Effect of tensile force on expression of PTHrP and thickness of hypertrophic zone in organ-cultured mouse spheno-occipital synchondroses. Arch Oral Biol. 2008;53:690-9.

81. Cendekiawan T, Wong RW, Rabie AB. Temporal expression of SOX9 and type II collagen in spheno-occipital synchondrosis of mice after mechanical tension stimuli. Angle Orthod. 2008;78:83-8.

82. Melsen B, Melsen F. The postnatal development of the palatomaxillary region studied on human autopsy material. Am J Orthod. 1982 Oct;82(4):329-42.

83. Baccetti T, Franchi L, The Fourth Dimension in Dentofacial Orthopedics: Treatment Timing for Class II and Class III Malocclusions. World J Orthod. 2001;2:159-67

84. Kudlick, E.M. A study utilizing direct human skulls as models to determine how bones of the craniofacial complex are displaced under the influence of midpalatal expansion. in: Master's thesis. ed 3. Fairleigh Dickinson University, Rutherford, New Jersey; 1973.

85. Sun Z, Hueni S, Tee BC, Kim H. Mechanical strain at alveolar bone and circummaxillary sutures during acute rapid palatal expansion. Am J Orthod Dentofacial Orthop. 2011;139:219-28.

86. Cross DL, McDonald JP. Effect of rapid maxillary expansion on skeletal, dental, and nasal structures: a postero-anterior cephalometric study. Eur J Orthod. 2000;22:519-28.

87. Chung CH, Font B. Skeletal and dental changes in the sagittal, vertical, and transverse dimensions after rapid palatal expansion. Am J Orthod Dentofacial Orthop. 2004;126:569-75.

88. Ramires T, Maia RA, Barone JR. Nasal cavity changes and the respiratory standard after maxillary expansion. Braz J Otorhinolaryngol. 2008;74:763-9.

89. Cordasco G, Nucera R, Fastuca R, Matarese G, Lindauer SJ, Leone P, Manzo P, Martina R. Effects of orthopedic maxillary expansion on nasal cavity size in growing subjects: a low dose computer tomography clinical trial. Int J Pediatr Otorhinolaryngol. 2012;76:1547-51.

90. Palaisa J, Ngan P, Martin C, Razmus T. Use of conventional tomography to evaluate changes in the nasal cavity with rapid palatal expansion. Am J Orthod Dentofacial Orthop. 2007;132:458-66.

91. Garrett BJ, Caruso JM, Rungcharassaeng K, Farrage JR, Kim JS, Taylor GD. Skeletal effects to the maxilla after rapid maxillary expansion assessed with cone-beam computed tomography. Am J Orthod Dentofacial Orthop. 2008;134:8-9.

92. Krebs, A. Midpalatal suture expansion studies by the implant method over a seven years period. Trans Europ Orthod Soc. 1964;40:131-42.

93. Memikoglu TU, Iseri H. Effects of a bonded rapid maxillary expansion appliance during orthodontic treatment. Angle Orthod 1999;69:251-6

94. da Silva Filho OG, Boas MC, Capelozza Filho L. Rapid maxillary expansion in the primary and mixed dentitions: a cephalometric evaluation. Am J Orthod Dentofacial Orthop. 1991;100:171-9.

95. da Silva Filho OG, Montes LA, Torelly LF. Rapid maxillary expansion in the deciduous and mixed dentition evaluated through posteroanterior cephalometric analysis. Am J Orthod Dentofacial Orthop. 1995 Mar;107(3):268-75.

96. Acar YB, Motro M, Erverdi AN. Hounsfield Units: a new indicator showing maxillary resistance in rapid maxillary expansion cases? Angle Orthod. 2015;85:109-16.

97. Wertz R, Dreskin M. Midpalatal suture opening: a normative study. Am J Orthod. 1977 Apr;71(4):367-81.

98. Cevidanes LH, Heymann G, Cornelis MA, DeClerck HJ, Tulloch JF. Superimposition of 3-dimensional cone-beam computed tomography models of growing patients. Am J Orthod Dentofacial Orthop. 2009;136:94-9.

99. Cevidanes LH, Styner MA, Proffit WR. Image analysis and superimposition of 3-dimensional cone-beam computed tomography models. Am J Orthod Dentofacial Orthop. 2006;129:611-8.

100. Grauer D, Cevidanes LS, Proffit WR. Working with DICOM craniofacial images. Am J Orthod Dentofacial Orthop. 2009;136:460-70.

101. Habersack K, Karoglan A, Sommer B, Benner KU. High-resolution multislice computerized tomography with multiplanar and 3-dimensional reformation imaging in rapid palatal expansion. Am J Orthod Dentofacial Orthop. 2007;131:776-81.

102. Kunz F, Linz C, Baunach G, Böhm H, Meyer-Marcotty P.Expansion patterns in surgically assisted rapid maxillary expansion: Transpalatal distractor versus hyrax appliance. J Orofac Orthop. 2016;77:357-65.

103. Garreau E, Bouscaillou J, Rattier S, Ferri J, Raoul G Bone-borne distractor versus tooth-borne distractor for orthodontic distraction after surgical maxillary expansion: The patient's point of view. Int Orthod. 2016;14:214-32.

104. Seeberger R, Abe-Nickler D, Hoffmann J, Kunzmann K, Zingler S.One-stage tooth-borne distraction versus two stage bone-borne distraction in surgically assisted maxillary expansion (SARME). Oral Surg Oral Med Oral Pathol Oral Radiol. 2015;120:693-8.

105. Zandi M, Miresmaeili A, Heidari A.Short-term skeletal and dental changes following bone-borne versus tooth-borne surgically assisted rapid maxillary expansion: a randomized clinical trial study. J Craniomaxillofac Surg. 2014;42:1190-5.

106. Baka ZM, Akin M, Ucar FI, Ileri Z. Cone-beam computed tomography evaluation of dentoskeletal changes after asymmetric rapid maxillary expansion. Am J Orthod Dentofacial Orthop. 2015 Jan; 147: 61-71.

107. Bjork A. Sutural growth of the upper face studied by the implant method. Acta Odontol Scand 1966;24:109-27.

108. Bjork A, Skieller V. Facial development and tooth eruption. An implant study at the age of puberty. Am J Orthod 1972;62:339-83.

109. Bjork A, Skieller V. Growth of the maxilla in three dimensions as revealed radiographically by the implant method. Br J Orthod 1977;4:53-64.

110. Bjork A, Skieller V. Normal and abnormal growth of the mandible. A synthesis of longitudinal cephalometric implant studies over a period of 25 years. Eur J Orthod 1983;5:1-46.

111. Doppel DM, Damon WM, Joondeph DR, Little RM. An investigation of maxillary superimposition techniques using metallic implants. Am J Orthod Dentofacial Orthop 1994;105:161-8.

112. Johnston LE Jr. Balancing the books on orthodontic treatment: an integrated an alysis of change. Br J Orthod 1996;23:93-102.

113. Cevidanes LHS, Bailey LTJ, Tucker GR Jr, Styner MA, Mol A, Phillips CL, et al. Superimposition of 3D cone-beam CT models of orthognathic surgery patients. Dentomaxillofac Radiol 2005;34:369-75.

114. Magnusson A, Bjerklin K, Kim H, Nilsson P, Marcusson A. Three-dimensional assessment of transverse skeletal changes after surgically assisted rapid maxillary expansion and orthodontic treatment: a prospective computerized tomography study. Am J Orthod Dentofacial Orthop. 2012;142:825-33.

115. Ballanti F, Lione R, Baccetti T, Franchi L, Cozza P. Treatment and posttreatment skeletal effects of rapid maxillary expansion investigated with low-

dose computed tomography in growing subjects. Am J Orthod Dentofacial Orthop. 2010;138:311-7.

116. Lee SP, Paik KS, Kim MK. Anatomical study of the pyramidal process of the palatine bone in relation to implant placement in the posterior maxilla. J Oral Rehabilitation. 2001;28:125-32.

117. Moon W, Wu KW, MacGinnis M, Sung J, Chu H, Youssef G, Machado A. The efficacy of maxillary protraction protocols with the micro-implant-assisted rapid palatal expander (MARPE) and the novel N2 mini-implant-a finite element study. Prog Orthod. 2015;16:16.

118. Doruk C, Sökücü O, Biçakçi AA, Yilmaz U, Taş F. Comparison of nasal volume changes during rapid maxillary expansion using acoustic rhinometry and computed tomography. Eur J Orthod. 2007;29:251-5.